DEFECT DETECTION ON ELECTRICAL POWER EQUIPMENT USING THERMAL IMAGING TECHNOLOGY

GEOFFREY ASIEGBU OGADIMMA

A thesis submitted in fulfillment of the requirement for the award of the degree of Master of Engineering in Electrical Engineering

Faculty of Electrical and Electronics Engineering
UNIVERSITI MALAYSIA PAHANG

January 2013

UNIVERSITI MALAYSIA PAHANG

DECLARATION OF THESIS AND COPYRIGHT

Author's full name : GEOFFREY OGADIMMA ASIEGBU

Date of birth : 15/08/1973

Title : DEFECT DETECTION ON ELECTRICAL POWER EQUIPMENTS USING THERMAL IMAGING TECHNOLOGY

Academic Session : 2012/2013

I declare that this thesis is classified as :

☐ **CONFIDENTIAL** (Contains confidential information under the Offical Secret Act 1972)*

☐ **RESTRICTED** (Contains restricted information as specified by the organization where the research was done)*

☑ **OPEN ACCESS** (I agree that my thesis be published as online open access Full text)

I acknowledge that Universiti Malaysia pahang reserve that right as follows:

1. The Thesis is the Property of Universiti Malaysia Pahang.
2. The Library of Universiti Malaysia Pahang has the right to make copies for the purpose of research only.
3. The has the right to make copies of the thesis for academic exchange.

Certified By

_____ _____

(Student's Signature) (Signature of Supervisor)

A09006352 DR. MOHD RAZALI BIN DAUD

New IC / Passport Number Name of Supervisor

Date: Date:

NOTES :*If the thesis is CONFIDENTIAL or RESTRICTED please attach with the letter from the organization with period and reasons for confidentiality and restriction.

SUPERVISORS' DECLARATION

We hereby declare that we have checked this project and in our opinion, this project is adequate in terms of scope and quality of the award of the degree of Master of Engineering in Electrical Engineering.

Signature :
Supervisor : DR. MOHD RAZALI BIN DAUD
Position : SENIOR LECTURER
Date : 27/06/2013

Signature :
Co-supervisor : ASSO. PROF. DR. KAMARUL HAWARI BIN GHAZALI
Position : SENIOR LECTURER
Date : 27/07/2013

STUDENT'S DECLARATION

I hereby declare that the work in this thesis is my own other than quotations and summaries, which have been duly acknowledged. This project has neither been accepted for any degree nor concurrently submitted for award of another degree.

_____

OGA

Signature :

Name : GEOFFREY ASIEGBU OGADIMMA

ID Number : MEE11003

Date : 27/06/2013

DEDICATION

I dedicate this thesis to my parents for their flagging faith in me, especially my surviving mother, my brothers and sisters and my dearest beloved fiancée without their devotion, support, patience, and encouragements throughout the period of my study, this work would not have been possible. In all,

TO GOD BE ALL THE GLORY

ACKNOWLEDGEMENT

I must express my sincerest thanks to GOD ALMIGHTY for sustaining my life to this day. I give kudos to my supervisor Dr. Mohd Razali Bin Daud towards insuring that my project and thesis are successfully completed. I give thanks to Associate Professor Dr. Kamarul Hawari Bin Ghazali for his act of co-supervision and my most respect for Dr. Ahmed Mohamed Ahmed Haidar for his guidance, patience, and support throughout my research project. My special thanks go to Universiti Malaysia Pahang for her financial encouragement within this period of faithful research work. I would like to use this very opportunity to appreciate my dearest beloved fiancée Amalachukwu Nnamaka Jiagbogu for her invaluable assistance through committed backup prayers.

ABSTRACT

Electrical power equipment and components are vital constituent portions of human existence. They are found virtually in every domestic home and manufacturing industries. These electrical power equipment, operates at a temperature above absolute zero, certainly emit infrared radiation. In some power distribution systems, existing station equipment could no longer withstand the short circuit current capacity causing equipment break down. The electrical equipment failures can be avoided if the temperature threshold is detected in order to take timely corrective action. Quality control and part inspection have done considerably well in the area of manufacturing but not yet gotten to its fully robust thermal imaging technology application. Thermal image is a term comes from the infrared thermography. It has gained its popularity in the last few decades over other predictive maintenance techniques due to its many advantages such as contact-less, easy to interpret the thermal data, large area of inspection as well as free from dangerous radiation. This research project proposed defect detection on electrical power equipment using thermal imaging technology. The aim is to study the thermal characteristic of electrical power equipment, secondly, to design defect detection technique and make a fault decision as well as comparing results with other defect detection techniques and international thermal evaluation standard. A thermal imager is used to acquire thermal images of the tested electrical facilities under various operating conditions. The thermal image in RGB color space is normalized and morphologically dissected using image mean, variance, and covariance which is applied on the mixtures of Gaussian Probability Distribution Function (GPDF) through which threshold values were determined. Using the threshold values similar pixels are connected via maximum likelihood criterion been function of short circuit OR logic operator. The predetermined threshold values are optimized using Receiver Operating Characteristic (ROC) curve and the area under convex hull. Regions of electrical thermogram are segmented using the optimal threshold values. Various features in the infrared thermal (IRT) image are extracted in order to detect anomalies. Classification and decision are made in terms of colors and temperature difference values. Matlab image processing software is used to implement these procedures. Application of this system is quite simple, user friendly, time and cost effective. In conclusion, a total of 111 different electrical power distribution facilities was experimentally inspected. Within the limits of experimental errors, the results of the analysis showed that 99.9% sensitivity and 99.72% accuracy was achieved with an error rate of 0.28 that was attributed to mistakes due to over and less caution during experimental thermal inspection of electrical facilities. The results suggested that, the method provides an accurate identification of defective parts can be extended for further applications. The results also suggest that the system works well enough to help improve the value and efficiency of consumable electrical power equipment reducing the number of faults in the power distribution line, ensuring safety of the workers and users of electricity, protecting electrical power facilities from damage due to over-heating or fire. Above all, testing, inspection and preventive maintenance work become safer, easier, and faster with a reasonably high degree of accuracy with this result-oriented defect detection scrutiny system on electrical power facilities.

ABSTRAK

Peralatan kuasa elektrik dan komponennya merupakan konstituen penting kewujudan manusia. Mereka dijumpai hampir di setiap rumah domestik dan industri pembuatan. Peralatan kuasa elektrik, beroperasi pada suhu di atas sifar mutlak, sudah tentu mengeluarkan sinaran inframerah. Dalam sesetengah sistem pengagihan kuasa, peralatan yang sedia ada tidak dapat lagi menahan kapasiti arus litar pintas yang menyebabkan peralatan rosak. Kerosakan peralatan elektrik boleh dielakkan jika ambang suhu dikesan untuk mengambil tindakan pembetulan yang tepat pada masanya. Penggunaan pengimejan haba di dalam bidang kawalan kualiti dan pemeriksaan komponen dalam bidang pembuatan adalah agak baik tetapi belum mencapai tahap automatik sepenuhnya. Imej haba adalah istilah yang berasal dari termografi inframerah. Ia telah mendapat populariti dalam beberapa dekad yang lalu berbanding teknik-teknik penyelenggaraan ramalan lain kerana banyak kelebihan seperti kurang-sentuhan, mudah untuk mentafsirkan data haba, kawasan pemeriksaan yang besar serta bebas daripada sinaran berbahaya. Projek penyelidikan ini mencadangkan pengesanan kerosakan pada peralatan kuasa elektrik menggunakan teknologi pengimejan haba. Tujuannya adalah untuk mengkaji ciri-ciri haba peralatan kuasa elektrik, dan untuk mereka bentuk teknik pengesana kerosakan serta memberitahu pengguna bahagian yang mengalami kerosakan. Keputusan yang dikeluarkan oleh projek ini akan dibandingkan dengan lain-lain teknik pengesanan kerosakan dan standard penilaian haba antarabangsa. Kamera pengimejan haba digunakan untuk memperolehi imej haba daripada peralatan elektrik digunakan di dalam pelbagai keadaan operasi. Imej haba dalam ruang warna RGB dinormalkan dan dipecahkan secara morfologi menggunakan imej min, varians dan kovarians yang digunakan pada campuran Gaussian Kebarangkalian Pengagihan Fungsi (GPDF) di mana nilai-nilai ambang ditentukan. Piksel yang mempunyai nilai-nilai di dalam lingkungan nilai ambang akan disambungkan melalui kriteria kebolehjadian maksimum bagi fungsi litar pintas ATAU operator logik. Nilai ambang yang telah ditetapkan dioptimumkan menggunakan keluk "Receiver Operating Characteristic (ROC)" dan kawasan di bawah cembung badan. Pelbagai ciri dalam imej haba inframerah (IRT) imej yang diambil diekstrak untuk mengesan anomali. Klasifikasi dan keputusan dibuat dari segi warna dan nilai perbezaan suhu. Fungsi pemprosesan imej di dalam Matlab digunakan untuk melaksanakan prosedur ini. Penggunaan sistem ini adalah agak mudah, mesra pengguna, masa dan kos efektif. Ujian dijalankan ke atas sebanyak 111 peralatan elektrik yang berbeza. Dalam had kesilapan eksperimen, keputusan analisis menunjukkan bahawa 99.9% kepekaan dan ketepatan 99.72% telah dicapai dengan kadar kesilapan 0.28 yang telah dikaitkan dengan kesilapan kerana kurang atau terlalu berhati-hati semasa pemeriksaan terma eksperimen kemudahan elektrik. Keputusan menunjukkan bahawa, kaedah menyediakan pengenalan tepat bahagian yang rosak boleh dilanjutkan bagi permohonan yang selanjutnya. Keputusan juga menunjukkan bahawa sistem kerja-kerja yang cukup baik untuk membantu meningkatkan nilai dan kecekapan guna peralatan kuasa elektrik mengurangkan jumlah kerosakan dalam talian pengagihan kuasa, memastikan keselamatan pekerja dan pengguna elektrik, melindungi kemudahan kuasa elektrik daripada kerosakan yang disebabkan oleh kepada lebih-pemanasan atau api. Paling penting, ujian, pemeriksaan dan kerja-kerja penyelenggaraan pencegahan menjadi lebih selamat, lebih mudah, dan lebih cepat dengan tahap yang cukup tinggi ketepatan dengan ini kecacatan berorientasikan hasil pengesanan sistem penelitian mengenai kemudahan elektrik.

TABLE OF CONTENTS **PAGE**

DECLARATION OF THESIS AND COPYRIGHT ii
SUPERVISOR'S DECLARATION iii
STUDENT'S DECLARATION iv
DEDICATION v
ACKNOWLEDGEMENTS vi
ABSTRACT vii
ABSTRAK viii
TABLE OF CONTENTS ix
LIST OF TABLES xii
LIST OF FIGURES xiii
LIST OF SYMBOLS xv
LIST OF ABBREVIATIONS xvi

CHAPTER 1 INTRODUCTION

1.1 Introduction 1
1.2 Fundamental Problem 1
1.3 Research Problem Addressed to Electrical Equipment 3
1.4 Recommended Solution 4
1.5 Objectives of Research Project 5
1.6 Scope of Research Project 5
1.7 Thesis Outline 6

CHAPTER 2 LITERATURE REVIEW

2.1 Introduction 7
2.2 Terminology 7
2.3 What is Thermography? 8
2.4 Why Thermography is Important? 8
2.5 Qualities of A Good IRT Image 8
2.6 The Electromagnetic Spectrum 9

2.7	Infrared Radiation	9
2.8	Radiometric Temperature	10
2.9	Reflectivity	10
2.10	Ambient Temperature	10
2.11	Review of Thermal Defect Detection Analysis	10

CHAPTER 3 RESEARCH METHODOLOG
DEFECT DETECTION SYSTEM DESIGN

3.1	Introduction	23
3.2	Supervised Optimal Threshold Selection Technique	30
3.3	RGB Optimal Threshold Segmentation Algorithm	36
3.4	Measurement of Segmentation Operation	41
3.5	Performance Measure of Defect Detection Algorithm	44
3.6	Evaluation of Sensitivity of Defect Detection System	48
3.7	Classification of Extracted Thermal Regions	49
3.8	Comparative Study on Electrical Equipment Defect Detection Technique	56

CHAPTER 4 RESULTS AND DISCUSSIONS

4.1	Introduction	60
4.2	Tools and Image Acquisition	60
4.3	Quality Image Acquisition	60
4.4	Defect Detection Evaluation	62
4.5	Results of RGB Optimal Threshold Algorithm	63
4.6	Interpretation of Classified Regions	67
4.7	Decision-making, Sensitivity, and Accuracy Results	74
4.8	Results of K Means Clustering Algorithm	81
4.9	Defect Detection Comparison Study Results	92

CHAPTER 5 CONCLUSION AND RECOMMENDATIONS

5.1	Introduction	103
5.2	Achievement	105
5.3	Recommendation for future work	106

REFERENCES 107

APPENDICES 114

A	Table A Ti25 Fluke Thermal Imager Specification	114
B-1	Table B-1 Emissivity Values for Metals	115
B-2	Table B-2 Emissivity Values for Non Metals	116
C-1	Tools And Materials	118
C-2	Thermal Picture Acquisition	118
C-3	Factors for Measurement Accuracy	120
C-4	Internal Calibration of Camera	121
C-5	Factory Calibration of Camera	121
C-6	Emissivity Correction	121
C-7	Reflected Temperature Compensation	122
C-8	Distance-To-Spot Size Ratio	123
C-9	Instantaneous Field of View (IFOV)	124
C-10	Minimum Distance for Focus	125
C-11	Correction Measurement	125
D	List of Publications	126

UMP

LIST OF TABLES

Table No.	Title	Page
3.1	Experimental thermal inspection result	29
3.2	Optimal threshold values (low temperature equipment)	45
3.3	Optimal threshold values (medium temperature equipment)	45
3.4	Optimal threshold values (high temperature equipment)	45
3.5	Low temperature equipment classification ($\Delta T \geq 40$℃)	49
3.6	Medium temperature equipment classification ($\Delta T \geq 65$℃)	50
3.7	High Temperature Equipment Classification ($\Delta T \geq 105$℃)	50
3.8	Standard analysis report base on temperature difference (℃)	51
3.9	Comparison between measured results, mathematical evaluation and international maintenance testing standards	53
4.1	Sensitivity, predictive positive value (PPV) and false positive rate (FPR) (low temperature equipment)	78
4.2	Sensitivity, predictive positive value (PPV) and false positive Rate (FPR) medium temperature equipment	79
4.3	Sensitivity, predictive positive value (PPV) and false positive Rate (FPR) high temperature equipment	79
4.4	Description of thermal inspection of electrical facilities and accuracy	80
4.5	Comparison analysis result table	101

LIST OF FIGURES

Figure No.	Title	Page
3.1	Visual spectrum photos and normal view of electrical facilities	25
3.2	Ambient reference temperature from de-energized and energized electric motor thermogram	26
3.3	Segments of backgrounds and foregrounds IRT images	28
3.4	Transformer IRT image; (a = Non-normalized IRT image), (b = Non-normalized grayscale IRT image), (c = Non-normalized IRT image histogram), (d = Normalized IRT image), (e = Normalized grayscale IRT image), (f = Normalized IRT image histogram)	32
3.5	Circuit breaker IRT image; (a = Non-normalized IRT image), (b = Non-normalized grayscale IRT image), (c = Non-normalized IRT image histogram), (d = Normalized IRT image), (e = Normalized grayscale IRT image), (f = Normalized IRT image histogram)	32
3.6	Real-time inspected electrical facilities	41
3.7	Ideal receiver operating characteristics curve	42
3.8	Area under convex hull	43
3.9	Original IRT image, (b) True Negative (TN), (c) True Positive (TP)	43
3.10	Original IRT image, (b) Result of flawed threshold, (c) Result of optimal threshold	44
3.11	Defect detection training flow process	52
3.12	Computer aided defect detection scrutiny system final flow process	55
3.13	K-means clustering algorithm flowchart	58
4.1	Well-focused and flawed IRT images; (a = Electric Motor), (b =Contactor), (c = Capacitor), (d = Transformer),	62

(e = Circuit Breaker)

4.2 Typical fault of overload or loose connection; 64
(a = normal view),
(b = thermal spectrum view),
(c = Image Histogram)

4.3 Screen print of Matlab processed results 67
(a = Abnormal thermal condition),
(b = Abnormal thermal condition),
(c = Normal thermal condition),
(d = Warming thermal condition),
(e = Abnormal thermal condition),
(f = Warming thermal condition),
(g = Warming thermal condition).

4.4 Thermogram of electrical components at warming stage 70
(A = Molded case circuit breaker IRT image),
(B = Electric motor bearing IRT image),
(C = Electric motor IRT image),
(D = Connector IRT image).

4.5 Thermogram of electrical components under critical condition 74
(A = Bolted joint and connector IRT image),
(B = Distribution transformer IRT image),
(C = Distribution transformer IRT image),
(D = Dry type transformer IRT image),
(E = Circuit breaker IRT image).

4.6 RGB optimal threshold classification result of abnormal transformer 75

4.7 RGB optimal threshold classification result of high thermal fuse box 75

4.8 RGB optimal threshold classification result of warm thermal condition electric motor 76

4.9 RGB optimal threshold classification result of normal thermal condition minitured circuirt breaker 77

4.10 RGB optimal threshold classification result of electric motor within ambient temperature 77

4.11 Results of unsupervised k-means clustering algorithm 85

4.12 Results of supervised K means classification 91

4.13 Defect detection comparison results; 100
(a = RGB optimal threshold algorithm),
(b = K-means clustering algorithm).

LIST OF SYMBOLS

μ_r, μ_g, μ_b	Mean value of red, green, blue colors in the IRT image
r_i, g_i, b_i	Pixel value of red, green, blue colors in the IRT image
N	Total Number of image pixels of the IRT image
$\sigma_r^2, \sigma_g^2, \sigma_b^2$	Variance values red, green, blue color components in the IRT image
$\sigma_{rg}^2, \sigma_{rb}^2, \sigma_{gb}^2$	Covariance values of pixel similarity between color combinations in the IRT image
e	Exponential Function Applied in Gaussian PDF
π	Pi = 3.1429 (constant)
ΔT	Temperature difference between equipment and ambient
Δt	Temperature difference between similar equipment
N_{gv}	Normalized grayscale value
T_i	Optimal threshold value of each extracted regions

LIST OF ABBREVIATIONS

RGB	Red, Green, Blue color model or space
IRT	Infrared Thermal Image
ROC	Receiver Operating Characteristics
TN	True Negative
TP	True Positive
FN	False Negative
FP	False Positive
PPV	Predictive Positive Value
FPR	False Positive Rate
TPR_{value}	Actual pixel value but does not represent real thermal value
TH_{real}	Real equipment thermal value

UMP

CHAPTER 1

1.1 INTRODUCTION

This chapter will explain explicitly the fundamental problems and lay emphasis on the importance of inculcating computer aided defect scrutiny system into testing and inspection of electrical equipment and components. Recommendations for the problems were discussed, and then objectives and scope of this research were listed.

1.2 FUNDAMENTAL PROBLEM

In the recent times, electrical power system network have experienced a quite number of new technologies (Pernkopfa and O'Leary, 2003; Wahab and Saidin, 2003) that have automated most of its major functions in a more focused commercial environment. Quality control and part inspection have done considerably well in the area of manufacturing but not yet gotten to its automated thermal imaging technology application.

Conventionally, preventive maintenance works were carried out on intensive direct-contact approaches. These conventional direct-contact methods of preventive maintenance works were based on physical contact to electrical equipment and components, which could be dangerous. Electrical power engineering systems like other engineering fields got its own hazards such as electrocution emanating from faulty electrical power equipment and components. In order to reduce the associated risk of electrocution due to direct-contact during testing and inspection on electrical power equipment and components, the use of thermal imaging technology provides a valuable solution. In addition, preventive maintenance works involving physical contact to electrical power equipment and components, requires that all equipment in operation should be de-energized before the commencement of testing and inspection. With

thermal imaging technology for preventive maintenance checks, testing and inspection at all levels and at all times gives reliable results without shutting down equipment in operation. In situations where a large number of equipment and components need to be tested or inspected, conventional direct-contact methods use statistical quality control system. The quality, efficiency and durability of all entire equipment is defined by a process of statistical inference drawn from the inspection and testing of a sample population of equipment and components taken from a number of equipment and components. Thermal imaging technology proves another good advantage of her ability to capture a wider view of objects at the same time detecting defective parts. Conventional direct-contact methods of testing and inspection of electrical power equipment and components usually done by a team of human inspectors that is technically prone to errors due to some inevitable situations like examining equipment and components that physically cannot be reached, very hot, damaged or contaminated and very difficult to shut off. Thermal imaging technology is very insensitive to all these limitations. A teaming number of elites have done some study as conclusively accounted by (Newman and Jain, 1995) even with a clear distinction of testing and inspection task, yet, direct-contact testing and examination can produce maximally 80% efficiency as reported by (Smith, 1993).

Based on the above statistics, conventional physical contact testing and inspection of equipment and components is inefficient, secondly, it is time consuming, and it is by no means cost effective, as the general cost of production increases at the end of the day. Above all, these negative factors; inefficiency or errors arising from conventional direct-contact inspection and testing of equipment has caused lots of industrial hazards leaving most field workers in fears especially in electrical power system engineering. Consequently, McGarry (1984) in his research discovered that delivery of poor quality finished products could cause a drop between 10% and 15% of total sales and 20% of manufactured equipment. Considering the whelming challenging nature of global end users and its expectation for higher targets of quality at constant devaluation state, producers can no longer implement the conventional method of testing and inspection. In view of this, this research project proposes a system known as Defect Detection on electrical equipment using thermal imaging technology and RGB optimal threshold algorithm to increase the level of safety assurance of electrical

equipment inspectors during testing and inspection periods, to speed up defect detection and analysis evaluation report from preventive maintenance checks.

1.3 RESEARCH PROBLEM ADDRESSED TO ELECTRICAL EQUIPMENT

With little or no doubts, electrical power equipment has formed the most vital constituent portion of human existence as it cuts across virtually every expect of human activity directly or indirectly. At industrial and domestic homes, it is most needed. Electrical power equipment ranging from heavy duty or high voltage down to lightweight or low voltage are all consumables hence degradation occurs on them per seconds in use.

Until now, there is no statistical record reporting the number of electrical equipment or components consumed on a daily basis. This is to say that among all the human consumables, electrical components and equipment are on the highest point of degradation due to the extent to which it is being demanded in the global consumer market. Because of this, testing and inspection, quality management control become more complex usually the bottleneck in manufacturing industries. Seemingly, more electrical components and equipment during either manufacturing or normal routine testing /inspection period, there is the likelihood that many equipment and components may have to be scrapped due to untimely defect detection and inefficiency or errors using direct-contact testing and inspection methods. The effect of this can be minimized to a very low level if a computer aided scrutiny system (automatic) is applied so that defects can be detected timely for appropriate preventive maintenance actions.

Defects occur when a corresponding output result from an input is not realized. More often than not, this is caused by constant undiscovered abnormal thermal dissipation within electrical power system components over a long period. If all electrical power equipment and its components need to be tested and inspected as it were, then direct-contact testing and inspection will no longer be considered as economic. Mair (1988) found out that direct-contact manual testing and inspection contributes to twenty percent (20%) of the total cost of production in the case of industries.

1.4 RECOMMENDED SOLUTION

Srivastava (2010) wrote an article titled "zero defect policy is a culture" he mentioned some techniques companies could adopt in order to improve their products and services. As there is incessantly high consumption and demand rate of electrical products across the globe for manufacturers to render products and services at a considerably low price as well as maintaining the ISO quality standard. In view of this, there is need to apply a computer aided scrutiny system for testing and inspecting all through the production and routine preventive maintenance checks. To override all the disadvantages of using conventional direct-contact inspection and testing methods, amalgamation of non-destructive contactless testing and inspection technique using thermal imaging technology inculcated with the automatic defect scrutiny system becomes more appropriate.

The defect detection on electrical equipment using thermal imaging technology and RGB optimal threshold algorithm will reasonably reduce cost, improve quality of operation of electrical facilities and safety assurance of both factory workers and end users of electrical products. In addition, the innovative application of a programmed system for defect detection on electrical power equipment would substantially cut down the amount of work force required in the testing and inspection section of maintenance department. The large number of unskilled laborers been replaced with just few well-informed competent workers as targeted by the developing and developed countries where employment wages is quite high, and visionary creativity is immensely needed for technological advancement.

Safety and quality are two inseparable contributing factors especially in electrical power systems network because of the inherent electrical hazards that might occur at any giving time if the said factors were not considered with utmost importance. The imperatives of these mentioned factors should by no means be overemphasized. In fact, the ever existing known tagged word *"safety first"* should be amended or be improved to "*quality safety first".* By improving the safety and quality standards of the electrical power systems network, the confidence in using electrical appliances or equipment both in domestic homes and at manufacturing industries would be

significantly increased and prices of finished products will be relatively low. Because there will be little or no cases of factory rejects, rework, unnecessary warranty and repair cost.

1.5 OBJECTIVES OF RESEARCH PROJECT

- To study the thermal characteristics and the impact of thermal radiation on electrical equipment.
- To design thermal imaging system that will identify parts of defective components and make a fault decision.
- To compare results of proposed RGB Optimal threshold algorithm with K-mean clustering algorithm.
- To compare the real time thermal defect measurement with the international thermal evaluation standard and prepare an enhanced situation report for proper repair and maintenance action.

1.6 SCOPE OF RESEARCH PROJECT

The following operations have been set up in order to accomplish the aim of this project: In this project, an overview of electrical equipment defect detection and vision system will be presented as background knowledge and understanding of the problem. The methodology to solve problems only pertinent and necessary facts in image processing technology will be elaborately discussed as it applies in this present research work.

As outlined in the objectives, this project also requires developing a system that will non-destructively detect anomalies in electrical power equipment and components such as overloaded transformers, loose contact also known as loose connections, load unbalancing, improper material insulation, overloading, short circuit and other similar electrical problems. The automated scrutiny system will identify, classify and make a decision on the captured thermal images of electrical power equipment. Development of the proposed scrutiny system is based on RGB optimal thresholding technique and germane choices available in the Matlab image processing toolbox will be used.

Real time thermal images of equipment and components within University Malaysia Pahang (UMP) environment, Kuala Lumpur and Pahang electrical power distribution substations as well as laboratory experimental setup and few online data are used. Procedures and processes of acquiring data for analysis will also be discussed in detail in the subsequent chapters.

1.7 THESIS OUTLINE

This thesis consists of five chapters. Chapter 2, describes an overview about effect of thermal radiation on electrical power equipment and components, review of previous researches on defect detection techniques using image processing technology. The advantages, disadvantages and applications of thermal imaging technology in both domestic and manufacturing industries will also be looked into. It also discusses different kind of defects in electrical equipment and components and current procedure of testing and inspection and ideas to control thermal defects. Overview on human vision and computer vision will also be briefly mentioned as well as their application in contemporary manufacturing industries. Chapter 3, deliberates on the development of defect detection using thermal imaging technology and RGB optimal thresholding technique. Chapter 4, presents the results and discussions. Finally, chapter 5, summarizes the findings of the research and listed the future research that will be needed to tackle the shortcomings of this work.

CHAPTER 2

LITERATURE REVIEW

2.1 INTRODUCTION

This chapter deliberates on a general survey of defect detection on electrical power equipment as foreknowledge of thermal characteristics of electrical power equipment, systematic procedures of how anomalies are being identified on electrical power equipment using thermography technology. Then, it is followed by definitions of some terminologies commonly applied in thermal imaging technology. This deliberation was aimed at taking a closer study of electrical power equipment thermal characteristics, explaining the potentiality of the present technique towards making sure that all electrical power equipment and components are free from hazards due to defects. In addition, this chapter presents reviews of previous researches related to this project. Lastly, a brief introduction of the proposed research project is given.

2.2 TERMINOLOGY

The ability of a thermographer to view and detect variation within the ambient temperature of the equipment and predict its profile or working status lies solely on the effective use of thermal camera, which is characterized by its ability to produce the infrared thermal image of the equipment in question. Other areas where thermal characteristics of an infrared thermal camera can be seen are in routine testing and inspection checks, preventive or predictive maintenance operation, loose electrical connections, overloaded electric motors, electric transformers, load unbalancing, improper material insulation, short circuits and other applications where the change of temperature reveals unacceptable thermal signatures. For a comprehensive study and

understanding of thermal characteristics of electrical equipment, there is need to note some thermography terms briefly explained in the next subsections.

2.3 WHAT IS THERMOGRAPHY?

Following the basic understanding of thermography using specially designed camera to detect and capture images of the heat emitted by objects. Unlike the normal digital cameras that capture images of visible light, that is reflected by objects; thermal cameras create pictures of heat essentially measuring infrared energy and convert the data into corresponding images of temperature.

2.4 WHY THERMOGRAPHY IS IMPORTANT?

Thermographic cameras or thermal imagers allow us to obtain infrared images. This provides fast, safe and accurate measurements of objects that are:

- Moving or very hot
- Difficult to reach
- Impossible to shut off
- Dangerous to contact

Thermal images can also be obtained in situations where contact to damaged or contaminated object or change the temperature of the object is very difficult.

2.5 QUALITIES OF A GOOD INFRARED THERMAL IMAGE

In order to have a good quality infrared thermal image, some basic thermal image acquisition rules and techniques should be considered before the actual morphological operation takes place. These rules are briefly explained. A good infrared thermal image should have following qualities such as:

- Focus
- Thermal Level
- Thermal span
- Thermal range
- Perspective

- Composition and
- Palette

Considering all these points, there will be little or no flawed images. False positive images that are so common in thermal images will be significantly reduced; hence, quality images are acquired.

Focus: A well-focused thermographic image provides clarity and details that cannot be seen in an unfocused image. This is a very important step in taking a quality IRT image and cannot be changed after the image has been saved.

Thermal level: This is equivalent of brightness in a normal photograph.

Thermal span: This is similar to contrast in a normal photograph. (Thermal range is the same the temperature range of the imager).

Perspective: This tells about the proper or accurate distance at which an image or object can be viewed and acquired yet covering all the meaningful targeted information.

Composition: A quality image should have an even mixture or equal proportion of all the constituent part that make up the whole image.

Palette: This is about the color combination that forms an image.

2.6 THE ELECTROMAGNETIC SPECTRUM

This refers to the four ranges of frequencies that characterize energy for example microwaves, light waves, x-rays and infrared radiation. The fluke thermal imager detects long wave infrared radiation in the 7.5 to 14 micron range. The lens and the detector rays are specially designed to take advantage of this long band, which is preferred for maintenance application.

2.7 INFRARED RADIATION

Infrared radiation is a form of electromagnetic energy that is radiated by all objects on earth in proportion to their temperatures. All infrared cameras and thermometers, detects this infrared radiation, which is also known as *radiant heat*. As objects become warmer, it radiates more energy, which the camera sees and converts, to a thermal image or thermogram. Some thermal imagers convert thermal information into a radiometric temperature measurement that provides tens to hundreds of thousands

of independent temperature values in each thermal image, depending upon the capabilities of the specific thermal imager.

2.8 RADIOMETRIC TEMPERATURES

Thermal imager measures the total temperatures coming from a surface this includes, radiation that is emitted by the object, reflected by the object and transmitted by the object. However, only emitted radiation relates to the actual temperature of the object, the reflected and transmitted temperatures produces false or incorrect object's temperature.

2.9 REFLECTIVITY

To capture an accurate object's temperature, it is important to consider reflectivity. Objects with low-emissivity are at the same time-highly reflective of their thermal surroundings. Many materials are highly reflective to infrared radiation. Note; that the reflected energy the imager sees is not related to the actual temperature of the object.

2.10 AMBIENT TEMPERATURE

Ambient temperature settings can be changed using the smartview software. In some situations, reflected objects, such as machines, furnaces, or other heat sources have a temperature much higher than that of the target. In some other cases, the reflected temperature may be lower than the target. Example, when a clear sky is reflected, it is always cold irrespective of the season.

2.11 REVIEW OF THERMAL DEFECT DETECTION ANALYSIS

Thermal imaging technology in recent years has gained lots of recognition in the field of engineering for detection of anomalies on equipment. Current researches in image processing technology have shown interest in the development of automatic scrutiny systems using thermographic technology. This is because of the robustness and

speed of defect detection analysis compared to the conventional method of testing, inspection and preventive/predictive maintenance. Numerous image formats have been used in detecting abnormalities in electrical equipment such as infrared thermal image, X-ray image, binary, grayscale images and other image formats. In addition, algorithms have been developed such as threshold operation, statistical inference, histogram calculation, and other image processing techniques. Procedures used in scrutinizing defective components can be classified into five stages thus; image acquisition, preprocessing, segmentation, classification and decision-making. This subsection reviews some defect detection techniques on electrical equipment using various forms of image analysis approaches in detecting and in making decisions on the severity of anomalies. Some advantages and disadvantages of these approaches are also elaborated.

Typical fault localization in connectors, relays, switches and transformer tap changers. Defects in these components occur within the contact points because of poorly secured, corroded, or current-overloaded hardware. Within semiconductors such as transistors, microprocessors, integrated circuits (ICs) and other semiconductor defects are found in poorly bonded, die-attached, open and shorted circuits, or leaky active devices. In circuit boards for instance, PCBs, Vero boards and direct-wired panels; defects on these circuit boards could be as a result of overstressed components, plated-through holes, poor heat sinks, and bad solder joints. Among discrete components; locate overstressed transformers, capacitors, and resistors. Often, loose contacts or connections and misalignment have been the most reoccurring faults found in electrical power system transmission and distribution lines. In fact, such problems are very difficult to detect by mere visual inspection, especially on steady state or no-load conditions. Martínez and Lagioia (2007) brought data that show thermographic inspection result. They found out that between 1999 and 2005, 48% power distribution system problems that were found in conductors were on loose contact parts and bolted connections, 45% of thermal faults were because of disconnectors and misalignments, rusted and rough or dirty contact joints, while, 7% were on other electrical faults.

Normally, defects are detected when an expected output result of an input is not realized. More often than not, this is caused by constant undiscovered abnormal thermal dissipation within electrical power system components over a certain period.

Consequently, electrical components suffer low life expectancy rates due to less attention to undesirable thermal radiations. This has become a case study to heat management researchers in electrical power systems engineering. Electric power components that have a temperature of operation above absolute zero emit infrared radiation. This radiation can be measured on the infrared spectral band of the electromagnetic spectrum produced by infrared thermal imaging technology. Awareness of thermal radiations' effect will go a long way in attenuating the alarming rate of defects on electrical components. However, this plays a vital role in stack performance, durability and overall system efficiency (Matian et al., 2010).

The electrical component failures can be avoided if the temperature threshold is detected in order to take timely corrective action. Generally, heat in electrical equipment occurs mainly due to the current increasing (I^2R) and in some cases in the form of free convection during a temperature or current dependent component variation on the internal and external surfaces of the stack fibers under different electrical loads and environmental conditions (Rada et al., 2008).

In many manufacturing operations, electrical power systems engineering has been the fundamental pillars whose contributions cannot be overemphasized. An unexpected failure of even a minor piece of component could have a major impact on production. Since nearly every component or equipment gets hot before it fails, non-destructive thermal inspection is a valuable and cost-effective diagnostic tool with many industrial applications, (NDT Resources Center). Adequate preventive or predictive maintenance culture is important in manufacturing industries to ensure smooth running of their production lines. However, provision of proper maintenance for many components has been the key objective for every manufacturing company, but the actualization of such a target has always suffered near-success-syndrome. Therefore, the strategies for proper maintenance of equipment are classified under these conditions thus; when equipment malfunctions, time–dependent, and status-dependent maintenance (Ying-Chieh and Yao, 2009). The most popular one is status-dependent maintenance, also known as preventive or predictive maintenance (Aksyonov el at., 1999).

Using infrared thermography of electrical equipment and components as a non-invasive adjunctive diagnostic methodology for defect detection on electrical equipment have given thermal imaging technology an edge over other fault detection technology. Other advantages of thermal imaging technology are contact-less, easy interpretation of thermal data, wide coverage of inspection, freedom from dangerous radiation, and robustness. More applications are in accurate measurements of objects that are moving, very hot, difficult to reach, impossible to shut off, dangerous to contact, also obtain thermal images in situations where contact with damaged or contaminated object, or change in temperature of the object is very difficult. Above all, this technology has been successfully used to solve many industrial problems (Lee, 2011; Heriansyah and Abu-Bakar, 2009; Cao el at., 2008; Grys, 2012; Chan el at., 1995).

Jabri el at., 2010, in their research work also reported that Infrared thermography technology is a robust non-destructive inspection technique. The inspection can be conducted efficiently by keeping a distance from the inspected equipment considering the specified minimum distance for focus of 15 centimeters or 6 inches (thermal-imaging-blog.com). There is no point halting equipment under operation for the purpose of inspection, because the collection of information for inspection is done through telemetrograph, therefore, harmful operations due to testing and inspection can be prevented. For these reasons, infrared thermography is widely used for many applications involving preventive or predictive maintenance work (Braunovic el at., 2007).

Experiment on infrared radiation was first conducted by William Herschel in 1800; it was proved that there were forms of lights that are invisible to the eyes of human beings (Chuck, H. 2001; Stojcevski and Kalam, 2010). This kind of radiation can be measured on the infrared thermal spectral band of the electromagnetic spectrum ranging from about 1mm down to 750 nm. Any equipment, operating at a temperature above absolute zero, certainly radiates infrared energy proportional to its surface temperature. Images within this range of electromagnetic spectra are not visible to human eyes. Therefore, a specially designed tool known as thermal camera or thermal imager is required to create pictures of heat essentially measuring infrared energy and convert the data into corresponding images of temperatures permissibly compatible to

human eyes to understand the internal status of electrical components. Thermal camera is characterized by its ability to capture an image of the thermal pattern and measures the emissive power of a surface in an area at various thermal ranges. Thermogram is the digital image produced by the infrared thermal camera. One pixel of a thermogram has a specific temperature value (more details in chapter 3), and contrast of the image is derived from the surface temperature gradient.

X-ray is another type of electromagnetic wave having a wavelength shorter than infrared wave. X-ray imaging technology is a diagnostic tool popularly used in medical fields for detecting abnormalities in human systems and contamination in food items (Butz el at., 2005; Graves el at., 1998; Abbott el at., 1997; J.A. Abbott. 1999; Jha and Matsuoka 2000; Graves el at., 1994; Wagner. 1987; Jayas el at., 2004; Chen el at., 2003; Lim and Barigou. 2004). A good literature study done by M. Edwards in his book D.F. Bodies in Food. (2007) reviews various detection technologies thus metal detectors, magnets, optical systems, microwave reflectance, nuclear magnetic resonance (NMR), radar, electrical impedance, ultrasound, and X-rays (Ronald el at., 2008).

New inventions prove the application of X-ray image in detecting anomalies on electrical power components base on digital silhouette technology and digital subtraction angiography. The combination of these two techniques is used in detecting defects in the scanned X-ray image of electrical power components. Its mode of operation is that it can get the X-rays before the vascular injection in the check parts, which is called mask image denoted by $r(x, y)$. Then after the injection vascular in the same parts of the X-ray image, another image is produced called surplus pieces also known as live image. The digitalized live image produces an output image represented as $d(x, y)$. The available silhouette obtained between the mask and the live image, contains only the characteristics of digital silhouette images of vascular as reported by Jin Li el at. (2012). It was evident that the digital silhouette and digital subtraction angiography technology were useful during the preprocessing/enhancement stage of image analysis to eliminate background interference between two images. This method neither shows the cause of defect nor identifies the part of affected components in an electrical power network system. Therefore, it is not an effective method of defect detection on electrical equipment. Secondly, the X-ray Imager presents its captured

image in gray scale level only and tells nothing about equipment or component temperature. Since nearly every component or equipment gets hot before it fails (NDT Resources Centers) therefore, X-ray Imager might not be an effective tool for defect detection on electrical equipment that has thermal problems.

This image processing operation used images taken from thermal cameras for defect detection normally take place under the auspices of image segmentation operation. The operation is confirmed by machines for machine vision or computers for computer vision applications. Image segmentation is an important task in machine and computer vision applications. The success of image vision analysis or operations is highly dependent upon the success of the autonomous segmentation of an object or an image. There are two approaches of image segmentation namely; discontinuity-based image segmentation and similarity-based image segmentation. In the discontinuity-based image segmentation approach, the subdivision or partition is based on some abrupt changes in the intensity level of an image or gray levels of an image. This image segmentation approach involves identification of isolated points, lines, and edges. An edge is a boundary between two regions in an image having distinct intensity or gray levels. Similarity-based image segmentation approach involves an idea of grouping those pixels in an image which are similar in some sense. There are three approaches under similarity based image segmentation: thresholding, region growing, and region splitting and merging techniques. Under the thresholding technique, there are four different types of thresholding operations: global, dynamic or adaptive, optimal, and local thresholding operations. The simplest approach under similarity based image segmentation approach is thresholding technique (Dong el at., 2008; Shah-Hosseini and Safabakhsh 2002; Lie. 1995; Sezgin and Sankur. 2004; Meola 2007; Chang el at 1997; Tao el at., 1997; Yong Wu el at., 2005; Sezgin and Sankd 2001). Because of its simplicity and fast computational result, the application of thresholding technique becomes more useful (Ning el at., 2010).

Many researchers like Thiruganam el at., (2010); Yingzi Du el at., (2004); Boberg 2008; Liu (2009) has applied Otsu thresholding methods for defect detection using image segmentation process. The Otsu's global thresholding technique has been used because of its simplicity and low computational cost. Segmentation using Otsu

method is based on calculations of the given first and second order moments. However, the Otsu method is insensitive in detecting objects in the neighborhood of the processed image so it cannot give detailed analysis of defective equipment. Sauvola's local thresholding technique attempts to solve the problem associated with Otsu's technique by calculating the local threshold *t(x,y)* from local average *m(x,y)* and the standard deviation *s(x,y)* (Shafaita el at., 2008; Mat Som el at., 2011; Jia Li el at., 2000). This method could have offered a solution but it takes a long computational time. In both thresholding techniques (Otsu's global and Sauvola's local), the input image is in grayscale level and the output is in the binary scale which is not very intuitive compared to the RGB color space input and output result.

K-means clustering algorithm and fuzzy C-means algorithm was used for color image segmentation and the feature extraction was unsupervised. Experimental results have shown that K-means algorithm is insensitive to the number of regions segmented and blocks in each cluster do not have to be neighboring blocks (Chitade and Katiyar 2010; Tavakol el at., 2008). This algorithm is insensitive to situations where attention to specific regions of interest is needed such as in electrical component defect detection, there were unnecessary repetitions and some regions were not segmented, above all, it is not time effective.

Suprathreshold Stochastic Resonance tends to solve the problem of K- means clustering algorithm by being sensitive to object size and position. The multi-object, multi-color image, input RGB color images with different color background were processed using bit-wise logical *OR* and *AND* operators. This operation provides the maximum connected regions of the object in the input noisy, blurred image corresponding to noise standard deviation one. Logical bit-wise *ANDing* of all R, G, and B frames together provides common segmented regions (Kumar Jha el at., 2010). However, the bit-wise *OR* and *AND* logical operator used for RGB images produced segmented binary output images more or less like Otsu's global and Sauvola's local thresholding method. This segmentation method is for extraction of objects from noise and varying intensity levels and cannot be implemented in electrical equipment defects detections.

There are many improvements in defect detection using image processing technology. Nowadays, some articulated researchers have automated the approach towards ensuring easy and fast means of finding faults in electrical power systems through image processing algorithms. Chou and Yao (2009) did some good work using thermographic technology to automate defect detection on electrical equipment. Their proposed system is based on the principle of Otsu's statistical threshold selection algorithm using gray-level histograms. The morphological algorithm adopted in their analysis was based on reference temperature of the equipment having similar loads and similar environmental conditions. Certainly, this system will find it difficult to operate in situations where there is no reference temperature. Therefore, defect detection using this algorithm is partial.

On the other hand, there were other approaches used in determining the thermal severity of electrical equipment. The qualitative analysis method is one of the techniques applied to estimate the maintenance priorities. This method can directly interpret and evaluate the severity of equipment hotspot temperature based on temperature difference between similar equipment (ΔT) criteria. The disadvantage of qualitative method is that ΔT criterion does not indicate the exceeded equipment's temperature limits. However, in quantitative method, as the reference temperature has to be measured, it requires a greater understanding of the variables influencing the radiometric measurement, as well as its limitations such as keeping a minimum distance for focusing, emissivity correction, ambient temperature correction, and distance to spot size ratio, among other quantitative measurement factors (Shawal el at., 2011).

Calculating the histogram distance is another method for finding the similarity between two objects. In this case, the histogram for each evaluated region is compared with another region in order to obtain the ΔT value. This method is good if bigger image is involved otherwise, there will be a problem if the image is very small. (Wretman, 2006).

Various threshold techniques have been used over years in the field of image processing technology. Among all the widely used threshold methods, the RGB optimal threshold method was rarely applied. Meanwhile some research work has been done.

Hideaki Sato el at. (2003) applied thresholds decision method for fast object detection system. On their approach, object extraction is based on a threshold value adjustment that is at the threshold is adjusted object color changes. For this purpose, two threshold values were necessary for object extraction; upper and lower thresholds. These upper and lower thresholds of RGB were determined simultaneously by using real-coded genetic algorithm and two fitness functions were applied to the optimization of the RGB color thresholds, and initial population of individual chromosomes which contains the RGB values was generated with color histograms for fast object detection. They found out that in two color thresholds, the extracted object contains less noise compared with single color threshold. There could be a better result if a three color threshold is applied.

Youngbae Hwang el at. (2006) also applied optimal threshold operation for determination of color space for accurate change detection. They were able to figure out that the threshold for RGB is nearly optimal because it has the almost the same amount of missing pixels and extra pixels. Stokman and Gever (2005) proposed a selection framework for a color model using the principles of diversification for image segmentation and edge detection. By means of statistical formulation and learning schemes, they found the optimal color channels and their weights. Wesolkowski S. et al. (2000) presented a comparison of color image edge detectors in multiple color spaces. Edge detectors such as the Sobel operator are evaluated against multiple color spaces.

Kaur and Sinha (2012) proposed an automated localization of optic disc and macula from fungus images using an RGB optimal threshold algorithm. Their idea was to detect retinal images of patients at different stages of retinopathy through iterative optimal threshold selection method by considering connected component analysis in disc localization necessary for the proper detection of exudates and for knowing the severity of the diabetic maculopathy.

Zhan and Yang (2012) proposed a real time and automatic vehicle type recognition system design and its application using an RGB optimal threshold algorithm. They got their RGB image segmented by calculating global optimal threshold and calculating binarization image through global optimal threshold value. Hari Kumar Singh el at. (2012) reviewed thresholding techniques applied for

segmentation of RGB and multispectral images. They segmented an RGB image and a multispectral image using iterative threshold techniques, Otsu's threshold technique, and local threshold technique. They concluded that the Otsu's method does not give any result when it is applied to multispectral image, but may be applied to other mono-spectral and RGB Images.

Funck, J.W., el at. (2003) reviewed the relevance of color image processing algorithm in wood defect detection. They pointed out that the use of color space (RGB, CILab and CILuv or CILuc) defect detection algorithm produces better defect detection results than thresholding and clustering algorithms using grayscale. Butler et al. (1989) showed that the use of RGB color information increased pixel-based defect detection accuracy for some subtle defects by over 20% points compared to grayscale accuracy. The use of all the three-color components could be expensive as a result; Brunner et al. (1992) and Conners et al. (1985) reported that almost all of the useful information could be stored in two of the three-color components in order to make the defect detection process both time and cost effective. Consequently, the same two color dimensions were found with flaw results across most wood features.

Željko Hocenski el at. (2006) gave an analysis result of the improved canny edge detector in ceramic tiles defect detection. In their approach, three types of threshold methods (quick and specialized good valley among the lobes of histogram, minimum cross entropy and histogram subtraction) were carried out on 20 RGB images of tiles supposedly with edge defects. For optimization, threshold parameters were manually adjusted further more, five smoothing operations were also applied (simple blur, simple blur without scaling, Gaussian smoothing, median blur and bilateral blur) in the end, very similar results were achieved.

Destain el at. (1998) proposed defects segmentation on 'Golden Delicious' apples by using color machine vision. This group of researchers came up with an algorithm that used all the three-color channels (RGB) which most researchers fail to apply. Eighty (80) samples of apples were tested with their algorithm consisting of three steps. The first is coarse defect segmentation based on a statistical comparison between the color of an individual pixel and the global color of the fruit, next is based either on a

global or on a local approach for defect detection. The (optimization) process was not clearly specified but, some expected results were shown.

To summarize this chapter, some published research literatures which are similar in some sense with the proposed technique are presented below;

Jin Li el at. (2012) proposed defect detection on electrical equipment in X-ray image using digital silhouette and digital subtraction angiography technology. It is good for elimination of background interference between two images. But not thorough on defect isolation.

Thiruganam el at., (2010); Yingzi Du el at., (2004); Boberg 2008; Liu, 2009 has applied Otsu thresholding methods for defect detection using image segmentation process. Otsu method is simple and cheap but insensitive in detecting objects in the neighborhood because it is based on histogram modal analysis.

Shafaita el at., 2008; Mat Som el at., 2011; Jia Li el at., 2000 applied Sauvola's local thresholding technique attempts to solve the problem associated with Otsu's technique by calculating the local threshold and the standard deviation. This method could have offered a solution but it takes a long computational time.

Chitade and Katiyar 2010; applied K-means clustering algorithms for automatic defect detection using color image. Experimental results showed that K-means algorithm produces empty clusters at high iteration and there is problem of segmentation of specific regions of interest. Because of this, evaluation report becomes very bothersome and unintuitive. Tavakol el at., 2008 also used fuzzy C-means algorithm to solve the problem of K-means clustering algorithm by not producing empty clusters even at high iteration, but there is problem of segmentation to specific regions of interest as well.

Wretman, 2006 used histogram distance to calculate and find the similarity between two objects. This method is good if bigger image is involved otherwise, there will be a problem if the image is very small.

Shawal El art., 2011 applied qualitative analysis technique to estimate the maintenance priorities by directly interpret and evaluate the severity of equipment hotspot temperature based on ΔT criteria. But does not indicate the exceeded equipment's temperature limits. Quantitative method provides the reference temperatures but it is not time effective as it requires a greater understanding of the variables influencing the radiometric measurement.

Chan el at., (2000) proposed a three-dimensional thermal imaging for power equipment monitoring. They designed a 3D thermal inspection that makes it easy to understand the geometrical structure and the surface temperature of equipment by swapping between the geometrical model and the thermal model. The key techniques involve a true regeneration of the 3D surfaces of the equipment using absolute dimensioning, based on on-site measurements and the integration of thermal images with the regenerated 3D surfaces. The surface of the object under measurement is divided into grid points whose absolute coordinates are measured with the aid of a laser-based distance measuring kit, the DMK. The piece of black wire is the RS-232 communication cord for communication with a PC. Panning and tilting functions are offered to the DMK by an assembly of two stepper motors. The horizontal and vertical angles of the assembly are controlled by the PC. The major problem here is with the correspondence between the DMK and the thermal system, that is matching every point sensed by the DMK onto a corresponding point on the thermal image. Secondly, getting clear optical and thermal images of target spots requires adequate space in front of the target. Therefore, this system is not quite applicable to very small plant room or under the condition that one or more faces of the equipment are close to the wall. The thermal image acquired by the system will be flawed if the surface of the target is not flat and smooth enough. Another issue is that the whole process is computationally intensive, demanding a very high-graded PC and time consuming as it takes hours to scan a piece of equipment. The hardware (including the thermal imager, the distance measuring kit and the PC) is reasonably expensive. Finally, only skillful technicians are required to operate the whole system to obtain vivid 3D images of high quality for further analysis.

Chou and Yao, 2009 did some good work using thermographic technology to automate defect detection on electrical equipments. Their proposed system is based on the principle of Otsu's statistical threshold selection algorithm using gray-level histograms. The morphological algorithm adopted in their analysis was based on reference temperature of equipments having similar loads and similar environmental conditions. Certainly, this system will find it difficult to operate in situations where there is no reference temperature. Therefore, defect detection using this algorithm is partial.

Because of all these backdrops found with those defect detection techniques, brought about this improved method which is by analyzing the thermal gradient of the segmented regions. One of the advantages of using the thermal gradient analysis is that the source of the hotspot (abnormality) that occurred in electrical equipment will be identified. This is done using thermal imaging technology and RGB optimal threshold technique to scrutinize defective electrical equipment. This is an improved system developed to detect defects on electrical equipment and components irrespective of equipment and component reference temperatures. The input data are taken as a thermogram of electrical equipment with different regions of thermal signatures in RGB color space and the output results were in RGB color space that makes this technique more intuitive. This technique is explicitly detailed in chapter 3.

CHAPTER 3

RESEARCH METHODOLOGY

DEFECT DETECTION SYSTEM DESIGN

3.1 INTRODUCTION

An analytical infrared thermography is characterized with a thermogram showing the thermal view and the visible view, as indicated in Figure 3.1. Some of the thermal images captured from real time operating equipment and components include circuit breakers, isolator switches, transformers, fuse boxes, contactors, capacitors, electric motors, resistors, and other electrical power distribution equipment and components.

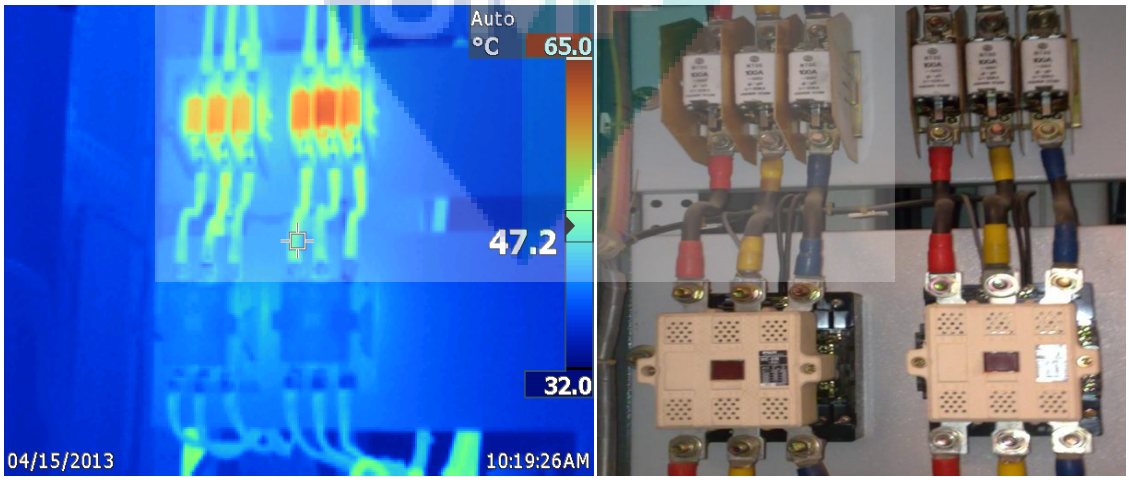

Thermal view and visible view of fuse and contactor

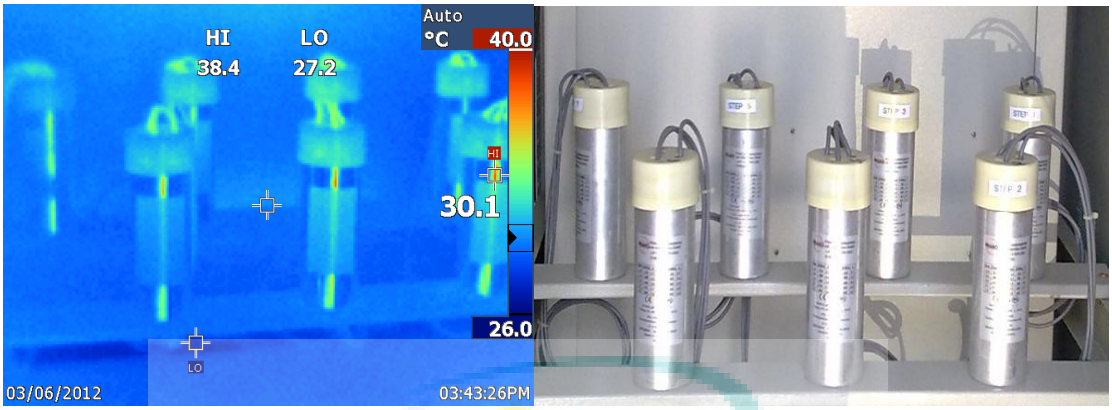

Thermal view and visible view of AC power capacitors

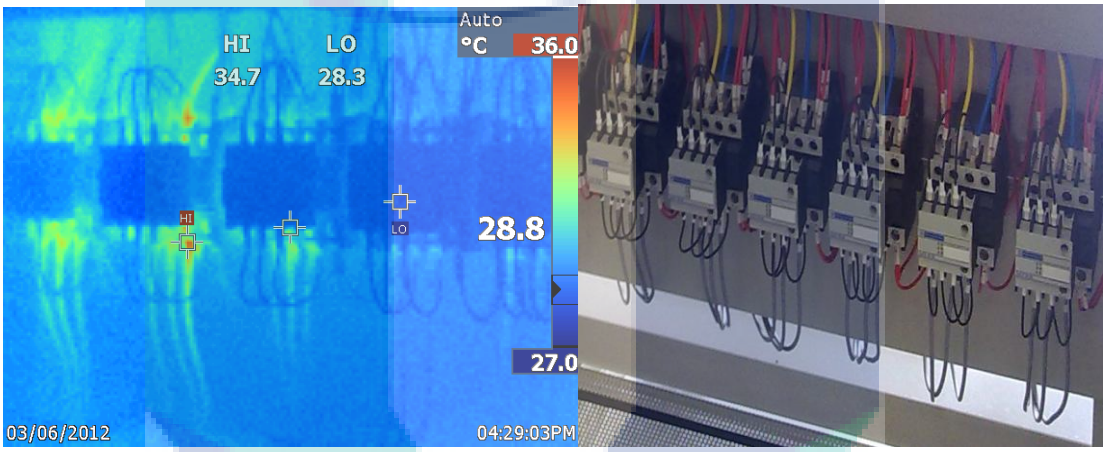

Thermal view and visible view of contactor

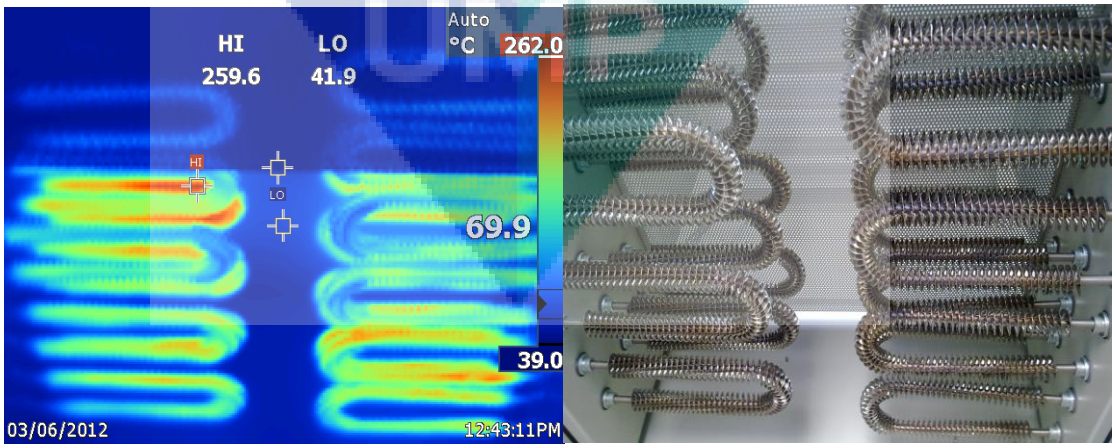

Thermal view and visible view of heating elements (resistors)

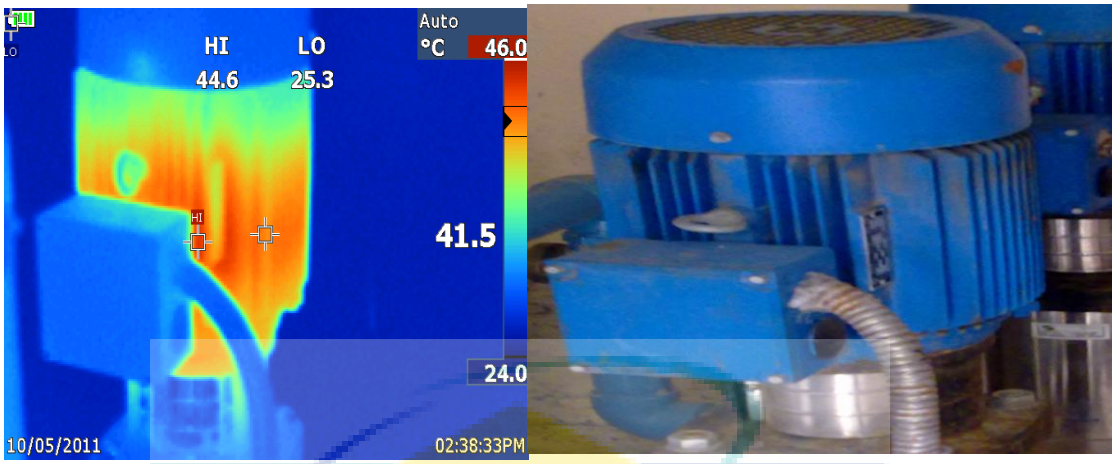

Thermal view and visible view of electric motors

Figure 3.1: visual spectrum photos and normal view of electrical facilities

It is important to acknowledge that infrared thermal imagers have a common limitation which is its inability to measure the internal temperature of enclosed equipment such as transformers, contact point of switches such as relays, circuit breakers, contactors, and all the similar enclosed switchgears. Electric motors are also among this enclosed electrical power equipment. In other words, thermal imagers or cameras can only measure surface temperatures of equipment. Though with acceptable degree of accuracy good enough for the system monitoring and protection, preventive and predictive maintenance operation. "The infrared survey is a great initial screening or detection tool for potential problems, but additional electrical tests should be performed in order to confirm initial conclusions. It is extremely easy to have a false positive thermal image; therefore, other measurements such as millivolt drop tests, current readings, harmonic analysis, power factor, and others should be performed on suspect observations." (Don A. Genutis, 2007).

The case of determining the right ambient air temperature is one of the limitations of infrared thermal imagers which affects the accuracy of thermal inspection. In order to ascertain the ambient air temperature prior to actual equipment thermography operation, the ambient air temperature can be obtained from the emergent environment where the equipment in question is installed such as the walls, roofs, floor and so on. It is also possible to obtain the ambient air temperature based on reference temperatures of similar equipment. In this case one of the similar equipment should be

de-energized while the other is in full operation as shown in Figure 3.2. The thermogram of these electric motors where taking almost at the same time in the same environment under the same atmospheric weather condition. The temperature difference of the targeted spots can be used as the approximated measured ambient air temperature of these electric motors. Obtaining ambient air temperature with thermal imager can be burdensome. Therefore, other radiometric temperature measurements may be required in order to obtain an ambient air temperature of electrical power equipment and components.

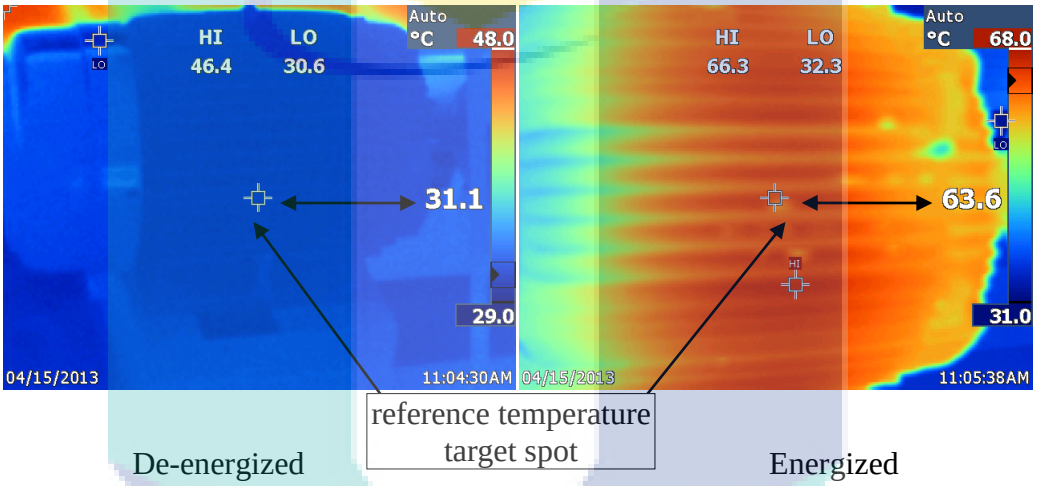

Figure 3.2: Ambient reference temperature from de-energized and energized electric motor thermogram

When thermal images are wrongly captured, the image colors can appear to be too bright or too dark, monotonous or noisy (Vadivel el at., 2003). Infrared thermal images with flaws increases the amount of false positive images that leads to wrong equipment and components evaluation. It is therefore advised by this report that, infrared thermal images should by all means discriminate distinctively between the foregrounds and the backgrounds in order to have a reasonable accuracy level during equipment thermal status evaluation and quantitative analysis process. The procedure is by subtracting the background region from the entire image using image subtraction technique performed in Matlab image processing toolbox. Figure 3.3(a – c) shows examples of backgrounds and foreground images extracted from their original IRT images.

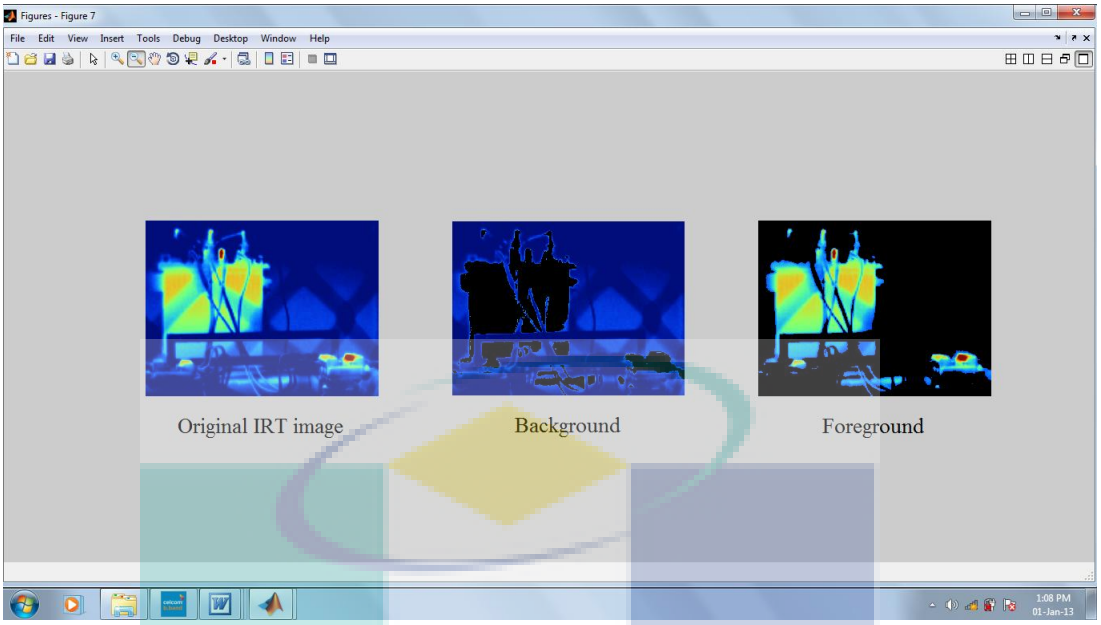

(a)

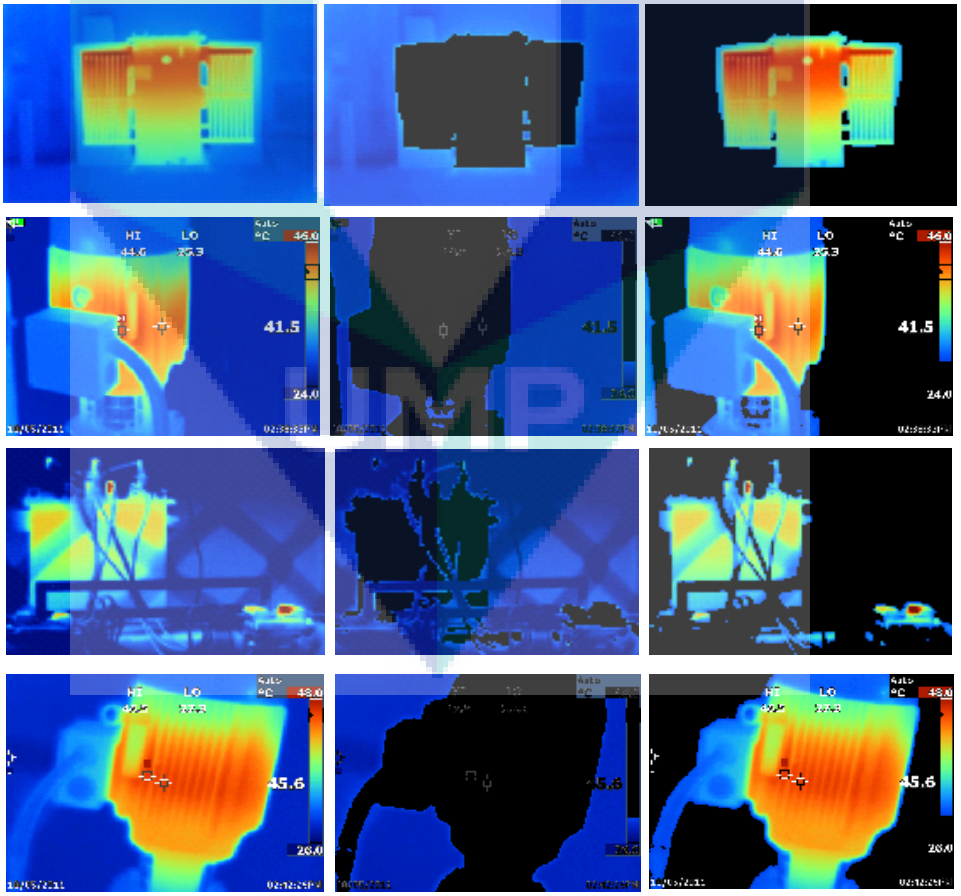

Original IRT image Background Foreground

(c)

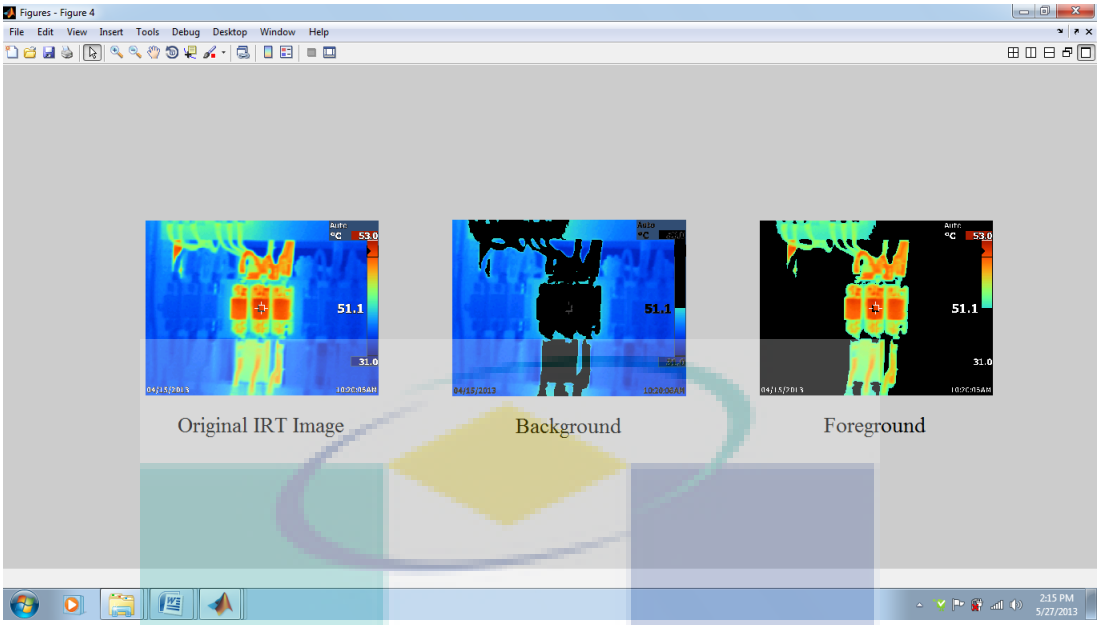

(c)

Figure 3.3: Segments of backgrounds and foregrounds IRT images

Different colors depict corresponding thermal values often shows equipment thermal status at the time of testing and inspection measurements. The thermal pattern of inspected equipment shows the severity of thermal faults. For instance, connectors, relays and switches show thermal abnormalities in the contact points which could be because of poorly secured contacts, corroded surfaces hampering the free flow of electric current, or current overloaded hardware. This research project deliberates on the prevailing thermal issues caused by defective components since it focuses on inspection of electrical equipment and power distribution facilities. In conducting equipment inspection and analyzing its thermal variations (ΔT), this involves taking a closer study of thermal characteristics of electrical equipment. The results of experimental thermal inspections are tabulated, in Table 3.1. Secondly it requires identifying part of defective equipment and components and finally to compare the real time thermal inspection measurement and the mathematical evaluation with the international thermal evaluation standard. (Jim White, 2008; Don A. Genutis, 2007).

Table 3.1: Experimental thermal inspection result

Equipment/ Components	Equipment Rated Temp. (℃)	Approx. Ambient Temp. (℃)	Maximum Temp. Rise (℃)	Measured Temp. (℃)			Measured Average Temp. (℃)
				1st	2nd	3rd	
Low Temperature Equipment/Components							
Molded Case Circuit Breaker	40	30	70	30.9	34.9	33.6	33.1
Miniature Circuit Breaker	30	30	60	32.7	38.1	33.2	34.6
Connector	35	30	65	26.2	27.2	26.3	26.6
Medium Temperature Equipment/Components							
Oil-Immerse Distribution Transformer	60	30	90	38.4	44.8	40.8	41.3
Dry Type Distribution Transformer	60	30	90	33.0	36.4	32.4	33.9
Fuse Box	60	30	90	42.4	61.6	51.1	51.4
Contactor	50	30	80	40.2	47.2	44.3	43.9
High Temperature Equipment/Components							
Power Capacitor	75	30	105	33.3	35.3	34.3	34.4
Electric Motor	75	30	105	64.8	66.3	66.0	65.7

Defect detection processes start from equipment testing and inspection. In this project, testing and inspection are carried out based on the non-contact approach. The non-contact approach is done with the aid of thermal camera or thermal imager which is the major tool used in this research project. The acquired thermal images of inspected electrical equipment and components are processed using the proposed defect detection scrutiny system. This technique which uses infrared thermal image and the RGB optimal threshold algorithm will scan through the thermogram of the inspected electrical equipment and regionalize the thermal gradients in terms of colors. The starting point is acquiring electrical equipment thermogram and transfers it into a

computer. Next is the preprocessing of the electrical equipment thermogram using the pixel equalization method. Pixel equalization is aimed at reducing the effect of lighting to the individual RGB color components thereby normalizing the thermal image and makes it suitable for proper segmentation operation. The next stage is the segmentation operation which involves an iterative procedure. First step is to choose arbitrarily an initial threshold value for the three color components (T_{ir}, T_{ig}, T_{ib}). Using this initial value of threshold, feature extraction algorithm (short circuit OR logic operator) will extract groups of similar pixels. So when segmenting the image using this initial value of threshold, the segmentation will basically partition or divide the image into (N) number of regions or groups of pixels. One group of pixels will be termed as group G_1 and another group of pixels will be termed as group G_2 and G_3 down to group G_N. Here the intensity values in group G_1 will be similar and the intensity value in group G_2 likewise G_3 up to group G_N, but these groups or regions will be different. Once the partitioning or separation of the image pixel intensities into groups or regions G_1, G_2 and G_3 up to G_N. The next operation is classification and decision making which is based on the equipment and components thermal gradients.

Any spot in the colored thermal image has a corresponding thermal value. This will be detailed in the subsequent sub-chapters of this chapter. In order to ascertain the accuracy of the thermal analysis results, reference is made to the international thermal evaluation standard (Infraspection Institute 2008), or from equipment of the same structure and similar features within the same ambient temperature and load condition if possible. The purpose of this scrutiny system is to increase the efficiency of electrical power equipment, to avoid the risk associated with conventional direct-contact defect detection, to reduce the cost due to after breakdown repair and maintenance, to improve the speed of defect detection processes.

3.2 SUPERVISED OPTIMAL THRESHOLD SELECTION TECHNIQUE

Image segmentation processes normally take place under the auspices of image processing operations. A properly segmented IRT image is tested and confirmed by machines for machine vision or computers for computer vision applications. In this

research project, RGB optimal threshold values will be used for segmentation of the IRT images. Image segmentation in its simple definition is a process of subdividing an image into its constituent parts. Subdivision of the image should stop after extraction and classification of all targeted ensemble regions. However, the level of subdivision is application dependant. To achieve improved defect detection accuracy level and reduce the ills of false positive image during the quantitative thermal evaluation, this research project presents the effect of adjusting the threshold values in the color contrast of IRT image, which is in RGB color space to perform segmentation in images that contain luminance. The RGB color space has been widely used for processing color images. This RGB color space describes each color as a weighted combination of three base components Red, Green and Blue. On the other hand, high correlation between components and mixing luminance with chromaticity (contrast) makes it very sensitive to changes in imaging conditions such as lighting. Therefore, normalization of RGB color space reduces the dependence of each color component to the brightness of the pixel (Soriano el at., 2000). To normalize each color component the following equations 3.1 (a, b, c) are used;

$$red = \frac{R}{R+G+B} \tag{3.1a}$$

$$green = \frac{G}{R+G+B} \tag{3.1b}$$

$$blue = \frac{B}{R+G+B} \tag{3.1c}$$

The sum of the normalized components is approximately equal to one which depicts balanced RGB color image. The Figures 3.4 and 3.5 show the nature of non-normalized and normalized infrared thermal image with its respective grayscale images and histograms.

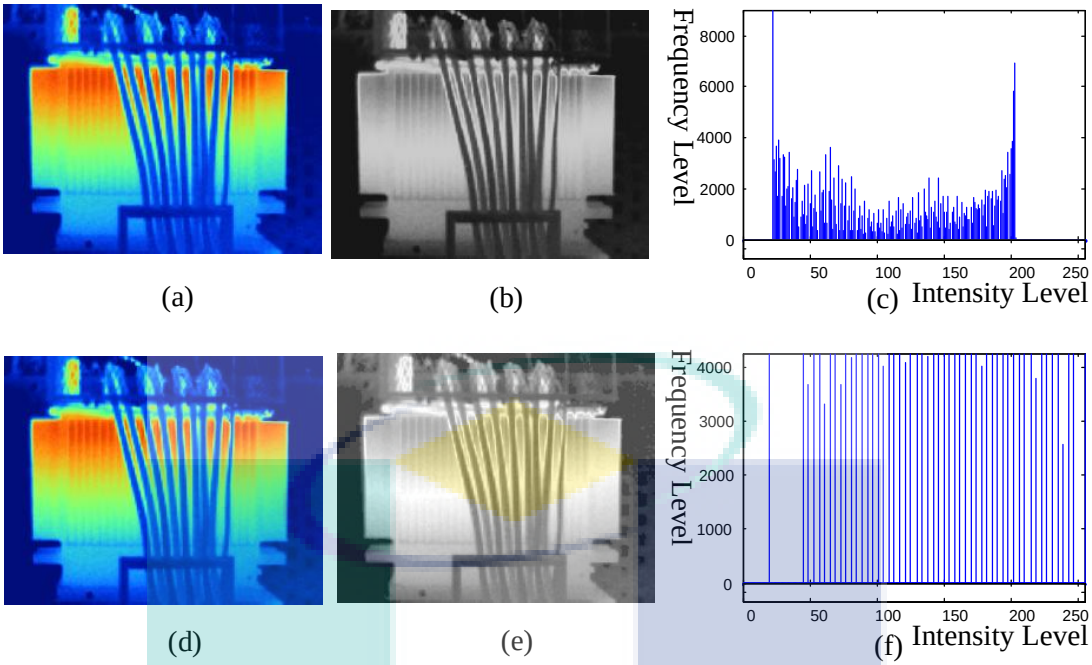

Figure 3.4: Transformer IRT image: (a = Non-normalized IRT image), (b = Non-normalized grayscale IRT image), (c = Non-normalized IRT image histogram), (d = Normalized IRT image), (e = Normalizedgrayscale IRT image), (f = Normalized IRT image histogram)

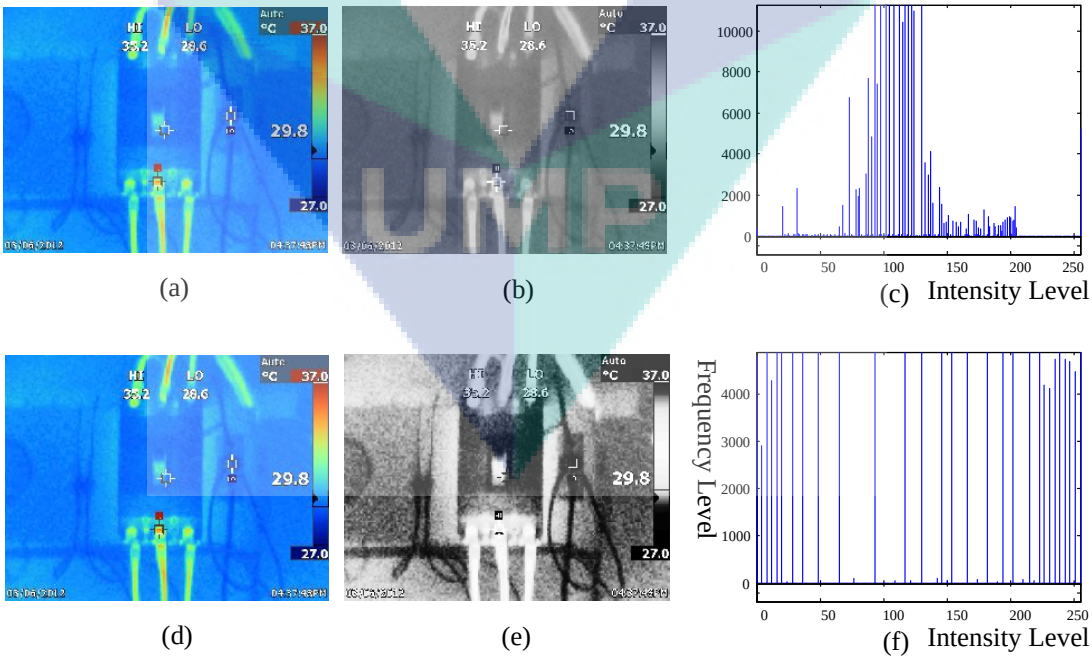

Figure 3.5: Circuit breaker IRT image: (a = Non-normalized IRT image), (b = Non-normalized grayscale IRT image), (c = Non-normalized IRT image histogram), (d = Normalized IRT image), (e = Normalized grayscale IRT image), (f = Normalized IRT image histogram)

The simplicity of RGB color spaces has been the prime reason for their popularity in color image processing. It is quite clear that IRT images of different equipment are more stable in the normalized color space. Considering the independence between the IRT samples of over 100 images, the Gaussian Probability Density Function (GPDF) model can be obtained from the maximum-likelihood criterion (short circuit OR logic operator) in Matlab image processing environment which has an analytical solution in GPDF (Hani, A., el at., 2007). The procedures of determining the RGB threshold values are summarized below;

Step 1, Choose initial threshold values (T_{irgb}) for the RGB colors.

Step 2, Partition the image into groups or regions G_1, G_2 and G_3 up to G_N using the initial threshold values T_{irgb}.

Step 3, Compute the mean μ for the individual RGB colors for G_1, G_2, G_3 and G_N.

Step 4, Compute the variance $\sigma_r^2, \sigma_g^2, \sigma_b^2$; the difference in the intensity value of the RGB colors.

Step 5, Compute the covariance $\sigma_{r,g}^2, \sigma_{r,b}^2, \sigma_{g,b}^2, \sigma_{r,g,b}^2$; the similarity in the intensity value between the RGB colors.

Step 6, Adjust new threshold values T_{rgb} for the RGB colors.

Step 7, Recompute the mean, the variance and the covariance values.

Step 8, Go back to step 2.

So what have been done was choosing the initial value of threshold T_i using this initial value of threshold to threshold the image, by thresholding the image, the intensity value of the image is separated into groups G_1, G_2 and G_3 up to G_N. For group G_1; find out the average intensity value μ_r, for group G_2 find the average intensity value μ_g likewise in the group G_3 the average intensity value μ_b and the rest groups G_N. Then, find the new threshold value T_{rgb}, which is the mean of these average intensity values that is $T_{rgb} = \frac{\mu_r + \mu_g + \mu_b + \mu_{NC}}{N}$, and use this new threshold to threshold the

image again so that these groups G_1, G_2, G_3 and G_N will be modified. Then go on with the iterative process that is from choosing initial threshold to grouping then finding the average intensity values in the N different separate groups and recalculating the variance and covariance. The entire process will be repeated until the variation in the two or more successive iterations in the computed value of T_{rgb} is less than or equal to the specified value of threshold. This operation has to continue until the difference between iteration T_i and iteration T_{i+1} is less than or equal to T-prime (T^I).

That is, $$| T_i - T_{rgb+1} | \leq T^I$$

Therefore once this condition is attained thresholding operation stops. The processes are simple; choose an initial threshold value then go on and modify this threshold value iteratively, until it finally converge to a situation where in two or more subsequent operations the value of the threshold does not change. In that position, the threshold value gotten becomes the final threshold value. These operations are implemented in the Matlab image processing environment.

Morphologically, parameters of mean, variance and covariance are determined from over 100 samples of IRT data of different electrical equipment and components. Equations 3.2 (a, b, c), 3.3 (a, b, c) and 3.4 (a, b, c, d) is used to calculate these parameters. The mean values representing the center of the individual RGB color components that constitutes the IRT color distributions are given in equation 3.2 (a, b, c) (Hani, A., el at., 2007);

$$\mu_r = \sum_{i=1}^{N} \frac{r_i}{N} \tag{3.2a}$$

$$\mu_g = \sum_{i=1}^{N} \frac{g_i}{N} \tag{3.2b}$$

$$\mu_b = \sum_{i=1}^{N} \frac{b_i}{N} \tag{3.2c}$$

Where N is the sum of the pixel intensity value of the IRT image.

The variance values that represent the pixel difference between the RGB colors in IRT image are given in equation 3.3 (a, b, c);

$$\sigma_r^2 = \frac{(r_i - \mu_r)^2}{N} \tag{3.3a}$$

$$\sigma_g^2 = \frac{(g_i - \mu_g)^2}{N} \tag{3.3b}$$

$$\sigma_b^2 = \frac{(b_i - \mu_b)^2}{N} \tag{3.3c}$$

The covariance values that measure similarity of the pixel in the RGB colors of the IRT image is given in equation 3.4 (a, b, c, d);

$$\sigma_{rg}^2 = \frac{(r_i - \mu_r)(g_i - \mu_g)}{N} \tag{3.4a}$$

$$\sigma_{rb}^2 = \frac{(r_i - \mu_r)(b_i - \mu_b)}{N} \tag{3.4b}$$

$$\sigma_{gb}^2 = \frac{(g_i - \mu_g)(b_i - \mu_b)}{N} \tag{3.4c}$$

$$\sigma_{rgb}^2 = \frac{(r_i - \mu_i)(g_i - \mu_i)(b_i - \mu_i)}{N} \tag{3.4d}$$

A multivariate elliptical Gaussia Probability Density Function (GPDF) model which takes the calculated parameters of mean, variance and covariance to represent IRT image color distribution can be found by;

$$f(r,g)=\frac{1}{2\pi}e^{\frac{-(r_i-\mu_r)^2}{2\sigma_r^2}\times\frac{(g_i-\mu_g)^2}{2\sigma_g^2}} \tag{3.5a}$$

$$f(r,b)=\frac{1}{2\pi}e^{\frac{-(r_i-\mu_r)^2}{2\sigma_r^2}\times\frac{(b_i-\mu_b)^2}{2\sigma_b^2}} \tag{3.5b}$$

$$f(g,b)=\frac{1}{2\pi}e^{\frac{-(g_i-\mu_g)^2}{2\sigma_g^2}\times\frac{(b_i-\mu_b)^2}{2\sigma_b^2}} \tag{3.5c}$$

$$f(r,g,b)=\frac{1}{2\pi}e^{\frac{-(r_i-\mu_r)^2}{2\sigma_r^2}\times\frac{(g_i-\mu_g)^2}{2\sigma_g^2}\times\frac{(b_i-\mu_b)^2}{2\sigma_b^2}} \tag{3.5d}$$

Where $f(r,g), f(r,b), f(g,b), f(r,g,b)$ are the IRT color distribution function in GPDF that determines the threshold values T_i (Tayyaba Azim, el at., 2011).

3.3 RGB OPTIMAL THRESHOLD SEGMENTATION ALGORITHM

Segmentation of various regions of IRT image can be achieved using threshold value obtained from GPDF. Since the IRT image is normalized, it is first converted into a grayscale image by joint probabilities in Equation 3.6,

$$P(IRTimage)=P_r\times P_{rg}\times P_g\times P_{gb}\times P_b\times P_{rb} \tag{3.6}$$

Equation (3.6) gives an estimation of likelihood of pixels of individual RGB color components or its combinations (RG, RB, or GB) in IRT image connecting to form regions. These probabilities are calculated as follows: Equations. (3.7), (3.8) and

(43.9) are the probability of segmenting Red pixels, Green pixels, and Blue Pixels in an IRT image.

$$P_{(\frac{IRTimage}{R})} = \frac{1}{2\pi\sigma_r} e^{\frac{-(r_i-\mu_r)^2}{2\sigma_r^2}} \Rightarrow \begin{cases} 1 \;\; if \;\; P_{IRTimage} \geq T_i \\ 0 \;\; if \;\; P_{IRTimage} < T_i \end{cases} \tag{3.7}$$

$$P_{(\frac{IRTimage}{G})} = \frac{1}{2\pi\sigma_g} e^{\frac{-(g_i-\mu_g)^2}{2\sigma_g^2}} \Rightarrow \begin{cases} 1 \;\; if \;\; P_{IRTimage} \geq T_i \\ 0 \;\; if \;\; P_{IRTimage} < T_i \end{cases} \tag{3.8}$$

$$P_{(\frac{IRTimage}{B})} = \frac{1}{2\pi\sigma_b} e^{\frac{-(b_i-\mu_b)^2}{2\sigma_b^2}} \Rightarrow \begin{cases} 1 \;\; if \;\; P_{IRTimage} \geq T_i \\ 0 \;\; if \;\; P_{IRTimage} < T_i \end{cases} \tag{3.9}$$

The output image is $P_{IRTimage/R}$ and the input image is $P_{IRTimage}$; while T_i is the optimal threshold value. This means, if the output image is equal to 1, then all the Red color component or pixels in the input image that is in the range of the optimal threshold value will be segmented otherwise none is found within the range likewise other color components.

Equations (3.10), (3.11), and (3.12) are the probabilities of segmented combinations of two colors, (Red-Green), (Red-Blue), and (Green-Blue) in an IRT image

$$P_{(\frac{IRTimage}{R,G})} = \frac{1}{2\pi\sigma_{r,g}} e^{\frac{-(r_i-\mu_r)(g_i-\mu_g)}{2\sigma_{r,g}^2}} \Rightarrow \begin{cases} 1 \;\; if \;\; P_{IRTimage} \geq T_i \\ 0 \;\; if \;\; P_{IRTimage} < T_i \end{cases} \tag{3.10}$$

$$P_{(\frac{IRTimage}{R,B})} = \frac{1}{2\pi\sigma_{r,b}} e^{\frac{-(r_i-\mu_r)(b_i-\mu_b)}{2\sigma_{r,b}^2}} \Rightarrow \begin{cases} 1 \;\; if \;\; P_{IRTimage} \geq T_i \\ 0 \;\; if \;\; P_{IRTimage} < T_i \end{cases} \tag{3.11}$$

$$P_{\left(\frac{IRTimage}{G,B}\right)} = \frac{1}{2\pi\sigma_{g,b}} e^{\frac{-(g_i-\mu_g)(b_i-\mu_b)}{2\sigma_{g,b}^2}} \Rightarrow \begin{cases} 1 \;\; if \;\; P_{IRTimage} \geq T_i \\ 0 \;\; if \;\; P_{IRTimage} < T_i \end{cases} \qquad (3.12)$$

This means if the output image is equal to 1, then all the pixels in the RGB color combinations (Red-Green), (Red-Blue), and (Green-Blue) in the IRT input image that is in the range of the optimal threshold value will be segmented otherwise none is found within the range

The procedures for determining the optimal threshold value are summarized as follows:

- Select samples of IRT images as in Figure 3.6 (a – f) to train the scrutiny system.
- Calculate the mean, the variance and the covariance of the color distribution in the IRT image; in RGB color space based on equations 3.2 (a, b, c), 3.3 (a, b, c) and 3.4 (a, b, c, d).
- Substitute the calculated parameters into equation 3.5 (a, b, c, d); the Gaussian Probability Distribution Function. Using the optimal thresholding technique (maximum-likelihood criterion) similar pixels are connected into different regions based on chromatic colors (various color contrast) available in the IRT image.

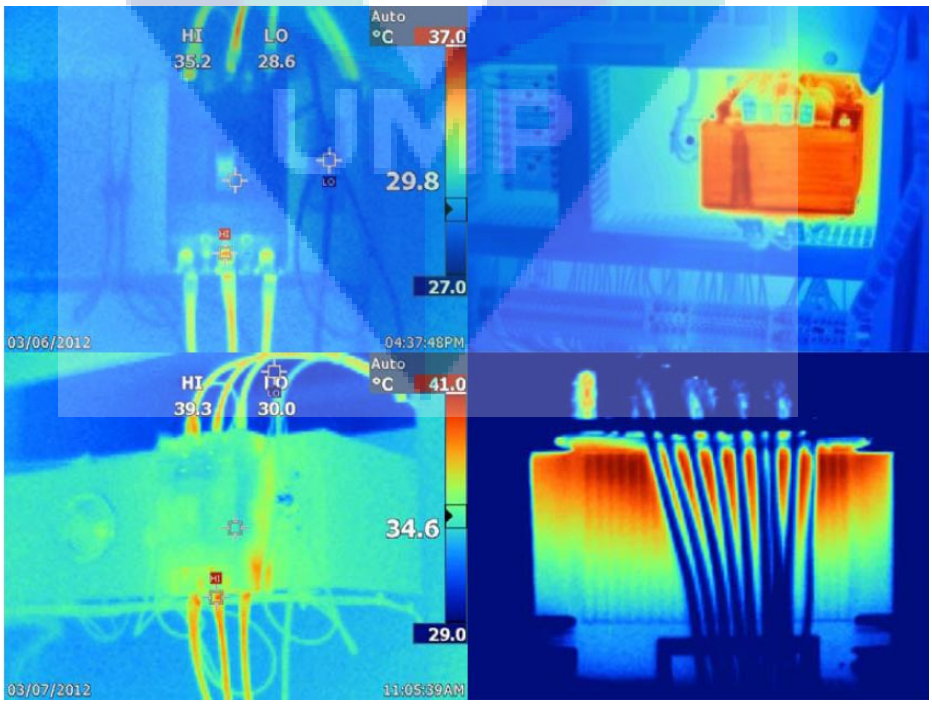

(a)

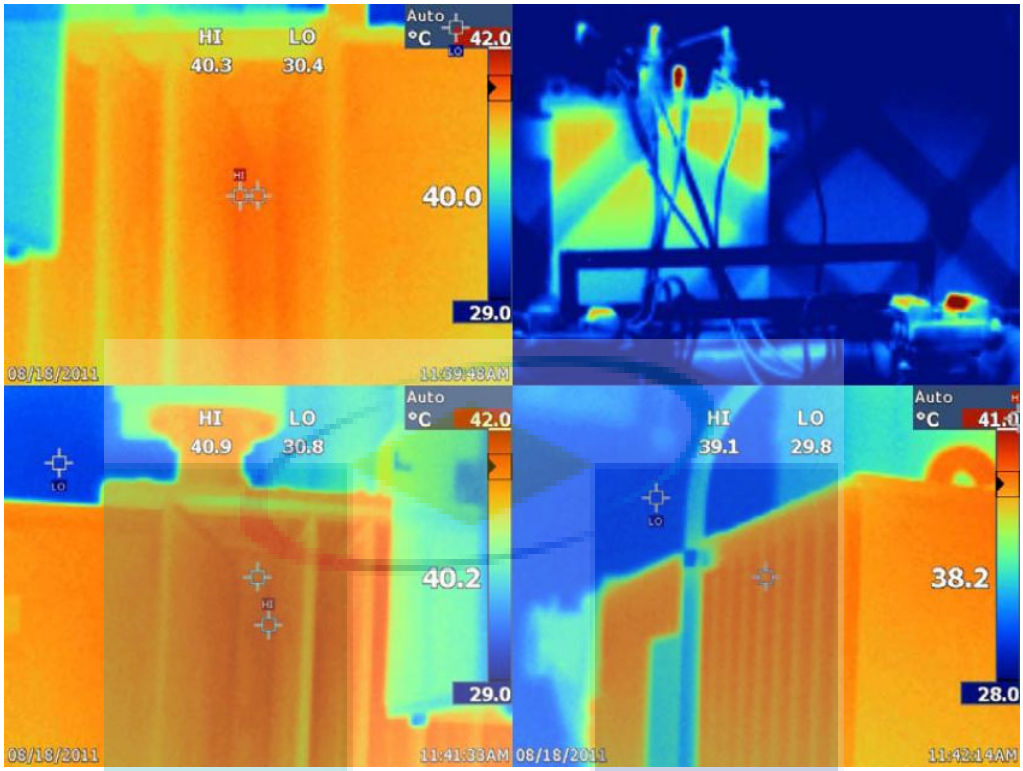
HI 40.3
LO 30.4
Auto °C 42.0
40.0
29.0
08/18/2011
HI 40.9
LO 30.8
Auto °C 42.0
40.2
29.0
08/18/2011
HI 39.1
LO 29.8
Auto °C 41.0
38.2
28.0
08/18/2011

(b)

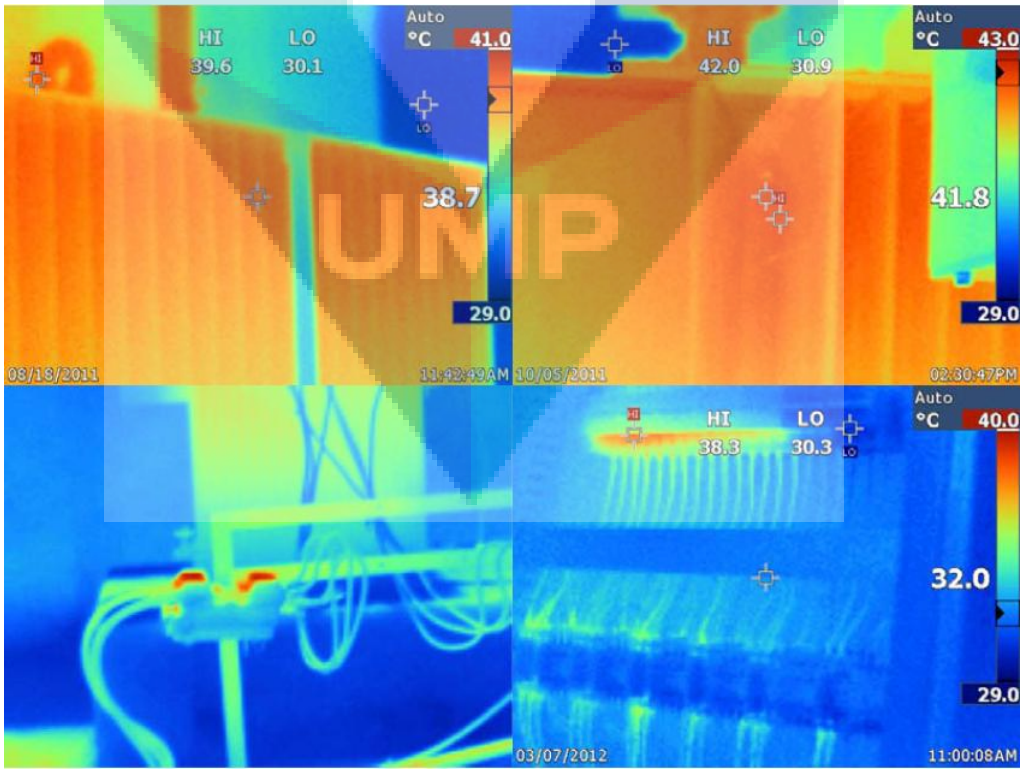
HI 39.6
LO 30.1
Auto °C 41.0
38.7
29.0
08/18/2011
HI 42.0
LO 30.9
Auto °C 43.0
41.8
29.0
10/05/2011
HI 38.3
LO 30.3
Auto °C 40.0
32.0
29.0
03/07/2012
11:00:08AM

(c)

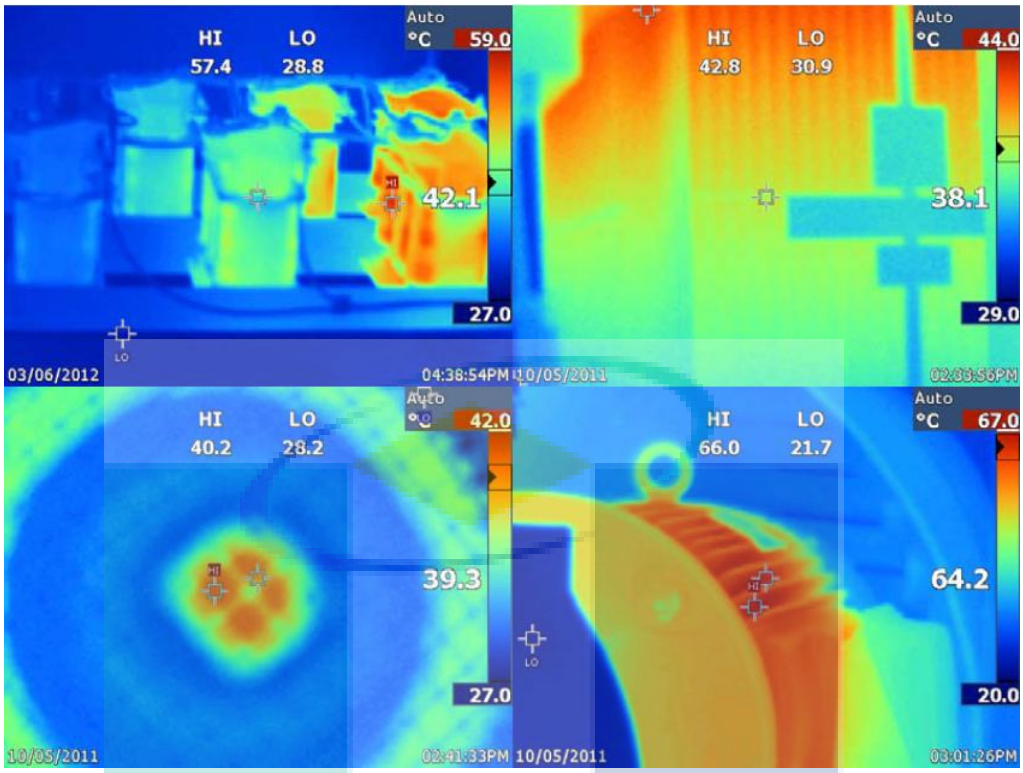
HI
LO
57.4
28.8
Auto
°C
59.0
42.1
27.0
03/06/2012
04:38:54PM
HI
LO
42.8
30.9
Auto
°C
44.0
38.1
29.0
10/05/2011
02:38:56PM
HI
LO
40.2
28.2
Auto
°C
42.0
39.3
27.0
10/05/2011
02:41:33PM
HI
LO
66.0
21.7
Auto
°C
67.0
64.2
20.0
10/05/2011
03:01:26PM

(d)

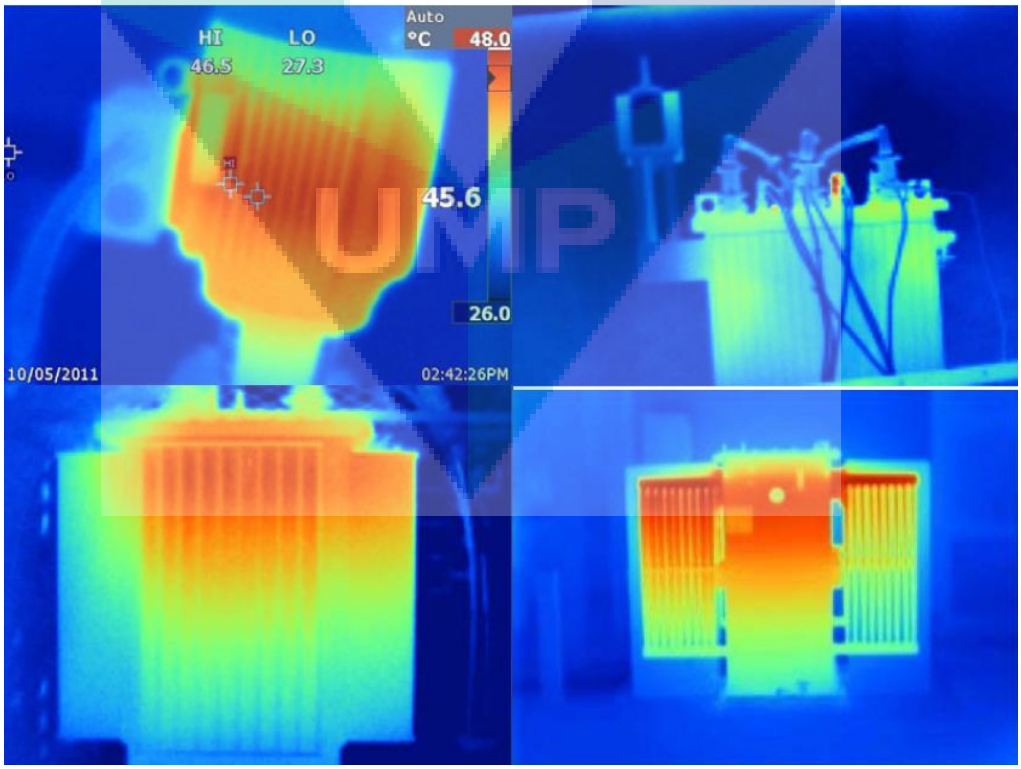
HI
LO
46.5
27.3
Auto
°C
48.0
45.6
26.0
10/05/2011
02:42:26PM

(e)

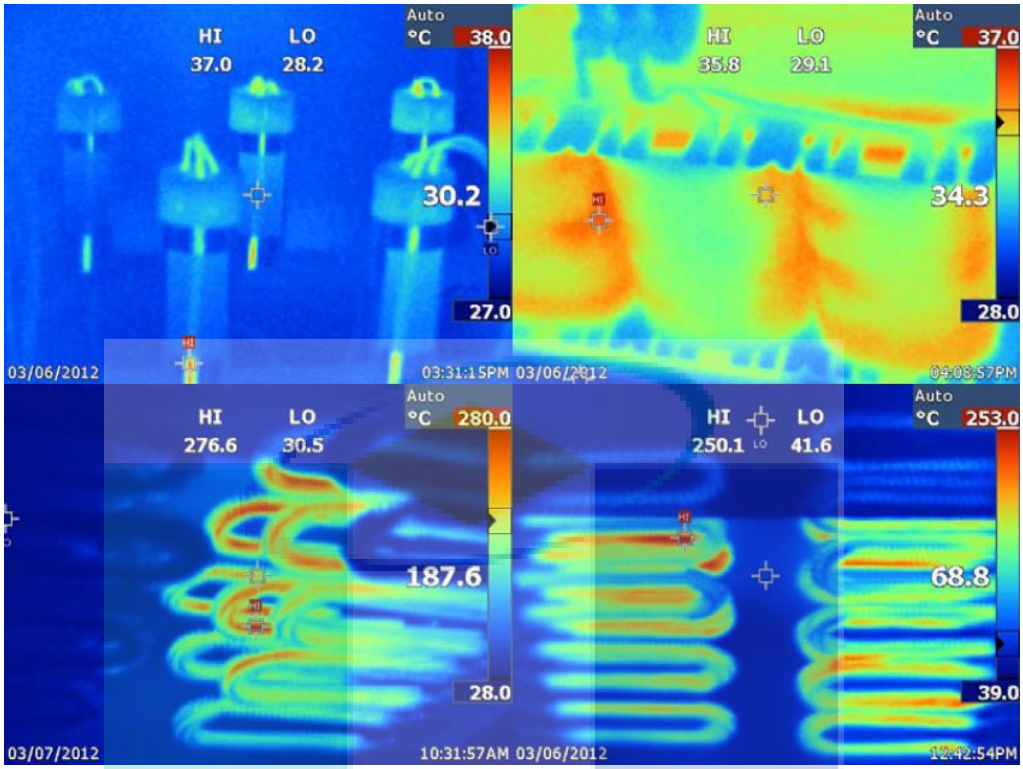

(f)

Figure 3.6: Real-time inspected electrical facilities

3.4 MEASUREMENT OF SEGMENTATION OPERATION

Optimal threshold values are authenticated by experiments conducted on many captured IRT images to prove the equation in (3.13). The equation reveals the desire to obtain an ideal Receiver Operating Characteristics (ROC) curve where the area under the curve is one (Alan el at., 1988). Figure 3.7 illustrates the ROC curve and Figure 3.8 shows the area under the convex hull while equation (3.13) is a proof of the concept of ROC curves.

$$TP + FN = 1 \quad or \quad TN + FP = 1; \qquad TN = TP \quad or \quad FN = FP \tag{3.13}$$

In Figure 3.7, the region labeled TP means True Positive image. It represents the object image also known as object pixel and the region labeled TN, which means True

Negative image represents the background image also known as background pixel. The portions labeled FP and FN are known as error boundary regions. This shows that a background point may be classified as object point (FP), likewise; object point may be classified as background point (FN). The above explanations mainly apply to binary image threshold operations. However, in RGB optimal threshold operation used in this research project, these terms that describes the ROC curve concept is being adopted and used as the threshold value optimization yardstick.

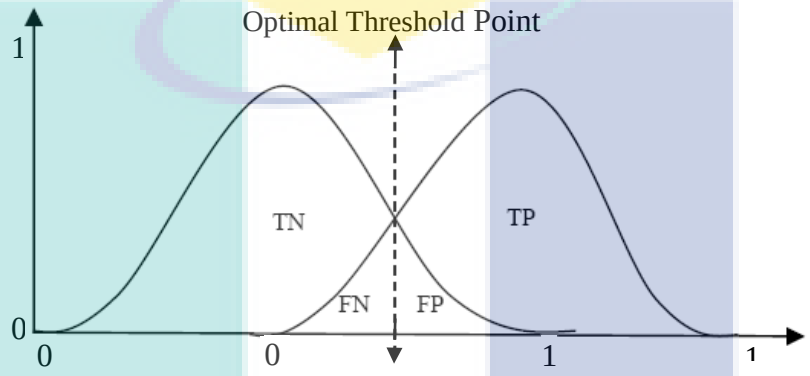

Figure 3.7: Ideal receiver operating characteristic curve

Convex Hull is another form of performance measure applied in this research work. It is defined as a set of smallest convex polygon that contains all the convex points within the polygon. These convex points are the scattered plot as shown in Figure 3.8 which represents the sum of the pixel intensity values or the sum of the optimal threshold values used for the IRT Image segmentation. How can this system ascertain accurate threshold operation? When the scattered plots which depicts the optimal threshold values are found within the confined space of the smallest convex polygon then the selected threshold values are optimal. In other words, if any of those scattered plots falls outside the walls of the smallest convex polygon it means that the chosen threshold values are not optimal. Cross-examination on the figure labeled "Area under Convex Hull" in Figure 3.8, it is seen that some points fall on the red line that is the boundary line of the convex polygon. These points on the red boundary line account for FN and FP errors previously explained. This FN and FP errors are attributed to over or less caution during thermal data acquisition. They are calculated and figured out using the derived Formulas in chapter 3.6. Convex Hull is produced in Matlab software.

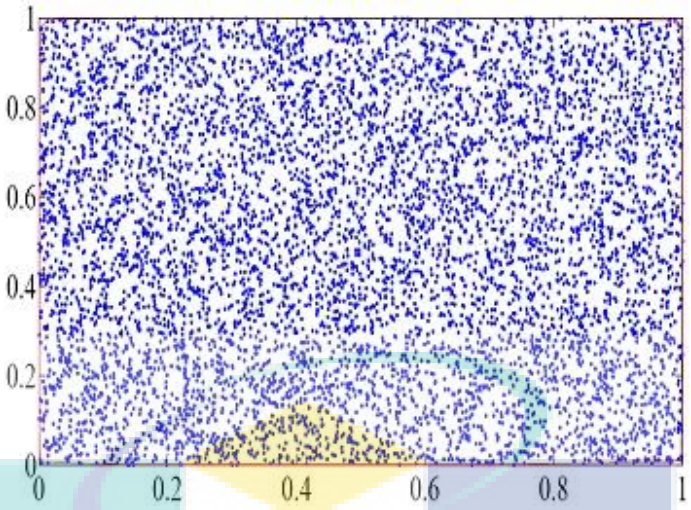

Figure 3.8: Area under convex hull

As an adaptive means of regionalizing IRT image pixels, an optimal threshold value should be obtained. The optimization is obtained when the proportion of the True Positive (TP) regions of IRT image, is approximately equal to the proportion of True Negative (TN) of the same regions. Equally, when the proportion of False Negative (FN) is approximately equal to the proportion of False Positive (FP), an optimal threshold value is achieved as pictorially illustrated in Figure 3.9 (a, b, c). Figure 3.9 (b) contains black regions, which is the TN of the extracted TP IRT image shown in Figure 3.9 (a). Figure 3.9 (c) is the TP of IRT image extracted from the original IRT image shown in Figure 3.9 (a). It can be seen from these Figures 3.9 (b and c), that the proportion of TN is approximately equal to the proportion of TP. Similarly, the proportion of FN is approximately equal to the proportion of FP, which shows that there is no boundary detection between them as indicated in Figure 3.9 (a). This result is a proof of accuracy of segmentation using an RGB optimal threshold algorithm.

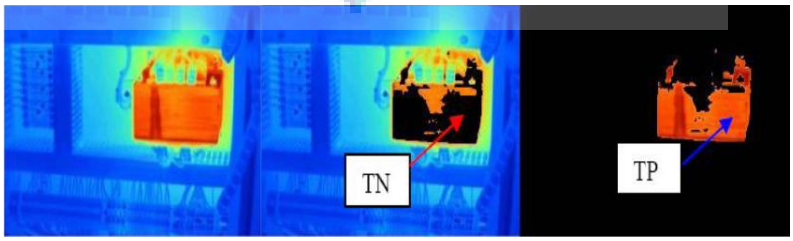

(a) (b) (c)

Figure 3.9: Original IRT image, (b) True Negative (TN), (c) True Positive (TP)

3.5 PERFORMANCE MEASURE OF DEFECT DETECTION ALGORITHM

Receiver Operating Characteristic (ROC) curve and the area under the convex hull have been used as the performance measure for threshold values that segments regions of IRT images accurately. Figure 3.10 (a) is an IRT image of electrical equipment thermogram containing different color contrast (chromatic pixel) regions. Figure 3.10 (b) contains boundary marks which are because of flawed threshold values (TP ≠ TN, FN ≠ FP likewise TP+FN≠1, TN+FP≠1) and Figure 3.10 (c) is an ensemble of 3.10 (a) which is because of optimal threshold values that proves the equation (3.13).

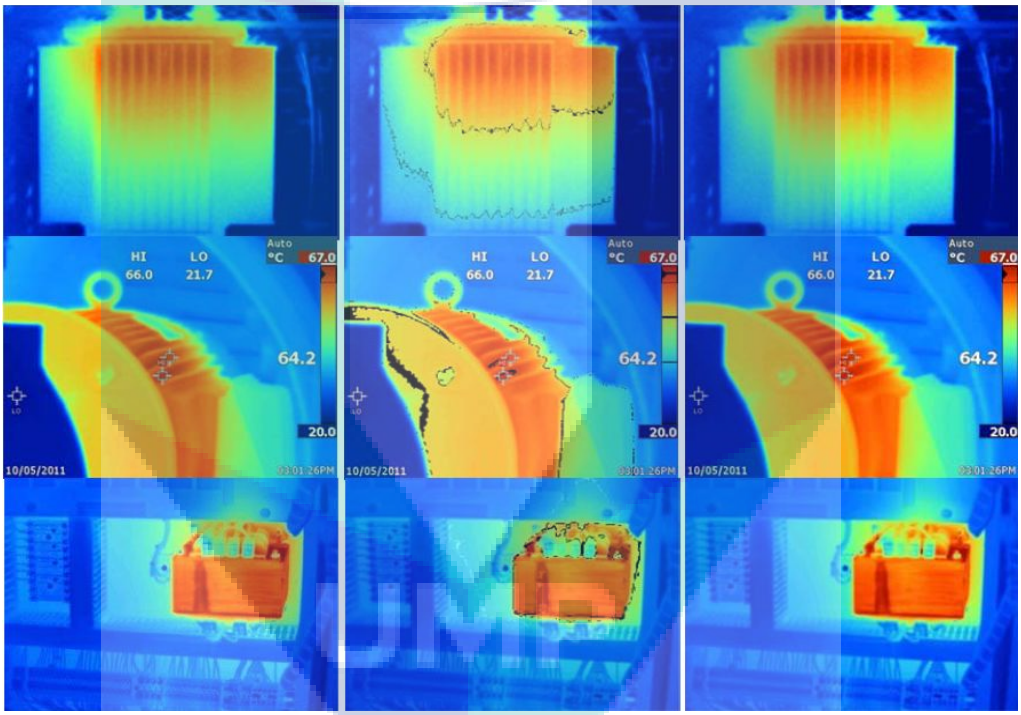

(a) (b) (c)

Figure 3.10: Original IRT image, (b) Result of flawed threshold, (c) Result of optimal threshold

The optimal threshold values generated during training process using various IRT images of low, medium and high temperature electrical equipment and components are presented in Tables 3.2, 3.3 and 3.4.

Table 3.2: Optimal threshold values (low temperature equipment)

Classified Temperature Regions	Red	Green	Blue
Abnormal Temperature Region	200	81	120
High Temperature Region	201	89	187
Warming Temperature Region	90	200	186
Normal Temperature Region	199	215	79
Ambient Temperature Region	200	216	120

Table 3.3: Optimal threshold values (medium temperature equipment)

Classified Temperature Regions	Red	Green	Blue
Abnormal Temperature Region	170	89	120
High Temperature Region	231	50	187
Warming Temperature Region	51	200	186
Normal Temperature Region	199	185	79
Ambient Temperature Region	200	186	120

Table 3.4: Optimal threshold values (high temperature equipment)

Classified Temperature Regions	Red	Green	Blue
Abnormal Temperature Region	150	81	120
High Temperature Region	241	40	187
Warming Temperature Region	41	201	186
Normal Temperature Region	200	185	79
Ambient Temperature Region	200	186	100

These optimal threshold values in Table 3.2, 3.3 and 3.4 will be used to calculate the percentage of the true positive rate (TPR) of the segmented regions. Since the IRT image is normalized through RGB color space as given in equation 3.1 (a, b, c) and further converted to a grayscale image through joint probability in equation (3.6), then the IRT image in RGB color space shares a common range of grayscale value (0, 255). Now the percentage of TPR can be calculated using Formula (3.16). Note: in equation (3.13) it was stated that TP+FN=1 for ideal Receiver Operating Characteristic (ROC) curve where the area under the curve is equal to (1) one. In this case, after converting the normalized IRT image into grayscale image the area under curve takes a different value (255) instead of (1). Therefore the calculation of the actual pixel values for each TP segmented regions of the IRT image can be done as follows:

$$TP + FN = N_{gv} \Rightarrow TP = N_{gv} - FN \tag{3.14}$$

But;

$$FN = \frac{\sum_{i=(T_{i(rgb)})}^{T_{i(rgb)}} T_i}{N_{gv}} \tag{3.15}$$

Substituting the value of FN in equation (3.15) into equation (3.14) then the TPR value is calculated using Formula (3.16),

$$TPR_{value} = N_{gv} - \left[\left(\frac{\sum_{i=(T_{i(rgb)})}^{T_{i(rgb)}} T_i}{N_{gv}} \right) \times 100 \right] (\%) \tag{3.16}$$

Where; N_{gv} is the normalized grayscale value; T_i is the regional threshold value of each extracted region; TPR_{value} is actual pixel value but does not represent real thermal value of equipment.

To obtain the actual thermal value, the thermal range of the imager should be known (the maximum temperature range which is readily available in any type and model of thermal imager) before the actual temperature can be calculated by converting the TPR_{value} in Formula (3.16) into real equipment thermal value using the Formula in (3.17),

$$TH_{real} = \frac{N_{gv}}{\mathrm{Im}\,agerT_{\max}} \times TPR \quad (°C) \tag{3.17}$$

Alternatively, absolute temperature criteria for electrical systems can be used in calculating electrical equipment temperature rise. The infrared thermographer may use absolute temperature criteria based on the following ANSI, IEEE and NEMA or other standards to identify electrical system exceptions. All temperatures of the following standards are specified in Celsius as follows: Ambient / Rated Rise / Maximum Allowable. Rated Ambient + Rated Rise = Maximum Allowable Temperature.

Note: Ambient = rated ambient temperature, Rated rise = Equipment Maximum Allowable Temperature. Unless noted otherwise, these absolute temperature criteria are based on equipment operating at the stated ambient temperature and at 100% of their rated load. Formula (3.18) can be applied to these absolute temperature criteria to give a corrected maximum allowable temperature ($T_{maxcorr}$) for the reduced operating load and actual ambient temperature of the exception:

$$T_{maxcorr} = \{(A_{meas} \div A_{rated})^2 (T_{rated\,rise})\} + T_{ambmeas} \tag{3.18}$$

Where:

$T_{maxcorr}$ = corrected maximum allowable temperature;

A_{meas} = measured load, in amperes;

A_{rated} = rated load, in amperes;

$T_{rated\,rise}$ = rated temperature rise (from standard);

$T_{ambmeas}$ = measured ambient temperature (Infraspection Institute 2008).

3.6 EVALUATION OF SENSITIVITY OF DEFECT DETECTION SYSTEM

The capability of the defect detection scrutiny system to yield a positive result for defective equipment with the diagnostic thermal signature is called sensitivity. In other words, sensitivity is the ability of the defect detection to query within the proportions of thermal regions based on the set criteria or decision tool to yield a positive result and can be calculated using Formula 3.19 (Alan el at., 1988).

$$Sensitivity = \frac{\sum region\ pixel\ value}{\sum IRT_{image}\ pixel\ value} \times 100(\%) \tag{3.19}$$

The *False Positive Rate* (FPR) is the proportion of non-defective equipment that yields defective inspection evaluation and can be calculated using Formula (3.20). In the context of this research work, an ideal ROC curve has been used to prove the accuracy of segmentation that produce an equalization of sensitivity and specificity.

$$FPR = 1 - specificity \tag{3.20}$$

Where, sensitivity is equal to specificity.

The *Positive Predictive Value* (PPV) of an equipment inspection result is the likelihood that equipment with regions of thermal signatures actually has the predicted attribute and can be calculated using Formula (3.21),

$$PPV = \frac{TP}{TP + FN} \times 100(\%) \tag{3.21}$$

Where; $TP = \sum region\ pixel\ value$ and $FN = \frac{TP}{N_{gv}}$

3.7 CLASSIFICATION OF EXTRACTED THERMAL REGIONS

In this section, over 100 samples of IRT images were processed to ascertain the practical authenticity of the proposed defect detection scrutiny system using the RGB optimal threshold technique described in the previous subsections of this chapter. The process is illustrated in a flowchart in Figure 3.11. The IRT images of transformers, circuit breakers, electric motors, and other electrical facilities are processed by the defect detection scrutiny algorithm because these facilities are pure and vital electrical equipment. First, the original IRT image is pre-processed by normalizing it through RGB color space as in equation 3.1 (a, b, c) after that it was morphologically dissected into various color segments using optimal threshold values given in Table 3.2, 3.3 and 3.4. In order to reduce the false positive rate to the lowest level, a maximum likelihood criterion which is function of short circuit OR logic operator is used to connect most similar pixels ensuring that prudence of ROC curve is satisfied (TP+FN=1; TN+FP=1; TN=TP; FN=FP) then different regions of the IRT image are extracted. The extracted regions are thoroughly scrutinized and classified based on the derived mathematical Formulas (3.16 and 3.17), based on temperature difference (ΔT) between the low, medium and high temperature equipment and their respective ambient temperatures as presented in Tables 3.5, 3.6 and 3,7. Lastly, the thermal gradient values from international thermal evaluation standards is used as a guide and for comparison purpose. This is shown in Table 3.8.

Table 3.5: Low temperature equipment classification ($\Delta T \geq 40℃$)

Situation Priority Report	**ΔT Between Equipment and Ambient**	**Recommended Action**
Abnormal	ΔT ≥40	Critical situation; repair immediately
High Thermal	20≤ΔT <40	Monitor until maintenance and repair is done
Warming	10<ΔT <20	Inspect and repair as time permits
Normal	ΔT ≤10	Minor problem; Normal inspection

Table 3.6: Medium temperature equipment classification ($\Delta T \geq 65℃$)

Situation Priority Report	ΔT Between Equipment and Ambient	Recommended Action
Abnormal	ΔT ≥65	Critical situation; repair immediately
High Thermal	45≤ΔT <65	Monitor until maintenance and repair is done
Warming	20<ΔT <45	Inspect and repair as time permits
Normal	ΔT ≤20	Minor problem; Normal inspection

Table 3.7: High temperature equipment classification ($\Delta T \geq 75℃$)

Situation Priority Report	ΔT Between Equipment and Ambient	Recommended Action
Abnormal	ΔT ≥75	Critical situation; repair immediately
High Thermal	65≤ΔT <75	Monitor until maintenance and repair is done
Warming	30<ΔT <65	Inspect and repair as time permits
Normal	ΔT ≤30	Minor problem; Normal inspection

Table 3.8: Standard analysis report base on temperature difference (℃)

Situation Priority Report	ΔT Between Equipment and Ambient	Δt Between Similar Equipment	Recommended Action
Abnormal	ΔT ≥40	ΔT ≥15	Critical situation; repair immediately
High Thermal	20≤ΔT <40	- - - - - -	Monitor until maintenance and repair is done
Warming	10<ΔT <20	4≤ΔT <15	Inspect and repair as time permits
Normal	ΔT ≤10	ΔT ≤3	Minor problem; Normal inspection

Electrical equipment anomaly detection carried out in this project starts with electrical power equipment and component thermogram acquisition. The raw thermogram (IRT image) is converted to grayscale after normalization via RGB color space. Then the electrical power equipment and components IRT image is thresholded using the optimal threshold algorithm in order to perform segmentation operation. In the segmentation operation, features of interest are extracted from the IRT image. Classification is the next anomaly detection operation which is based on the thermal difference of various thermal color contrasts available on the electrical power equipment and components thermogram. These processes are summarized in Figure 3.11.

Four thermal signatures observed were represented with different colors as shown in the defect detection training flow process in Figure 3.11. The green color region represents the normal thermal operation condition followed by the yellow color region classified as warming thermal operation condition, next red color region classified as a high thermal operation condition, lastly, the dark-red color region indicates the hottest thermal region classified as abnormal thermal operating condition.

Results of samples of the inspected electrical equipment and components processed using the proposed RGB optimal thresholding algorithm are presented in chatper 4.

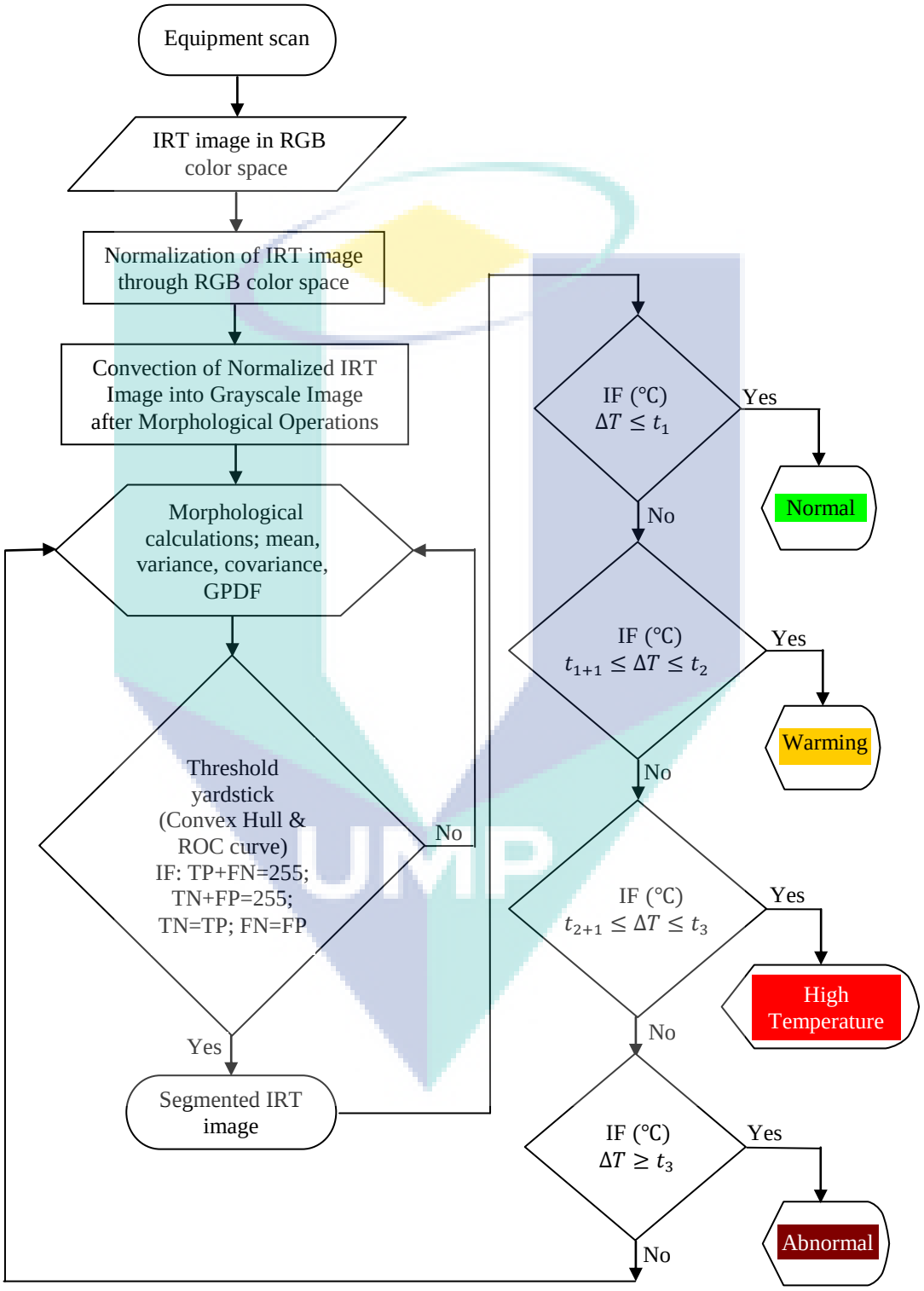

Figure 3.11: Defect detection training flow process

The comparison between experimental inspection measurement results (Table 3.2, 3.3 and 3.4) using the thermal imager, the calculated results using the derived Formulas (3.16 and 3.17), and international maintenance testing standards (Table 3.8) are tabulated in Table 3.9. In Table 3.9, it is observed that there is a balance between the calculated result and international maintenance testing standard specification. This further proved that the proposed defect detect scrutiny system offered a reliable electrical equipment and components thermal operation status report.

Table 3.9: Comparison between measured results, mathematical evaluation, and international maintenance testing standards

Low Temperature Equipment / Components

Equipment/ Component Samples	Thermal Imager Temp. Reading (℃)			Calculated ΔT Between Equipment and Ambient using Derived Formulas (Calculated Ambient 29.8℃)				NETA, ANSI, IEEE, NEMA Maintenance Testing Standard Based on ΔT Between Equipment and Ambient (Estimated Ambient 30℃)			
	Hotspot	Ambient	ΔT (℃)	Abnormal $\Delta T > 40$	High Temp. $\Delta T > 20$	Warming $\Delta T > 10$	Normal $\Delta T \leq 10$	Abnormal $\Delta T \geq 40$	High Temp. $40 < \Delta T \geq 20$	Warming $20 < \Delta T > 10$	Normal $\Delta T \leq 10$
MCCB	34.6	28.5	6.1				✓				✓
MCCB	35.3	28.3	10				✓				✓
MCCB	34.9	27.7	7.2				✓				✓
MCCB	35.0	27.0	8				✓				✓
MCCB	35.2	28.6	6.6				✓				✓
MCB	38.8	27.3	11.5			✓				✓	
MCB	38.3	30.3	8				✓				✓
MCB	37.5	27.5	10				✓				✓
MCB	35.2	27.0	8.2				✓				✓
MCB	39.3	29.0	10.3			✓				✓	
Connector	26.2	29.1	-2.9				✓				✓
Connector	26.7	29.9	-3.2				✓				✓
Connector	26.3	30.0	-3.7				✓				✓
Connector	71.7	27.4	44.3	✓				✓			
Connector	38.3	29.0	9.3				✓				✓

Medium Temperature Equipment / Components

Equipment/ Component Samples	Thermal Imager Temp. Reading (℃)		Calculated ΔT Between Equipment and Ambient using Derived Formulas (Calculated Ambient 29.8℃)				
	Hotspot	Ambient	ΔT (℃)	Abnormal $\Delta T \geq 60$	High Temp. $60 < \Delta T \geq 45$	Warming $45 < \Delta T > 20$	Normal $\Delta T \leq 20$
Transformer	35.2	27.0	8.2				✓
Transformer	43.0	29.0	14.0				✓
Transformer	40.9	29.0	11.9				✓
Transformer	39.1	28.0	11.1				✓
Transformer	40.6	29.0	11.6				✓

Table 3.9: Continued

Transformer	39.0	28.0	11.0				✓
Transformer	42.0	29.0	13.0				✓
Transformer	38.3	29.0	9.3				
Transformer	54.4	27.0	27.4			✓	
Transformer	42.8	29.0	13.8			✓	
Transformer	71.0	29.0	42.0		✓	✓	
Transformer	91.0	29.0	62.0	✓			
Fuse	51.1	31.0	20.1			✓	
Fuse	61.6	32.6	29			✓	
Fuse	42.4	31.0	11.4				✓
Fuse	47.2	30.2	17.0				✓
Fuse	55.8	29.0	26.8			✓	
Contactor	40.2	31.0	9.2				✓
Contactor	42.4	31.9	10.5				✓
Contactor	47.2	32.0	15.2				✓
Contactor	38.8	27.6	11.2				✓
Contactor	35	28.7	6.3				✓
High Temperature Equipment / Components							
	Hotspot	**Ambient**	**ΔT (℃)**	**Abnormal $\Delta T \geq 75$**	**High Temp. $75 < \Delta T \geq 65$**	**Warming $65 < \Delta T > 30$**	**Normal $\Delta T \leq 30$**
AC Power Capacitor	35.3	28.9	6.4				✓
AC Power Capacitor	35.8	28.9	6.9				✓
AC Power Capacitor	38.1	28.2	9.9				✓
AC Power Capacitor	37.0	29.3	7.7				✓
AC Power Capacitor	38.0	29.9	8.1				✓
Electric Motor	64.8	31.2	33.6			✓	
Electric Motor	66.3	31.1	35.2			✓	
Electric Motor	66.0	31.4	34.6			✓	
Electric Motor	63.1	29.8	33.3			✓	
Electric Motor	57.1	31.6	25.5				✓

NETA = National Electrical Testing Association, ANSI = Amarican National Standards Institute, IEEE = Institute of Electrical and Electronics Engineers, NEMA = National Electrical Maunfacturers Association

The computer aided defect detection scrutiny system final flow process for sorting and classifying inspected electrical power equipment and components according to the inspection result in terms of thermal gradient is summarized in Figure 3.12.

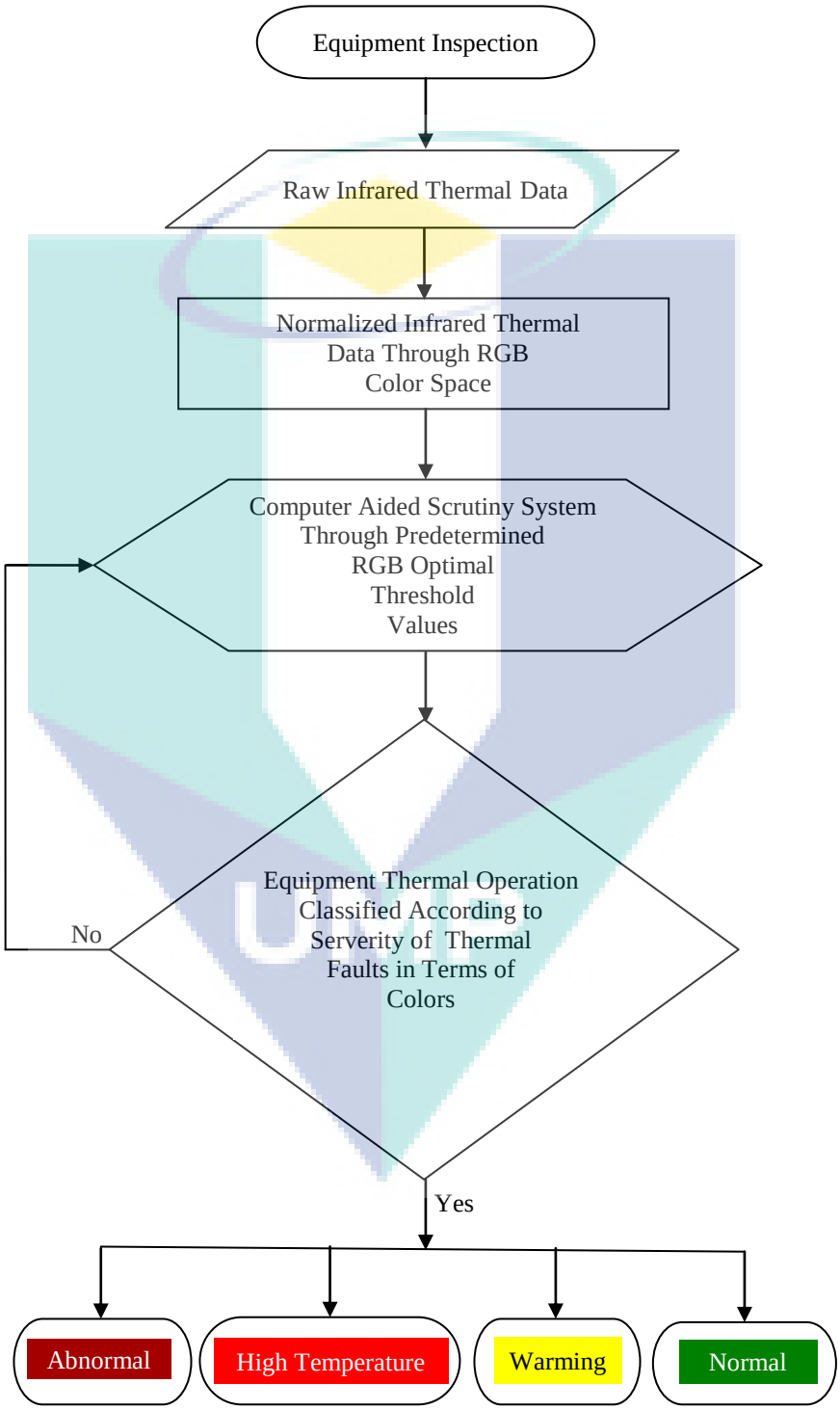

Figure 3.12: Computer aided defect detection scrutiny system final flow process

3.8 COMPARATIVE STUDY ON ELECTRICAL EQUIPMENT DEFECT DETECTION TECHNIQUE

There are many defect detection techniques based on image processing technology. Image segmentation is found to be very fundamental virtually in all the methods. Some of these methods were reviewed in chapter 2. During the literature review, it was discovered that most of the defect detection methods using equipment thermogram were based on grayscale and binary image. In this work, it is better to work with the original thermal image that appears in the color map. The image being analyzed is thermal image; which means that heat or temperature is involved. The different color contrasts in the thermal image have different temperature values. So analyzing the inspected equipment thermogram in terms of color gives more thermal information of the electrical equipment in question than its grayscale image. Because of these reasons, results of the processed IRT images were displayed in colors which make the proposed technique more intuitive and interpretation-made-easy.

To compare the proposed technique and evaluate its performance, a comparative study has been done. For this purpose, K-means clustering algorithm was compared with the proposed RGB optimal threshold algorithm. The selection was based on K-means clustering algorithm automatic property and ability to segment defects in thermal images. The results of the comparative analysis are summarized in chapter 4.9.

K-means clustering algorithm was used for color image segmentation and the feature extraction was unsupervised (automatic). Experimental results have shown that K-means algorithm is insensitive to the number of regions segmented and blocks in each cluster do not have to be neighboring blocks (Chitade and Katiyar 2010; Tavakol el at., 2008). According to the International Commission on Illumination (CIE), two approximately uniform color spaces (CIELUV and CIELAB) were recommended in 1976 (Li and Burgess 2010). Applying CIE, image segmentation involves converting RGB color space to CIELAB or CIELUV that enables quantification of visual color differences. The $'L^*a^*b^*'$ color space is derived from the CIE XYZ tristimulus values.

$$X = 0.4303R + 0.3416G + 0.1784B \quad (3.22)$$

$$Y = 0.2219R + 0.7068G + 0.0713B \quad (3.23)$$

$$Z = 0.0202R + 0.1296G + 0.9393B \quad (3.24)$$

The $CIEL^*a^*b^*$ color space consists of a luminosity layer $'L^*'$, chromaticity-layer $'a^*'$ which indicates where color falls along the red-green axis, and chromaticity-layer $'b^*'$ indicates where the color falls along the blue-yellow axis. CIELAB color space is morphologically formulated as follows:

$$L^* = 116[(h_q \frac{Y}{Y_s})] - 16 \quad (3.25)$$

$$a^* = 500[(h_q \frac{W}{W_s})] - (h_q \frac{Y}{Y_s}) \quad (3.26)$$

$$b^* = 200[(h_q \frac{Y}{Y_s})] - (h_q \frac{Z}{Z_s}) \quad (3.27)$$

Where W_s, Y_s and Z_s are the standard stimulus coefficients and

$$h_q = \sqrt[3]{q} \quad for \quad q > 0.008856 \quad (3.28)$$

$$h_q = 7.787_q + \frac{16}{116} \quad for \quad q \le 0.008856 \quad (3.29)$$

All the color information is in $'a^*'$ and $'b^*'$ chromaticity layers while the illumination is in the $'L^*'$ layers. The difference between two colors is measured using the Euclidean distance metric.

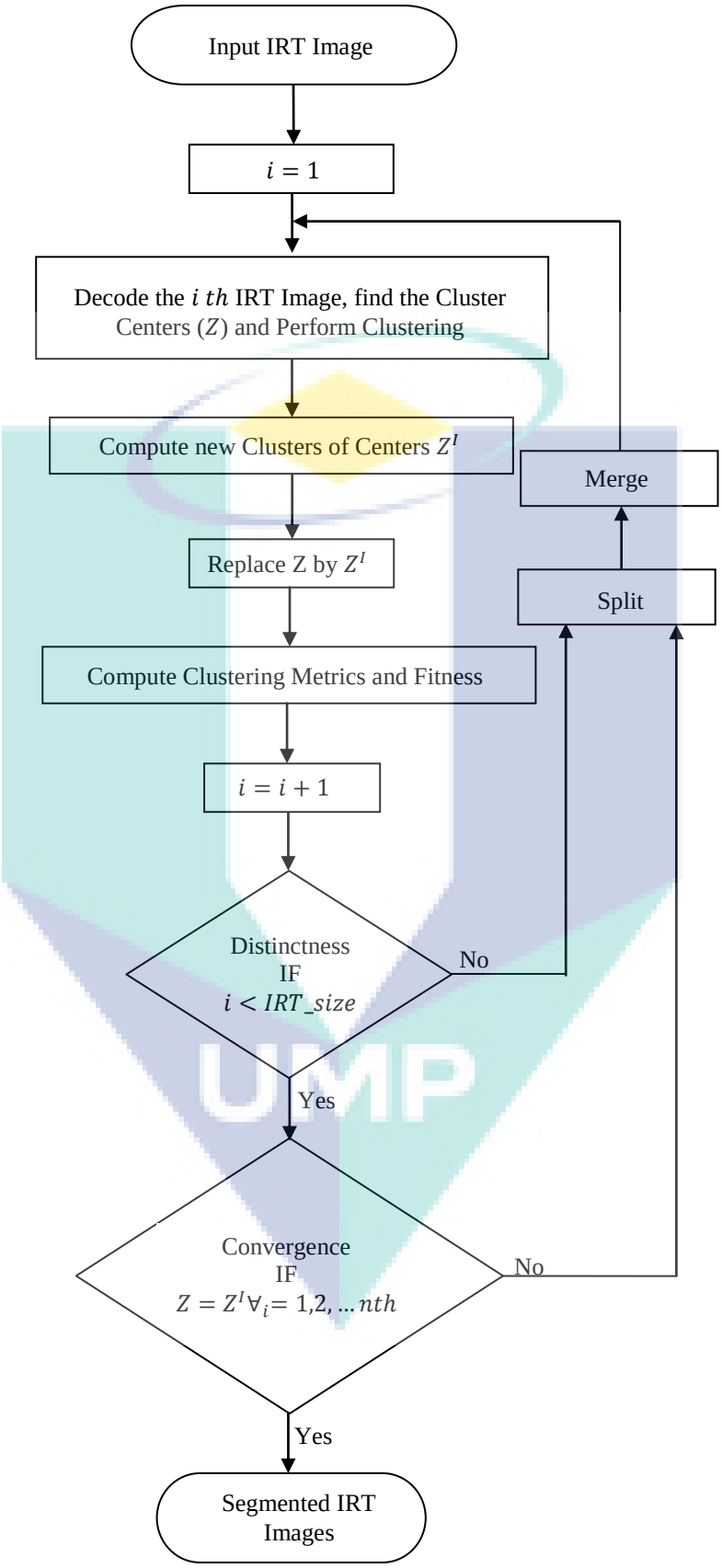

Figure 3.13: K-means clustering algorithm flowchart

Generally, K-Means clustering algorithm is based on the split and merge technique, as shown in Figure 3.13. This algorithm splits the given image into different clusters of center. Initially each pixel in the image is allocated to the nearest cluster. Then the new centers are computed with the new clusters. Using a similarity measure such as the weighted Euclidean distance metrics, the input vectors can be partitioned into subsets, each of which should be sufficiently distinct. Subsets which do not meet this criterion are merged. This procedure is repeated on all of the subsets until no further splitting of subsets or until convergence occurs. The results from K-means clustering algorithm is in chapter 4.8.

CHAPTER 4

RESULTS AND DISCUSSIONS

4.1 INTRODUCTION

This chapter presents the difference between a well-focused IRT images and flawed IRT images captured from Ti25 Fluke thermal imager refer to appendix (A) for Ti25 Fluke thermal imager specifications. The results from the developed defect detection scrutiny system were shown and discussed. Results of performance measure, comparison analysis and evaluation results were also presented and discussed.

4.2 TOOLS FOR IMAGE ACQUISITION

Ti25 fluke model thermal camera is the key tool used in this work for image acquisition (refer to Appendix B for specification details). All the images acquired are purely electrical equipment and components like oil-immerse distribution transformers, fuse boxes, dry type distribution transformers, circuit breakers, electric motors, connectors, contactors, capacitors, resistors, inductors, and other electrical equipment. Thermogram of all these equipments and components were taken under various operating conditions within University Malaysia Pahang (UMP) environment, Kuala Lumpur, Pahang electrical power distribution substations and some roadside distribution transformers.

4.3 QUALITY IMAGE ACQUISITION

The following features characterize quality thermal image thus: focus, perspective, composition, thermal span and range. Figures 4.1 (a – e) shows pictures of

well-focused and flawed infrared thermal images of some inspected electrical equipment and components. From the images shown in Figure 4.1 (a – e), it was observed that focused IRT images produce more accurate temperature value of the inspected equipment and vivid images were recorded which makes analysis evaluation process more easier.

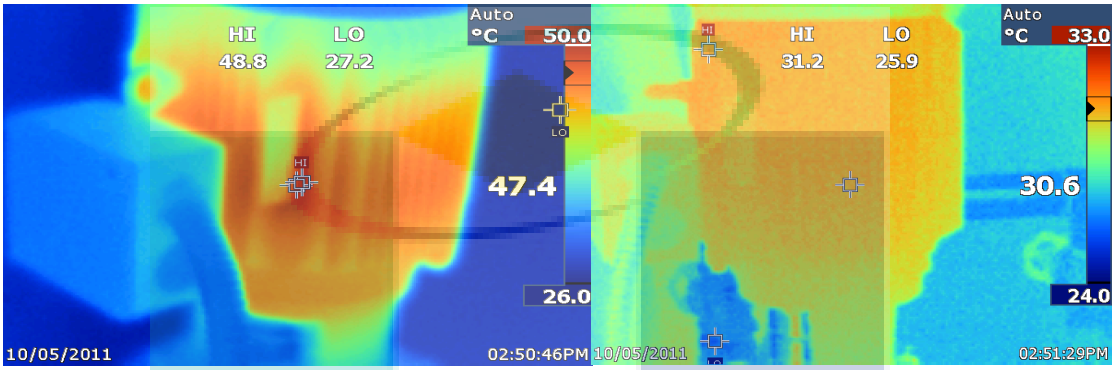

(a) Well-focused IRT image Flawed IRT image

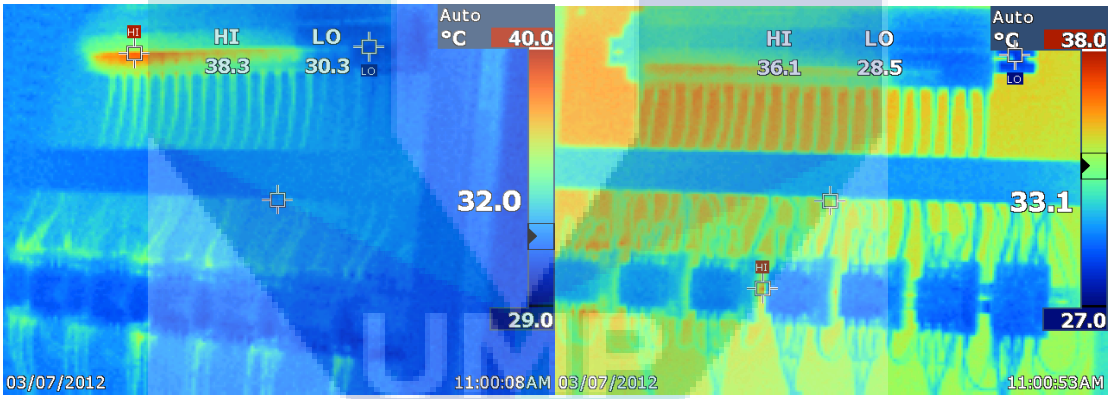

(b) Well-focused IRT image Flawed IRT image

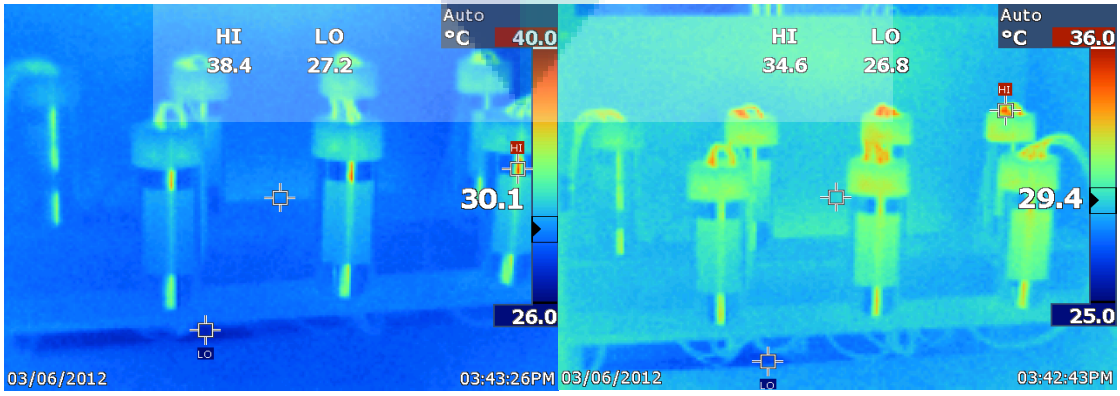

(c) Well-focused IRT image Flawed IRT image

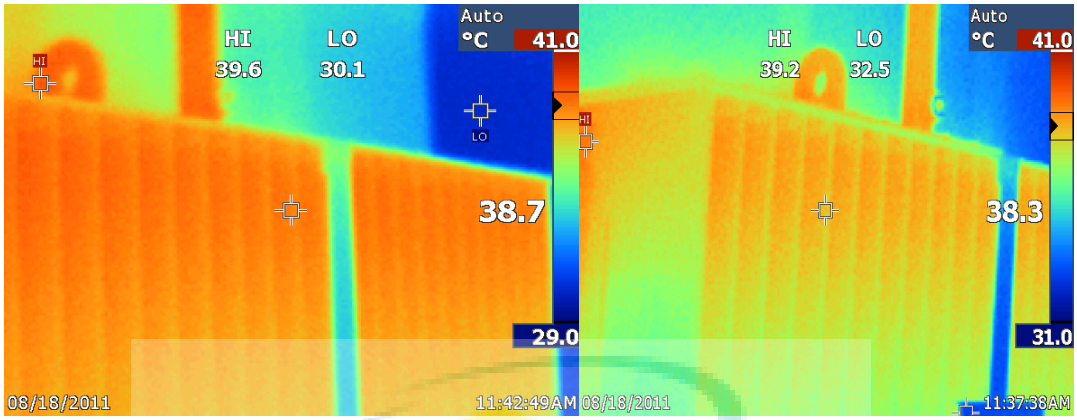

(d) Well-focused IRT image Flawed IRT image

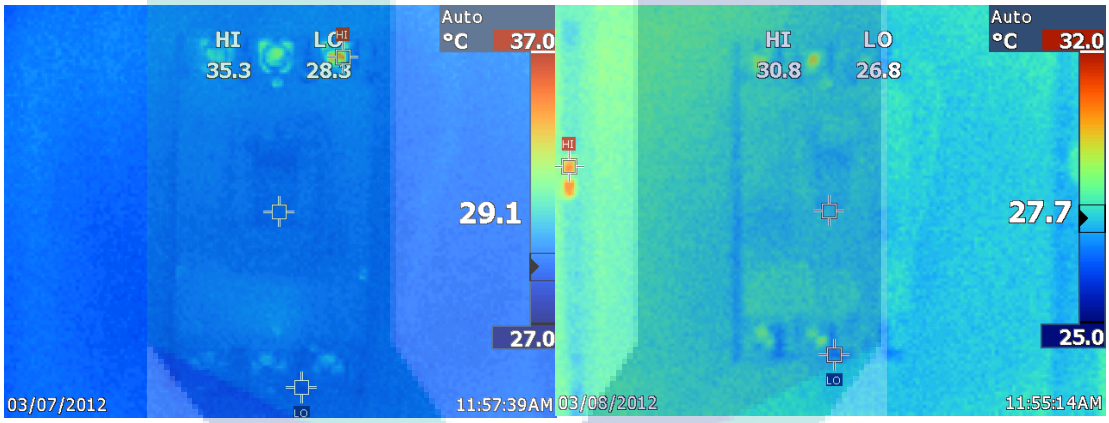

(e) Well-focused IRT Image Flawed IRT Image

Figure 4.1: Well-focused and flawed IRT images;
(a = Electric Motor),
(b =Contactor),
(c = Capacitor),
(d = Transformer),
(e = Circuit Breaker).

4.4 DEFECT DETECTION EVALUATION

More than fifty thermal images of different electrical equipment as presented in Table 4.1 were used for the defect detection scrutiny algorithm training. Some of the training data and other thermal data were used for the testing of the developed defect detection scrutiny algorithm. The same thermal images were also used in K means clustering algorithm for comparison purposes as explained in chapter 3.8. Most of the

IRT images were taken when the equipment was in operation. During the experimental inspection period, ambient temperatures are included only for experimental and comparison purposes otherwise not, because it varies a lot due to instability in atmospheric weather condition. Analysis of equipment thermal status was done via two ways, quantitative and qualitative. In quantitative image analysis, precise temperature or temperature distribution is very much needed. In this, various factors can influence the readings such as slight variations caused by changes in emissivity, atmospheric weather conditions, reflections, and size of the target object, the environment in the background, distance-to-spot size, and minimum distance for focus. Because of all these, it is difficult to maintain a high accuracy rate during evaluation. However, a more reliable qualitative measurement analysis that takes a general view of the equipment as well as the relative temperature values of the hot spots is implemented in this project. This is because qualitative measurement does not require much correction in the camera other than to be aware of emissivity and reflectivity. In real world applications, this method is often used especially in the preventive maintenance inspection. Following the international thermal evaluation standards, qualitative measurement rules are applied to classify the different situations in relation to a thermal inspection according to thermal range values, as indicated in Table 3.9 (Infraspection Institute, 2008). Temperature specifications vary depending on the exact type of equipment. Even in the same class of equipment, there are various temperature ratings. Heating is generally related to the square of the current (I^2R) therefore, the load current will have a major impact on ΔT, which is the difference between equipment and its ambient temperature, and Δt is the difference between similar equipment under similar load status. In the absence of consensus standards for (ΔT, Δt), the values in Table 3.9 provide reasonable guidelines (Don A. Genutis, 2007).

4.5 RESULTS OF RGB OPTIMAL THRESHOLD ALGORITHM

This research is done with the list of tools and materials listed in Appendix (C). Color selection is one of the important pre-settings made on the thermal camera before data acquisition. The pre-determined color palette (blue-red) selected from the thermal imager used; Red indicates areas of maximum radiated energy and blue indicates areas of minimum radiation. Figure 4.2 (a) is normal view of one of the inspected distribution

transformers with typical fault of either overload or loose connection with the bolted joint. Figure 4.2 (b) is the visible thermal spectrum view with different regions of thermal radiations, and Figure 4.2 (c) is the graphical representation of the different regions of thermal pattern/radiations; the pixel frequency represented on the y-axis shows the magnitude of various pixel regions. The x-axis indicates the pixel intensity level ranging from (0 - 255). Pixel intensity value can be converted to an actual equivalent temperature value, refer to the formula (3.17) in chapter 3.5 for more information. The extremely deep valley of the IRT image histogram as shown in Figure 4.2 (c) indicates maximum radiation meaning the hottest spot hence faulty part.

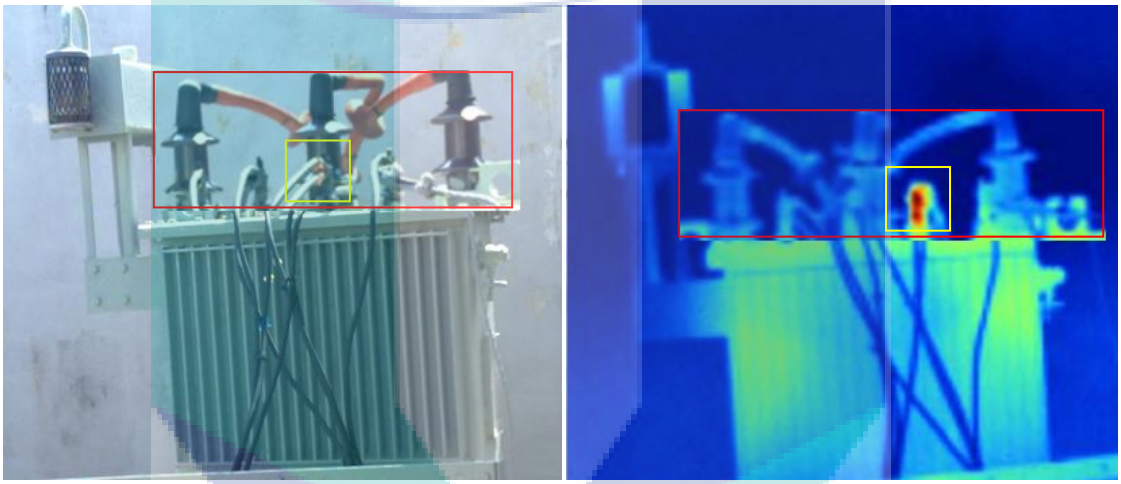

(a = Normal view) (b = Thermal spectrum view)

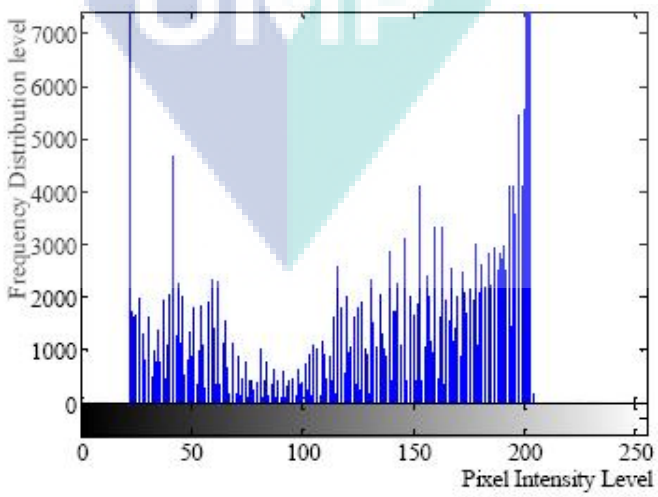

(c = Image histogram)

Figure 4.2: Typical fault of overload or loose connection

The IRT images in Figure 4.3 (a, b, c, d, e, f, and g) shows screen-print of some examples of the inspected equipment and components processed using the developed defect detection scrutiny system in the Matlab image processing environment. Figure 4.3 (a) is an abnormal case of cold defect on oil-immersed distribution transformer. This could be as a result of low oil pump pressure or blockage hampering the free flow of cooling oil through the transformer radiator tubes or fans, hence undesirable thermal rise occurred. Figure 4.3 (b) is a case of abnormal hot defect on connectors and bolted joints. This could be as a result of loose connections or overload causing undesirable thermal rise. More results of hot defect are presented in Figure 4.3 (c, d, e, f, and g).

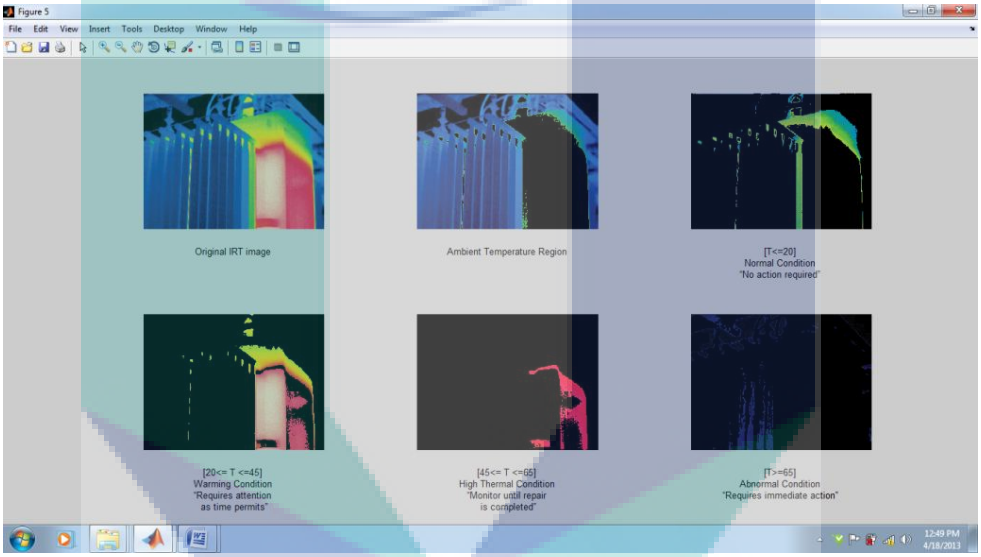

(a)

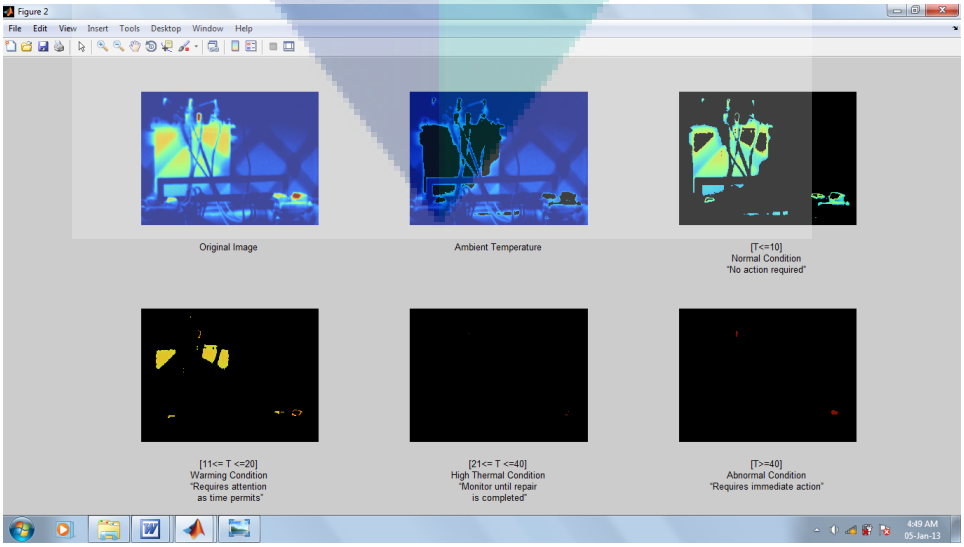

(b)

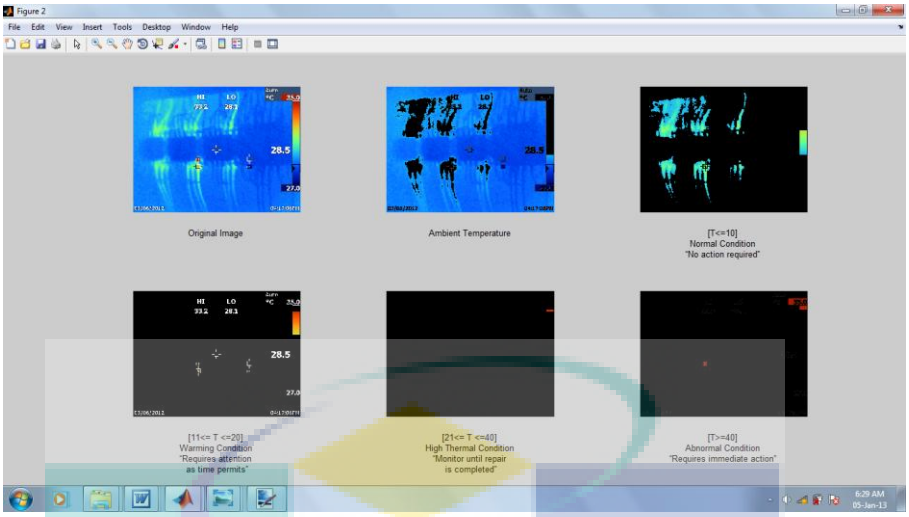
Figure 2
File Edit View Insert Tools Desktop Window Help
Original Image
Ambient Temperature
[T<=10]
Normal Condition
"No action required"
[11<= T <=20]
Warning Condition
"Requires attention
as time permits"
[21<= T <=40]
High Thermal Condition
"Monitor until repair
is completed"
[T>=40]
Abnormal Condition
"Requires immediate action"

(c)

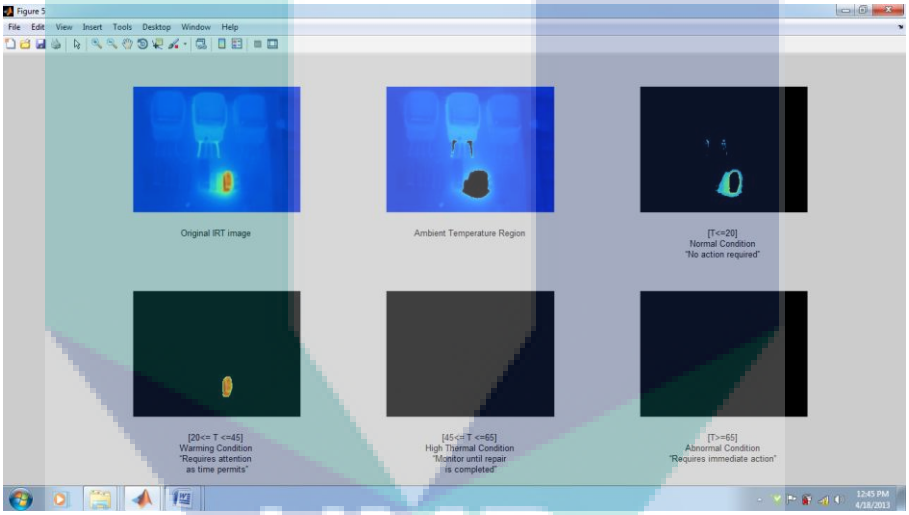
Figure 5
File Edit View Insert Tools Desktop Window Help
Original IRT image
Ambient Temperature Region
[T<=20]
Normal Condition
"No action required"
[20<= T <=45]
Warning Condition
"Requires attention
as time permits"
[45<= T <=65]
High Thermal Condition
"Monitor until repair
is completed"
[T>=65]
Abnormal Condition
"Requires immediate action"

(d)

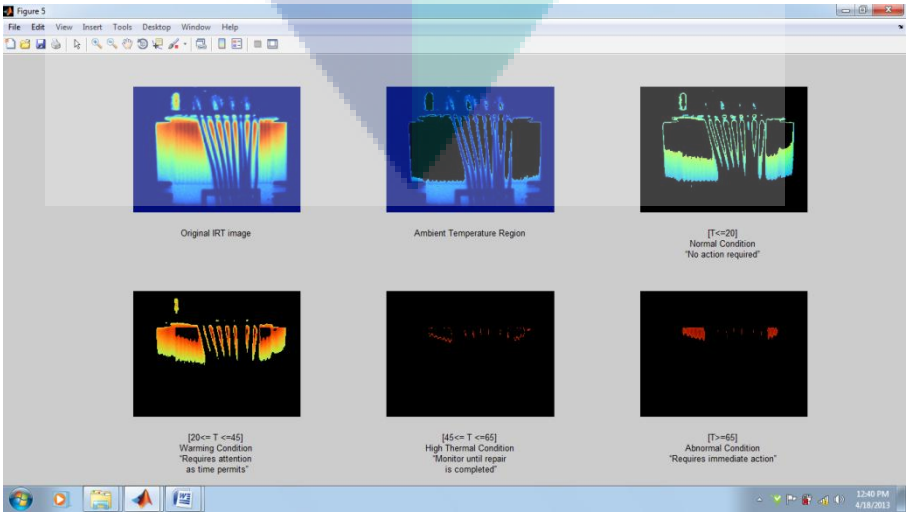
Figure 5
File Edit View Insert Tools Desktop Window Help
Original IRT image
Ambient Temperature Region
[T<=20]
Normal Condition
"No action required"
[20<= T <=45]
Warning Condition
"Requires attention
as time permits"
[45<= T <=65]
High Thermal Condition
"Monitor until repair
is completed"
[T>=65]
Abnormal Condition
"Requires immediate action"

(e)

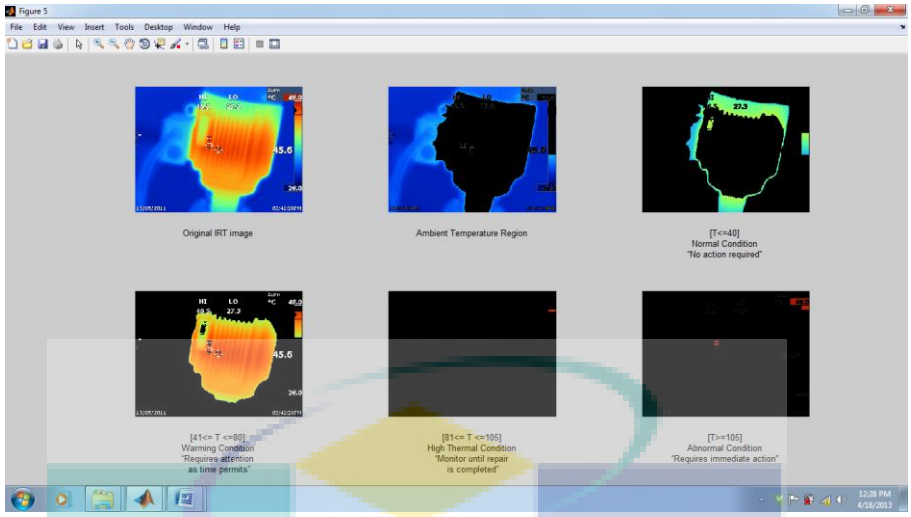

(f)

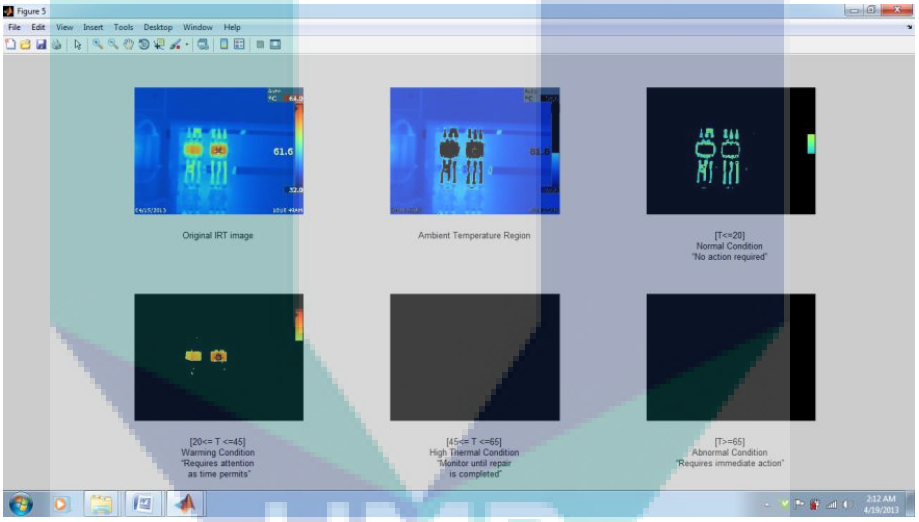

(g)

Figure 4.3: Screen print of Matlab program;
(a = Abnormal thermal condition),
(b = Abnormal thermal condition),
(c = Normal thermal condition),
(d = Warming thermal condition),
(e = Abnormal thermal condition),
(f = Warming thermal condition),
(g = Warming thermal condition).

4.6 INTERPRETATION OF CLASSIFIED REGIONS

Thermal analysis done in this project is qualitative and quantitative. Equipment's thermal status was classified into five namely: ambient temperature region,

normal temperature condition, warming temperature condition, high temperature condition and abnormal temperature condition. Among these five categories of thermal regions, four of them (normal temperature condition, warming temperature condition, high temperature condition and abnormal temperature condition) were considered in the thermal analysis evaluation report that describes electrical equipment components and operation status. Below each of the thermal regions other than the ambient temperature region, are the thermal range, the fault decision and the recommended action to be taken for proper maintenance and repair actions. This arrangement facilitates inspected equipment analysis and evaluation report. The defect detection analysis in this subsection 4.6 showed the results of processed IRT images of electrical facility with their respective string labels. The results presented in Figure 4.4 (A – D) and 4.5 (A – E) were achieved from the developed defect detection scrutiny system.

Figure 4.4 (A_e) indicates the abnormal thermal region of a distribution transformer under a critical situation hence "requires immediate attention". The IRT image in Figure 4.4 (A_d), shows the thermal signature of high temperature condition. Electrical equipment found within this high thermal region has serious faults therefore "requires some follow-up attention until repair is completed". Figure 4.4 (A_c), indicate the IRT region of the warming stage; equipment within this warming temperature region has minor fault; "requires maintenance and repair action as time permits". Figure 4.4 (A_b), indicates equipment under normal thermal condition with no fault therefore needs no attention other than the normal routine check. Ambient temperatures are rarely easy to ascertain because of variations in atmospheric weather condition, which affects the overall equipment temperature that leads to low accuracy rate in quantitative analysis result so may or not be included in the analysis report. It is shown in Figure 4.4 (A_a). Background images should not be included in the analysis report as mentioned in the introductory part of this chapter 4 because it has nothing to do with the equipment under inspection. The same analysis applies in Figures (4.4 $B_{(e-a)}$ to 4.4 $D_{(e-a)}$)

Based on the defect detection scrutiny analysis results, the mathematical operations performed in chapter 3.4, the application of the derived formulas (3.16) and (3.17), the conversion process of pixel values of each classified regions into its actual

equivalent thermal value (℃) and the IEEE thermal evaluation standards in Table 3.8. It was proved that Figures (4.4A to 4.4D) were found within warming thermal condition after thorough scrutinization in the developed defect detection scrutiny system, therefore these electrical facilities requires maintenance action as time permits.

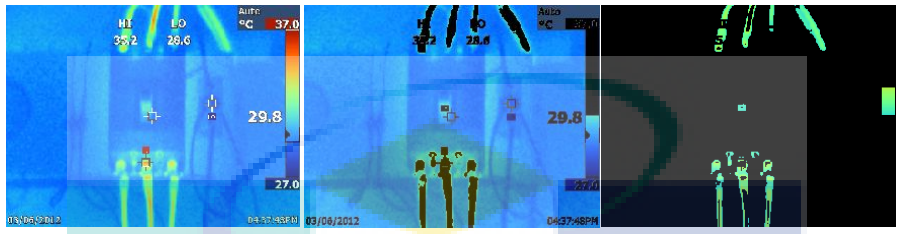

Original IRT Image (a) AmbientTemperature Region (b) $\Delta T \leq 10$ Normal Condition *"No action required"*

(c) $10 < \Delta T < 20$ Warming Condition *"Requires attention as time permits"* (d) $20 \leq \Delta T < 40$ High Thermal Condition *"Monitor until repair is completed"* (e) $\Delta T \geq 40$ Abnormal Condition *"Requires immediate action"*

(A)

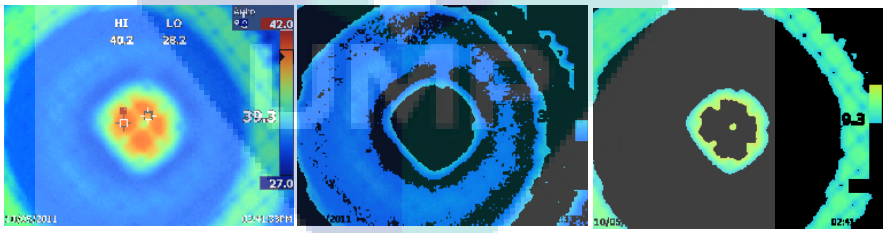

Original IRT Image (a) AmbientTemperature Region (b) $\Delta T \leq 30$ Normal Condition *"No action required"*

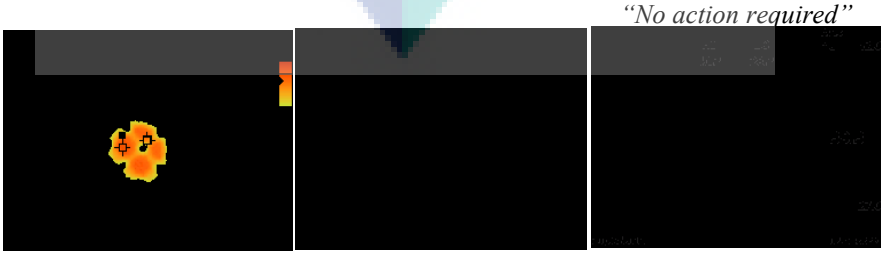

(c) $30 < \Delta T < 65$ Warming Condition *"Requires attention as time permits"* (d) $65 \leq \Delta T < 75$ High Thermal Condition *"Monitor until repair is completed"* (e) $\Delta T \geq 75$ Abnormal Condition *"Requires immediate action"*

(B)

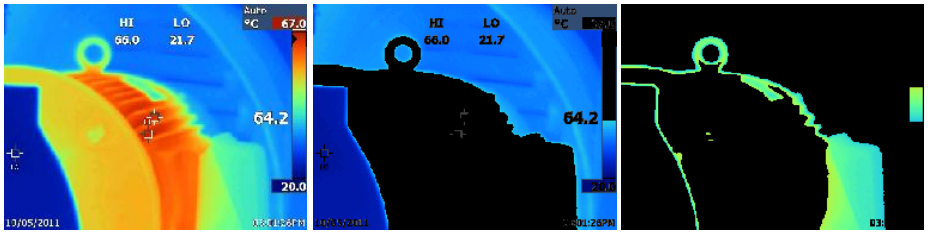

Original IRT Image

(a) AmbientTemperature Region

(b) $\Delta T \leq 30$ Normal Condition *"No action required"*

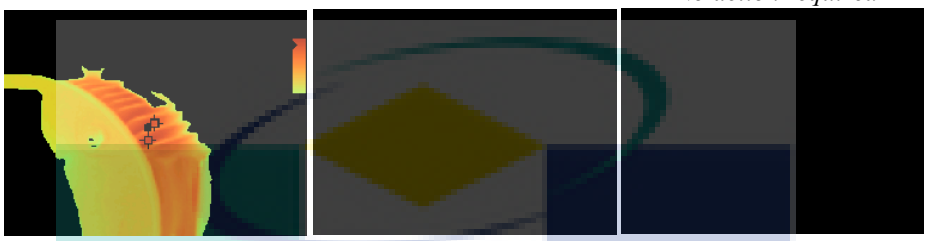

(c) $30 < \Delta T < 65$ Warming Condition *"Requires attention as time permits"*

(d) $65 \leq \Delta T < 75$ High Thermal Condition *"Monitor until repair is completed"*

(e) $\Delta T \geq 75$ Abnormal Condition *"Requires immediate action"*

(C)

Original IRT Image

(a) AmbientTemperature Region

(b) $\Delta T \leq 10$ Normal Condition *"No action required"*

(c) $10 < \Delta T < 20$ Warming Condition *"Requires attention as time permits"*

(d) $20 \leq \Delta T < 40$ High Thermal Condition *"Monitor until repair is completed"*

(e) $\Delta T \geq 40$ Abnormal Condition *"Requires immediate action"*

(D)

Figure 4.4: Thermogram of electrical components at warming stage;
(A = Molded case circuit breaker IRT image),
(B = Electric motor bearing IRT image),
(C = Electric motor IRT image),
(D = Connector IRT image).

Also the defect detection analysis results of processed IRT images of electrical facility in Figure 4.5 (A_e) indicates the abnormal thermal region of a distribution transformer under critical situation hence "requires immediate attention". The IRT image in Figure 4.5 (A_d), shows the thermal signature of high thermal condition. Electrical equipment found within this high thermal region has serious faults therefore "requires some follow-up attention until repair is completed". Figure 4.5 (A_c), indicate the IRT region of the warming temperature stage; equipment within this warming temperature region has minor fault; "requires maintenance and repair action as time permits". Figure 4.5 (A_b), indicates equipment under normal condition with no fault therefore, needs no attention other than the normal routine check. Ambient temperatures are rarely easy to ascertain because of variations in atmospheric weather condition, which affects the overall equipment temperature that leads to low accuracy rate in quantitative analysis result so may or not be included in the analysis report. It is shown in Figure 4.5 (A_a). Background images should not be included in the analysis report as mentioned in the introductory part of this chapter 4 because it has nothing to do with the equipment under inspection. The same analysis applies in Figures (4.5 $B_{(e-a)}$ to 4.5 $E_{(e-a)}$).

Based on the defect detection scrutiny analysis results, the mathematical operations performed in chapter 3.4, the application of the derived formulas (3.16) and (3.17), the conversion process of pixel values of each classified regions into its actual equivalent thermal value (℃) and the IEEE thermal evaluation standards in Table 3.8. It was proved that Figures (4.5A – 4.5E) are found to be critically abnormal after thorough scrutinization with the developed defect detection scrutiny system therefore; immediate attention is required on these equipments and components.

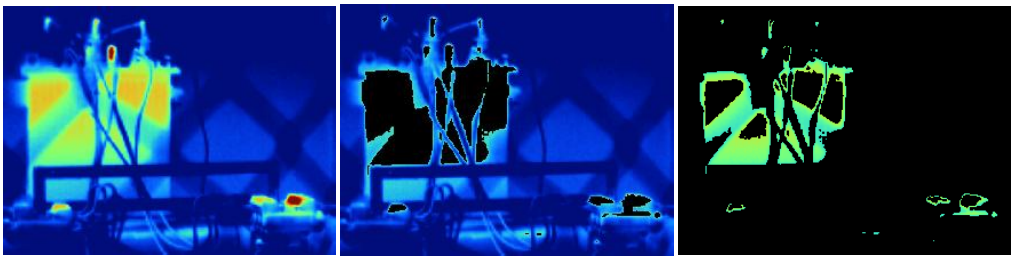

Original IRT Image

(a) AmbientTemperature Region

(b) $\Delta T \leq 10$
Normal Condition
"No action required"

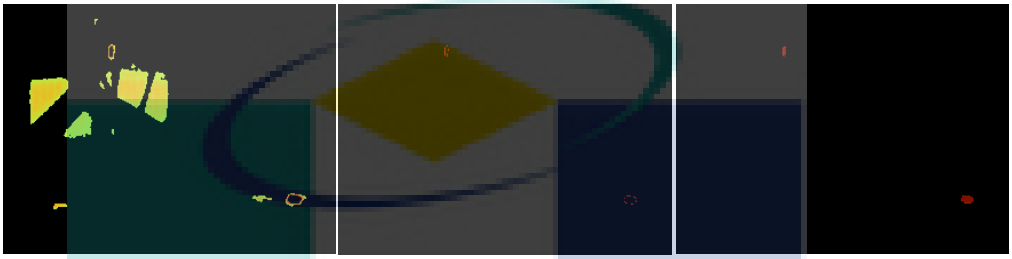

(c) $10 < \Delta T < 20$
Warming Condition
"Requires attention as time permits"

(d) $20 \leq \Delta T < 40$
High Thermal Condition
"Monitor until repair is completed"

(e) $\Delta T \geq 40$
Abnormal Condition
"Requires immediate action"

(A)

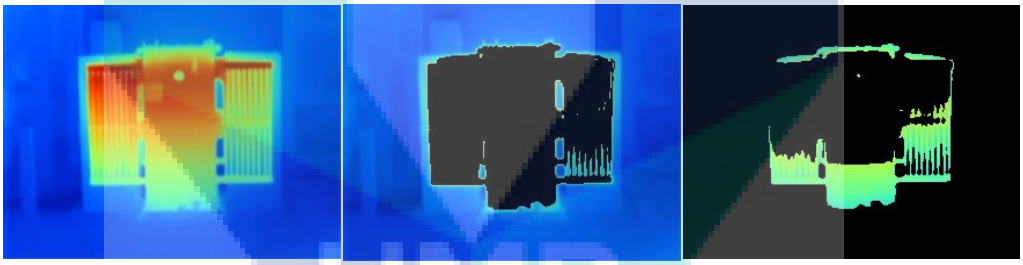

Original IRT Image

(a) AmbientTemperature Region

(b) $\Delta T \leq 20$
Normal Condition
"No action required"

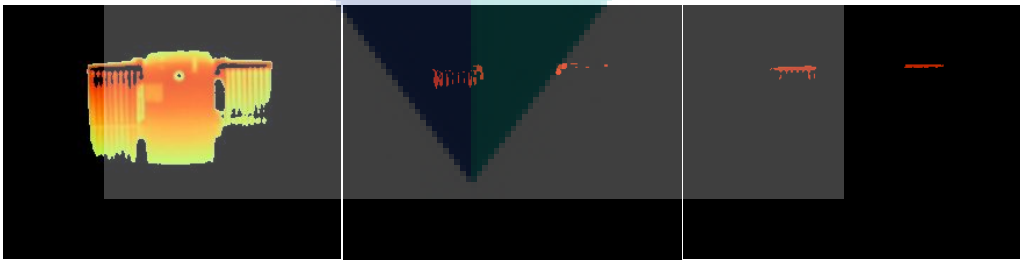

(c) $20 < \Delta T < 45$
Warming Condition
"Requires attention as time permits"

(d) $45 \leq \Delta T < 65$
High Thermal Condition
"Monitor until repair is completed"

(e) $\Delta T \geq 65$
Abnormal Condition
"Requires immediate action"

(B)

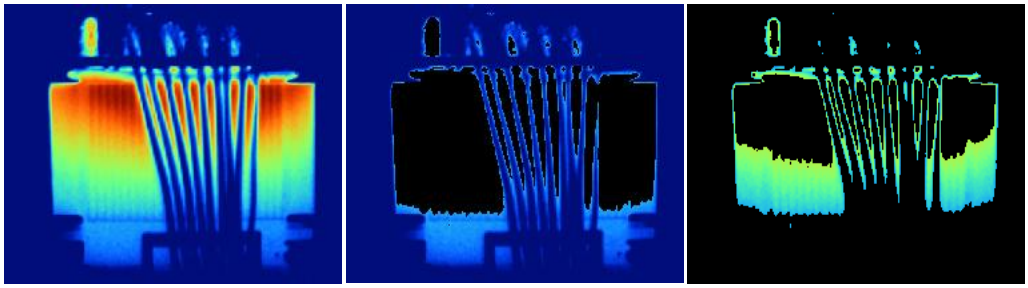

Original IRT Image (a) AmbientTemperature Region (b) $\Delta T \leq 20$ Normal Condition *"No action required"*

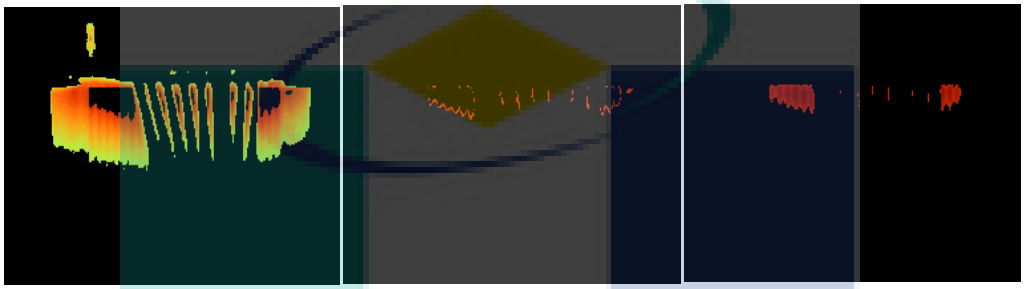

(c) $20 < \Delta T < 45$ Warming Condition *"Requires attention as time permits"* (d) $45 \leq \Delta T < 65$ High Thermal Condition *"Monitor until repair is completed"* (e) $\Delta T \geq 65$ Abnormal Condition *"Requires immediate action"*

(C)

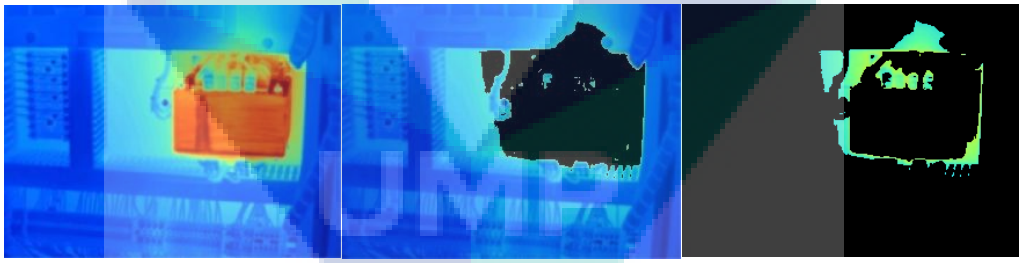

Original IRT Image (a) AmbientTemperature Region (b) $\Delta T \leq 20$ Normal Condition *"No action required"*

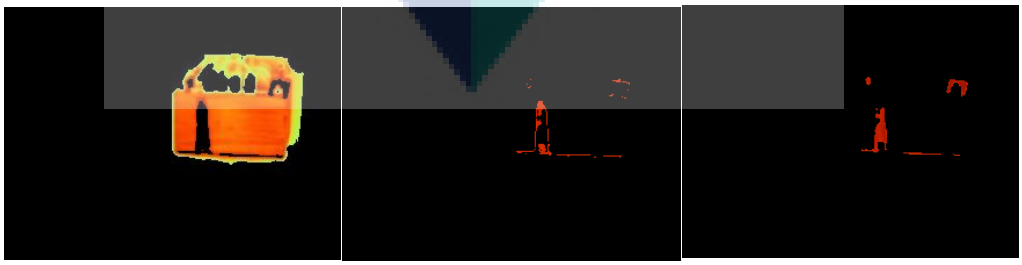

(c) $20 < \Delta T < 45$ Warming Condition *"Requires attention as time permits"* (d) $45 \leq \Delta T < 65$ High Thermal Condition *"Monitor until repair is completed"* (e) $\Delta T \geq 65$ Abnormal Condition *"Requires immediate action"*

(D)

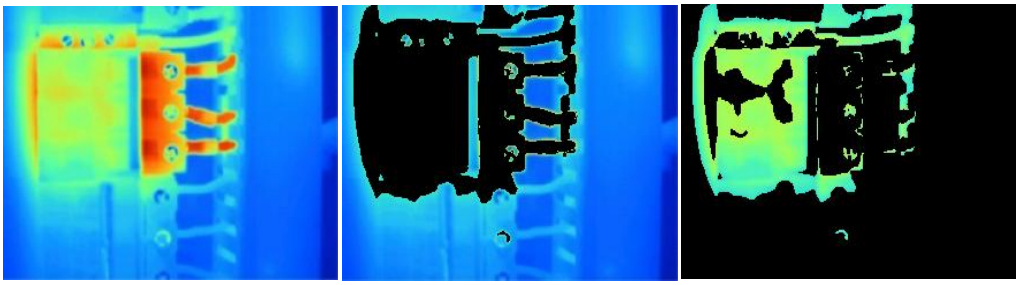

Original IRT Image (a) AmbientTemperature Region (b) $\Delta T \leq 20$ Normal Condition *"No action required"*

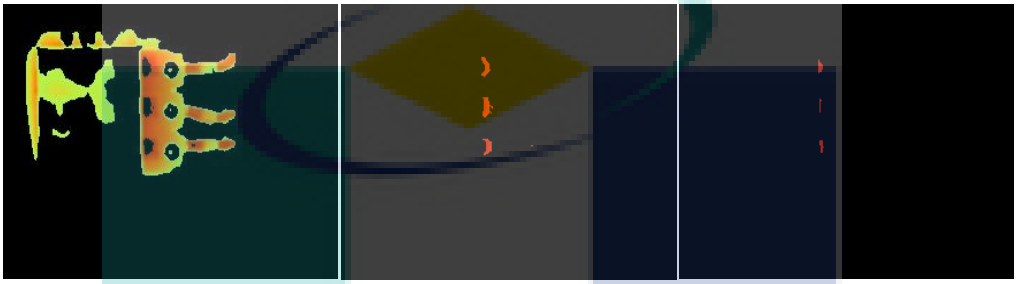

(c) $20 < \Delta T < 45$ Warming Condition *"Requires attention as time permits"* (d) $45 \leq \Delta T < 65$ High Thermal Condition *"Monitor until repair is completed"* (e) $\Delta T \geq 65$ Abnormal Condition *"Requires immediate action"*

(E)

Figure 4.5: Thermogram of electrical components under abnormal condition; (A = Bolted joint and connector IRT image), (B = Distribution transformer IRT image), (C = Distribution transformer IRT image), (D = Dry type transformer IRT image), (E = Circuit breaker IRT image).

4.7 DECISION-MAKING, SENSITIVITY, AND ACCURACY RESULTS

In summary, the efficacy of the proposed RGB optimal threshold algorithm and thermal imaging technology for defect detection on electrical power equipment can be seen from the infrared thermal image of the oil immerse distribution transformer under abnormal thermal conditions as presented in Figure 4.6. This conclusion was based on the fact that certain portions of the oil immerse distribution transformer thermogram are seen in the abnormal thermal region after thorough feature extraction and classification. Hence, the decision made; that this oil immerse distribution transformer was in critical thermal operating condition at the time of inspection. Therefore immediate action is required on this oil immerse distribution transformer to save it from total failure.

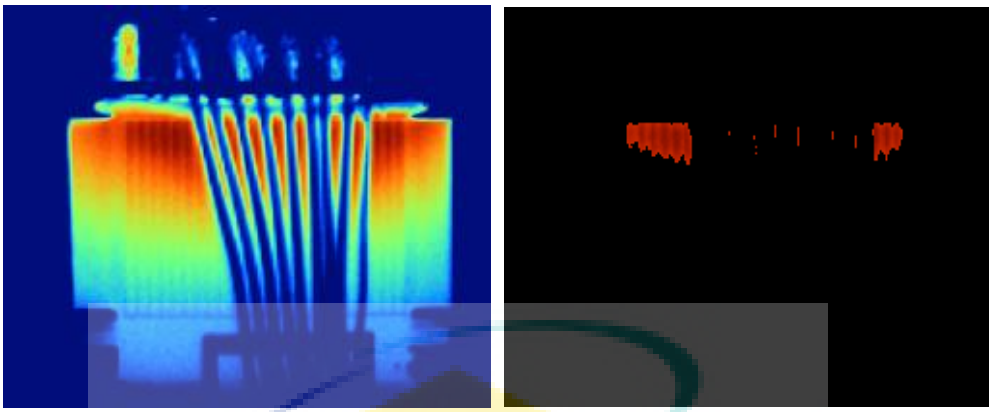

Original Infrared Thermal Image Abnormal Thermal Region
"Requires immediate action"

Figure 4.6: RGB optimal threshold classification result of abnormal transformer

In like manner, the efficacy of the proposed RGB optimal threshold algorithm and thermal imaging technology for defect detection on electrical power equipment can be seen from the infrared thermal image of the power fuse box under high thermal condition as presented in Figure 4.7. This conclusion was based on the fact that certain portions of the power fuse box thermogram are seen in the high thermal region after thorough feature extraction and classification. Hence, the decision made was that this power fuse box was in high thermal operating condition at the time of inspection. Therefore this power fuse box requires monitoring until repair is completed.

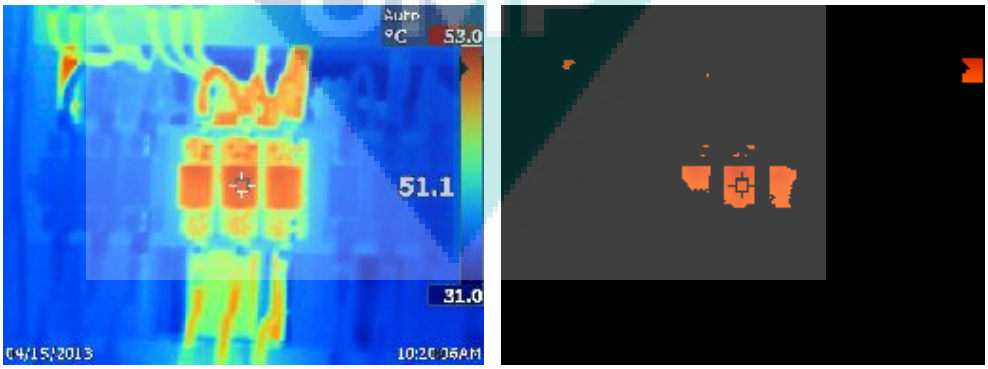

Original Infrared Thermal Image High Thermal Region
"Monitor until repairis completed"

Figure 4.7: RGB optimal threshold classification result of high thermal fuse box

In like manner, the efficacy of the proposed RGB optimal threshold algorithm and thermal imaging technology for defect detection on electrical power equipment can be seen from the infrared thermal image of the electric motor under warming temperature conditions as presented in Figure 4.8. This conclusion was based on the fact that certain portions of the electric motor thermogram are seen in the warming thermal region after thorough feature extraction and classification. Hence, the decision made was that this electric motor was in warming thermal operating condition at the time of inspection. Therefore this electric motor requires attention as time permits.

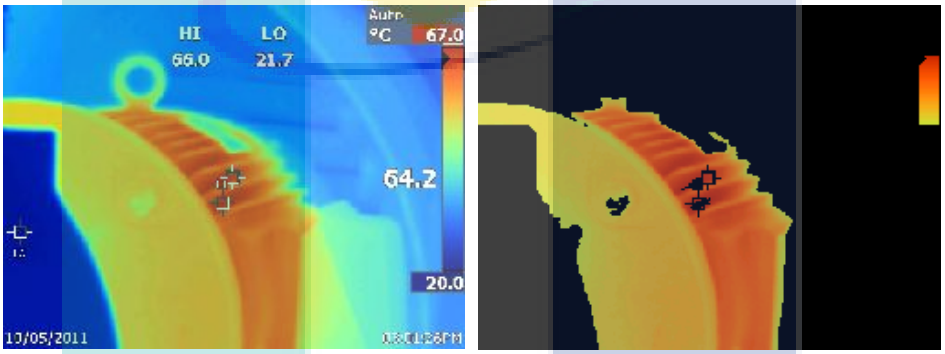

Original Infrared Thermal Image

Warming Region
"Requires attention as time permits"

Figure 4.8: RGB optimal threshold classification result of warm thermal condition electric motor

Also the efficacy of the proposed RGB optimal threshold algorithm and thermal imaging technology for defect detection on electrical power equipment can be seen from the infrared thermal image of the minitured circuit breaker under normal temperature conditions as presented in Figure 4.9. This conclusion was based on the fact that certain portions of the minitured circuit breaker thermogram are seen in the normal thermal condition region after thorough feature extraction and classification. Hence, the decision made was that this minitured circuit breaker was in normal thermal operating condition at the time of inspection. Therefore this minitured circuit breaker requires no repair and maintenance action other than the routine check.

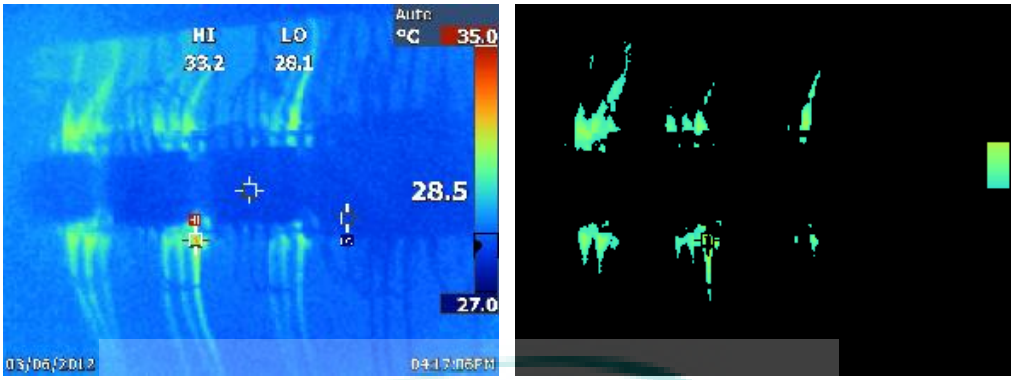

Original Infrared Thermal Image Normal Condition
"No action required"

Figure 4.9: RGB optimal threshold classification result of normal thermal condition minitured circuirt breaker

Also the efficacy of the proposed RGB optimal threshold algorithm and thermal imaging technology for defect detection on electrical power equipment can be seen from the infrared thermal image of the electric motor within ambient temperature conditions as presented in Figure 4.10. This conclusion was based on the fact that certain portions of the electric motor thermogram are seen in the within ambient temperature region after thorough feature extraction and classification. Hence, the decision made was that this electric motor was within ambient temperature operating condition at the time of inspection. Therefore this electric motor requires no attention other than the routine check.

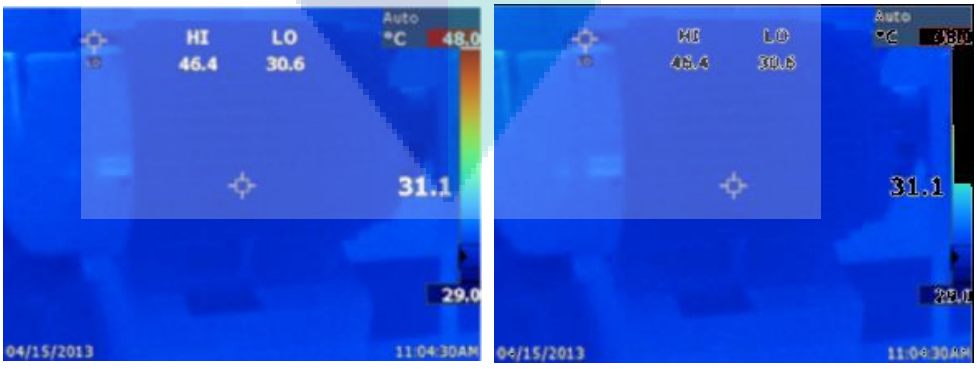

Original Infrared Thermal Image Ambient Temperature Region

Figure 4.10: RGB optimal threshold classification result of electric motor within ambient temperature

The comprehensive statistical inferences drawn from all the equations and Formulas applied in the development of the defect detection scrutiny system as well as mathematical analysis results from Sensitivity, Predictive Positive Value (PPV) and False Positive Rate (FPR) for low, medium and high temperature of inspected electrical power equipment and components are summarized in Table (4.1 – 4.3). It was recorded that the proposed defect detection technique gave 99.9% sensitivity from low temperature electrical power equipment and components. The error value of 0.1% was also calculated. This error value was encountered during experimental thermal inspection data acquisition which was attributed to either over caution or less caution. The sensitivity records from medium and high temperature electrical power equipment and components was found to be 100%.

Table 4.1: Sensitivity, predictive positive value (PPV) and false positive rate (FPR) (Low temperature equipment)

Optimal Threshold Values			Region Pixel Value	ΔT Criteria (℃)	Sensitivity (%)	PPV (%)
Red	**Green**	**Blue**				
200	81	125	406	ΔT≥40	16.9	99.7
201	89	150	440	20≤ΔT<40	18.3	99.6
90	200	196	486	10<ΔT<20	20.2	99.6
199	215	109	523	ΔT≤10	21.8	99.6
200	216	120	546	- - - - -	22.7	99.6
STATISTICS						
Sampled IRT Images		**FPR Value (%)**	**Total Pixel Value**	**ΔT Range (℃)**	**Overall Sensitivity (%)**	**Mean PPV (%)**
15		± 0.1	2401	ΔT ≥40	99.9	99.6

Table 4.2: Sensitivity, predictive positive value (PPV) and false positive rate (FPR) (Medium temperature equipment)

Optimal Threshold Values			Region Pixel Value	ΔT Criteria (℃)	Sensitivity (%)	PPV (%)
Red	Green	Blue				
190	55	70	315	ΔT≥60	14.7	99.6
191	55	105	351	45≤ΔT<60	16.4	99.6
56	200	175	431	20<ΔT<45	20.1	99.6
199	185	119	503	ΔT≤20	23.4	99.6
240	186	120	546	- - - - -	25.4	99.6
STATISTICS						
Sampled IRT Images	**FPR Value (%)**		**Total Pixel Value**	**ΔT Range (℃)**	**Overall Sensitivity (%)**	**Mean PPV (%)**
22	± 0		2146	ΔT ≥60	100	99.6

Table 4.3: Sensitivity, predictive positive value (PPV) and false positive rate (FPR) (High temperature equipment)

Optimal Threshold Values			Region Pixel Value	ΔT Criteria (℃)	Sensitivity (%)	PPV (%)
Red	Green	Blue				
100	35	35	170	ΔT≥75	8.4	99.6
215	40	70	325	65≤ΔT<75	16.1	99.6
41	201	196	438	30<ΔT<65	21.7	99.6
200	230	117	575	ΔT≤30	28.5	99.6
200	229	81	510	- - - - -	25.3	99.6
STATISTICS						
Sampled IRT Images	**FPR Value (%)**		**Total Pixel Value**	**ΔT Range (℃)**	**Overall Sensitivity (%)**	**Mean PPV (%)**
10	± 0		2018	ΔT ≥75	100	99.6

Description of experimental thermal inspection accuracy of electrical power equipment and components. A total of one hundred eleven (111) samples of electrical power equipment and components was inspected in this research project. Table 4.4 presents the description of the inspected equipment and components showing the statistics of accuracy in percentage. It was observed that 81.08(%) of all the inspected electrical power equipment and components was within warming thermal operating condition, 14.14(%) of all the inspected electrical power equipment and components was found within a high thermal operating condition, and 4.50(%) of all the inspected electrical power equipment and components was found within abnormal thermal operating condition. Statistically, the sum of the overall infrared thermal inspection accuracy was calculated as 99.72(%). In other words, an error value of 0.28(%) was attributed to mistakes due to over or less caution during the experimental thermal inspection on electrical power equipment and components.

Table 4.4: Description of thermal inspection of electrical facilities and accuracy

Equipment/Components	Number of Samples	Warming Condition	High Temp. Condition	Abnormal Condition
Oil-Immerse Distribution Transformers 11KV/415V	14	13		1
Dry Type Distribution Transformers 11KV/415V	1	1		
3-phase Panel Mount Auto Transformers	1			1
Molded Case Circuit Breaker 3-phase	16	13	2	1
Miniature Circuit Breakers 3-phase	22	22		
3-phase Electric Motors	17	12	4	1
3-phase Capacitors in capacitor bank	7	7		
Resistors 220V, 2kW heating elements	7	4	3	
3-Phase Transformers	7	4	3	
3-phase Connectors	6	4	1	1

Table 4.4:Continued

3-phase Contactors	9	6	3	
Fuse	4	4		
Total Samples	111	90	16	5

Accuracy of Inspected Electrical Equipment and Components

Warming Condition	High Temp. Condition	Abnormal Condition	Overall Accuracy
81.08**(%)**	14.14**(%)**	4.50**(%)**	99.72**(%)**

4.8 RESULTS OF K-MEAN CLUSTERING ALGORITHM

Each infrared thermal image represented by one attribute point is an example of the K means clustering algorithm and it is assigned automatically to one of the cluster as shown in Figure 4.11 (a – j). This is an unsupervised learning because the algorithm segments the IRT image automatically based on the criteria of minimum distance to the centroid.

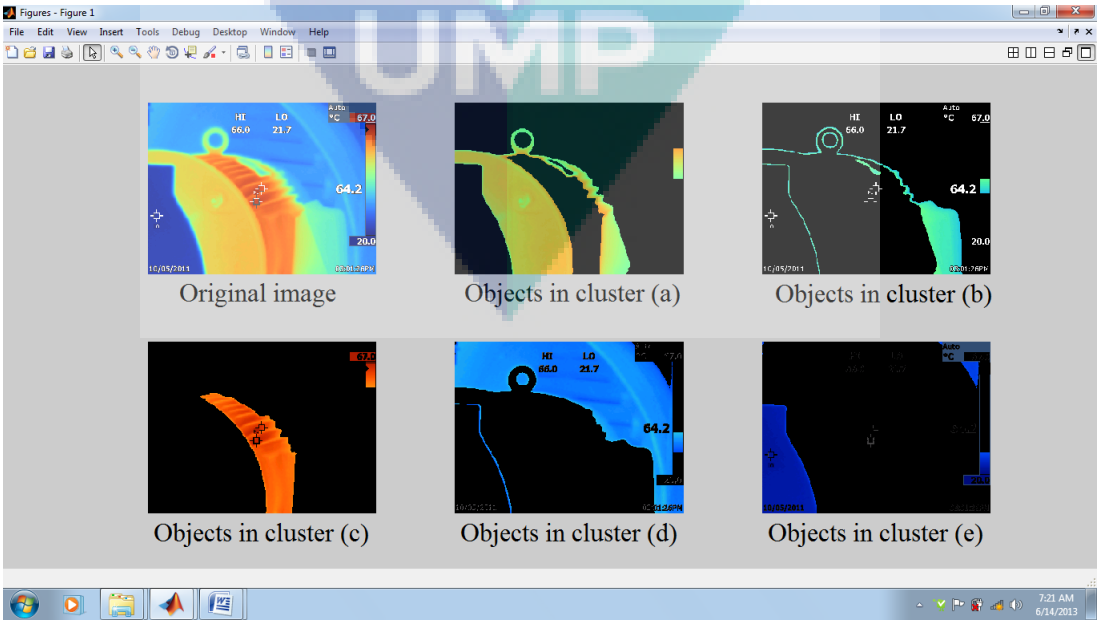

Screen print of unsupervised K means clustering algorithm

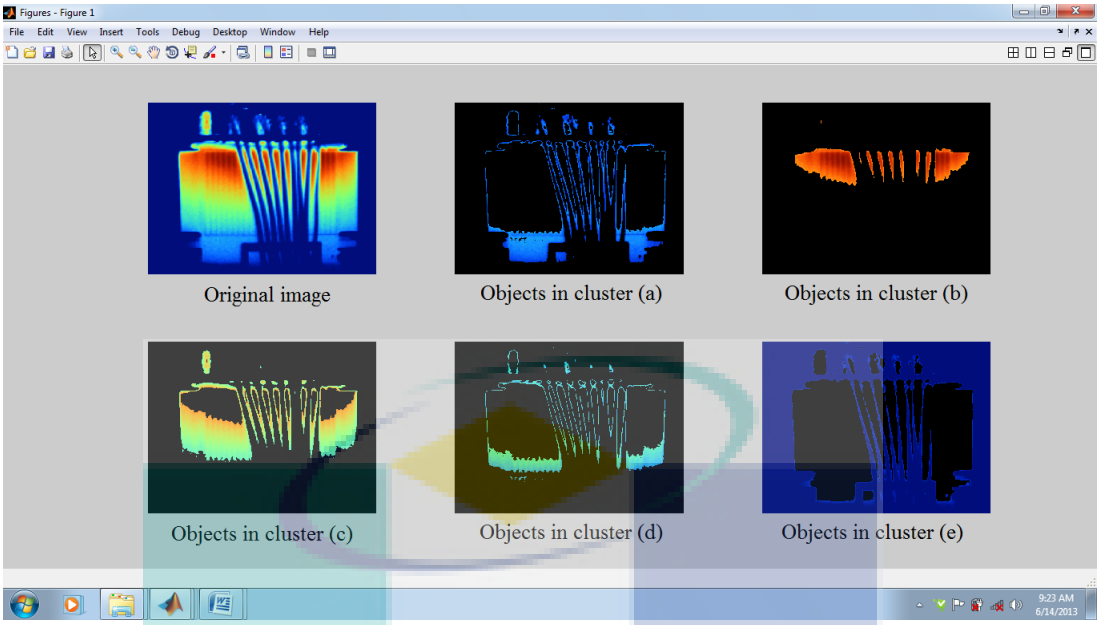

Screen print of unsupervised K means clustering algorithm

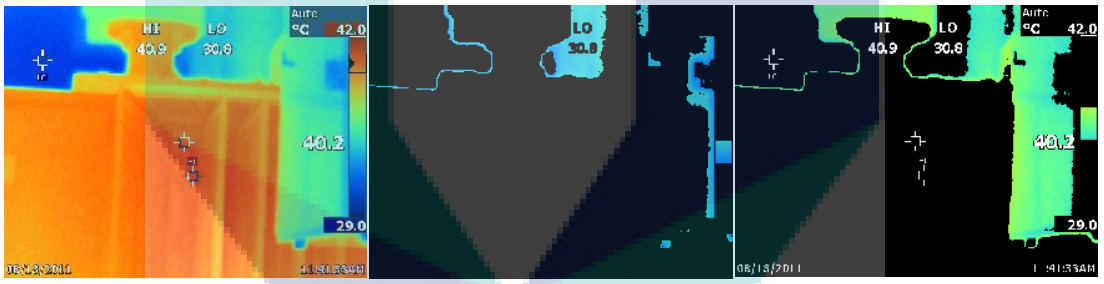

Original image Objects in cluster (a) Objects in cluster (b)

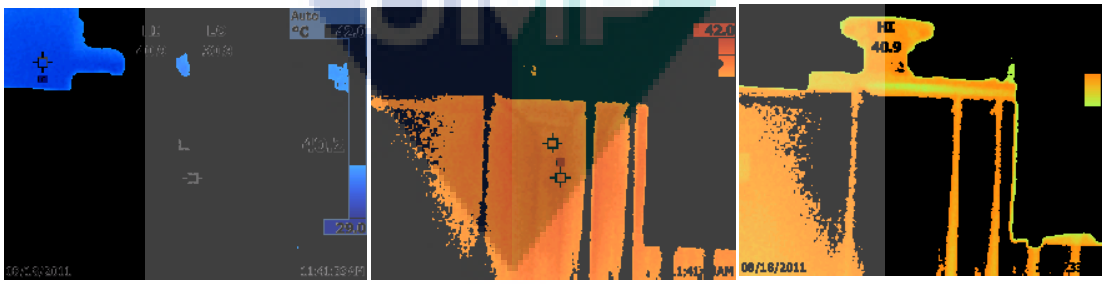

Objects in cluster (c) Objects in cluster (d) Objects in cluster (e)

(a)

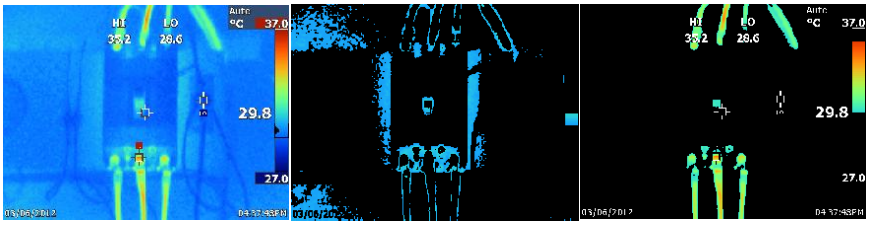

Original image | Objects in cluster (a) | Objects in cluster (b)

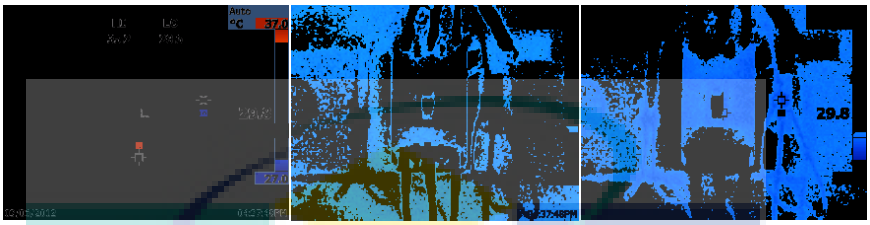

Objects in cluster (c) | Objects in cluster (d) | Objects in cluster (e)

(b)

Original image | Objects in cluster (a) | Objects in cluster (b)

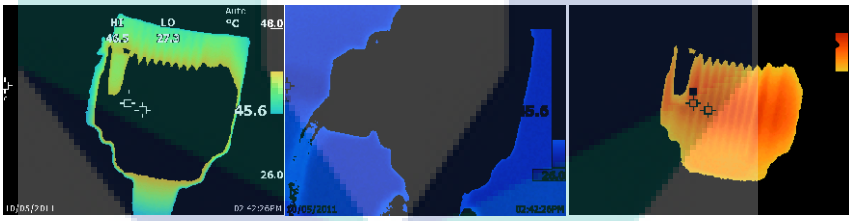

Ojects in cluster (c) | Objects in cluster (d) | Objects in cluster (e)

(c)

Original image | Objects in cluster (a) | Objects in cluster (b)

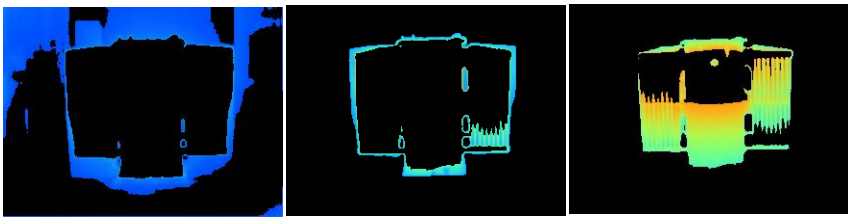

Ojects in cluster (c) | Objects in cluster (d) | Objects in cluster (e)

(d)

Original image Objects in cluster (a) Objects in cluster (b)

Ojects in cluster (c) Objects in cluster (d) Objects in cluster (e)

(e)

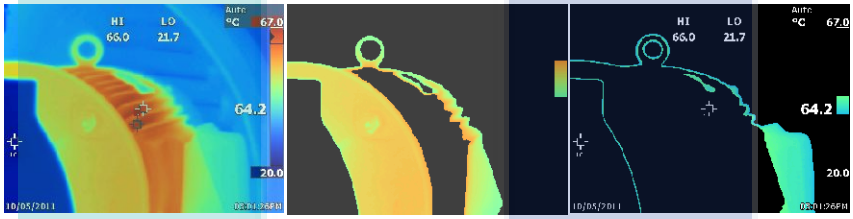

Original image Objects in cluster (a) Objects in cluster (b)

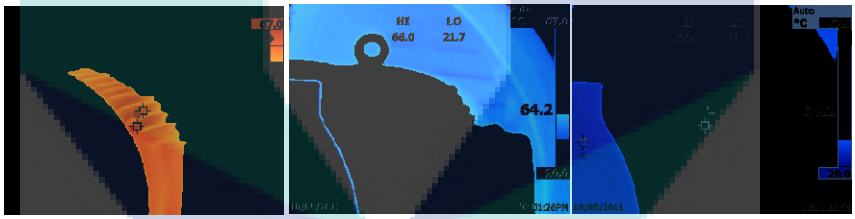

Ojects in cluster (c) Objects in cluster (d) Objects in cluster (e)

(f)

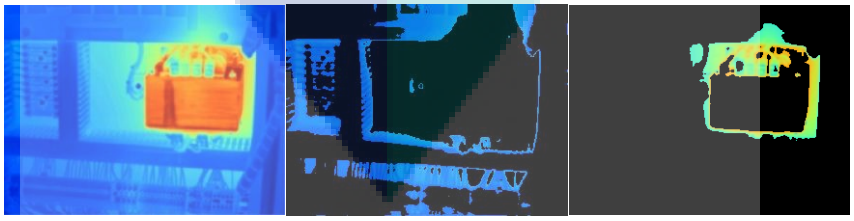

Original image Objects in cluster (a) Objects in cluster (b)

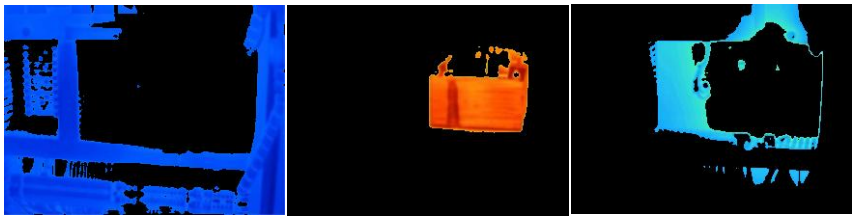

Ojects in cluster (c) Objects in cluster (d) Objects in cluster (e)

(g)

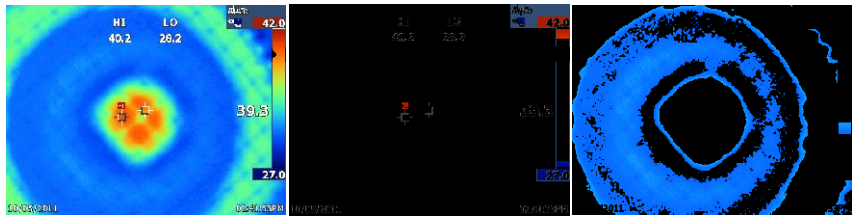

Original image | Objects in cluster (a) | Objects in cluster (b)

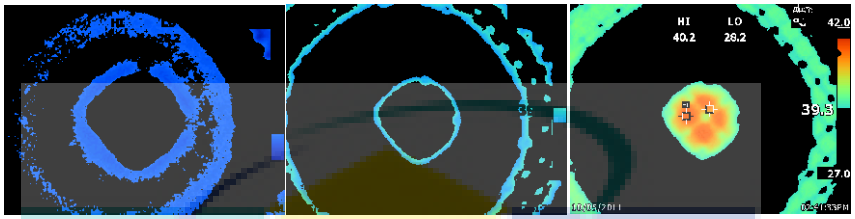

Ojects in cluster (c) | Objects in cluster (d) | Objects in cluster (e)

(h)

Original image | Objects in cluster (a) | Objects in cluster (b)

Ojects in cluster (c) | Objects in cluster (d) | Objects in cluster (e)

(i)

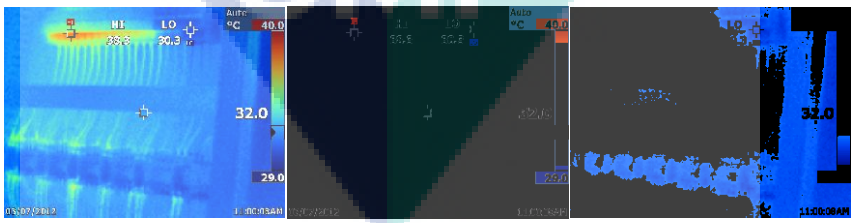

Original image | Objects in cluster (a) | Objects in cluster (b)

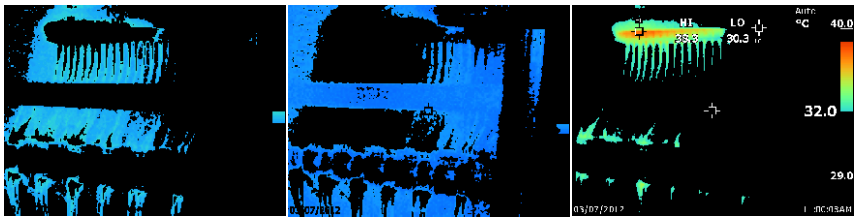

Ojects in cluster (c) | Objects in cluster (d) | Objects in cluster (e)

(j)

Figure 4.11: Results of unsupervised k-means clustering algorithm

The classification of the segmented IRT image clusters is done programmatically via supervised learning process. The learning process is depending on the training samples that were fed into the supervised K means classification algorithm. The results are presented in Figure 4.12 (a – j). All the Figures are thermogram of electrical facilities. The same samples of electrical facilities were used for the supervised training of the proposed RGB optimal threshold algorithm for defect detection on electrical power equipment and components. The results from the two algorithms (supervised K means classification and supervised RGB optimal threshold) have been compared with each other and discussed in chapter 4.9.

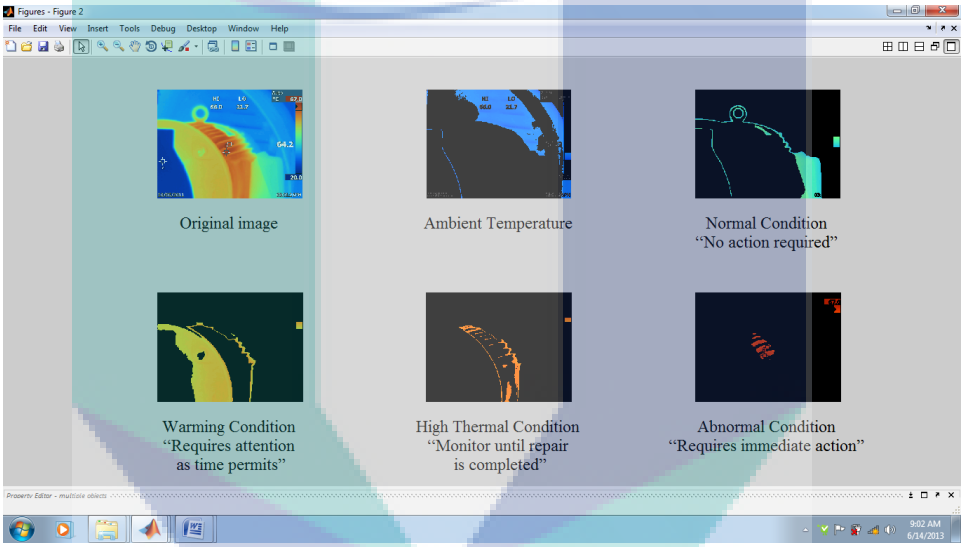

Screen print of supervised K means classification

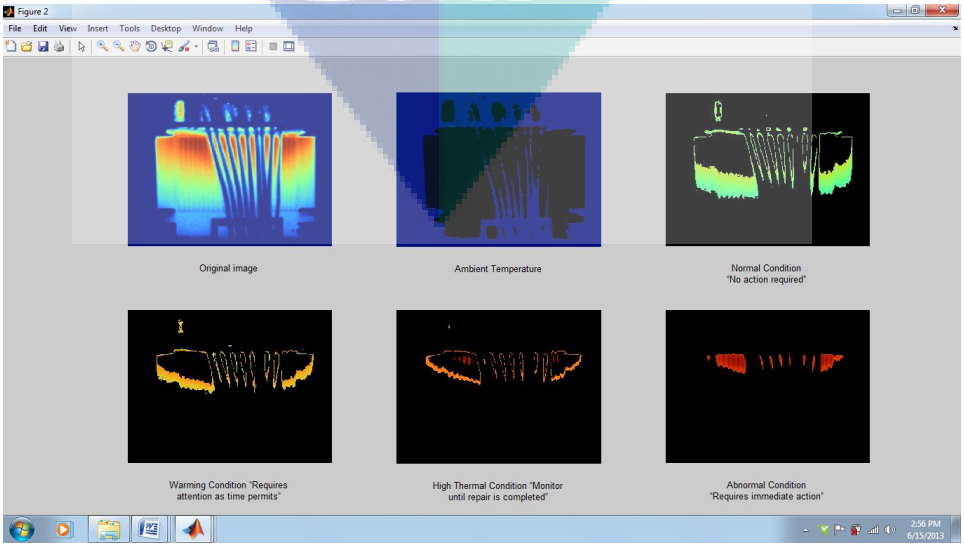

Screen print of supervised K means classification

Original image | Ambient Temperature Region | Normal Condition "No action required"

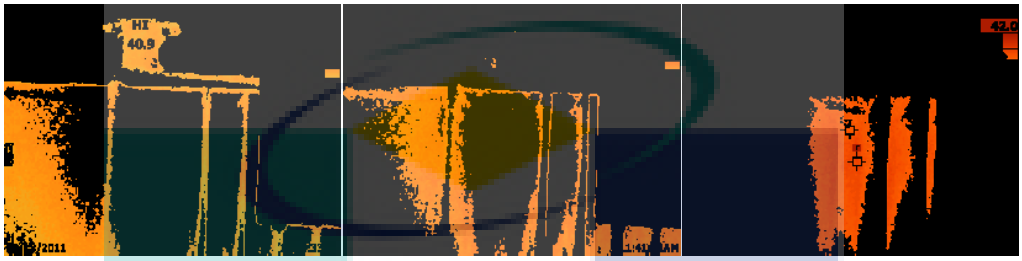

Warming Condition "Requires attention as time permits" | High Thermal Condition "Monitor until repair is completed" | Abnormal Condition "Requires immediate action"

(a)

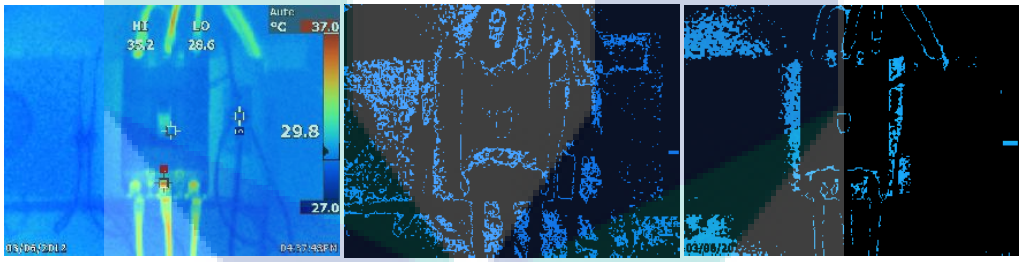

Original image | Ambient Temperature Region | Normal Condition "No action required"

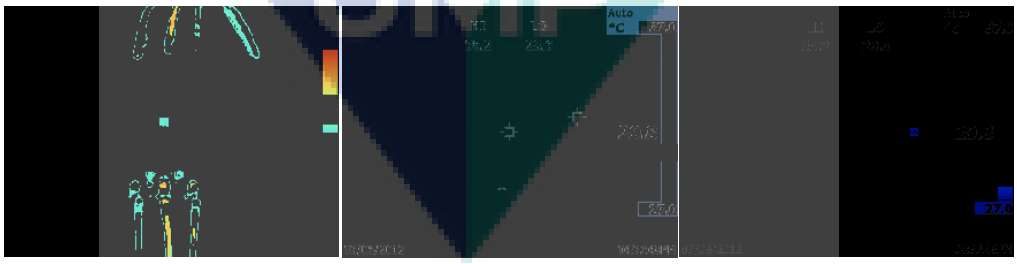

Warming Condition "Requires attention as time permits" | High Thermal Condition "Monitor until repair is completed" | Abnormal Condition "Requires immediate action"

(b)

Original

Ambient Temperature Region

Normal Condition
"No action required"

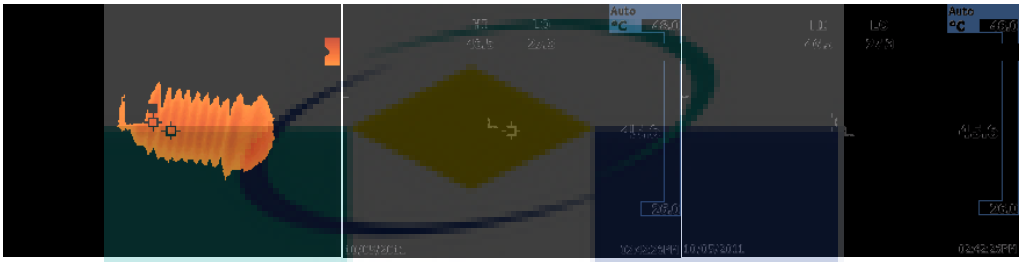

Warming Condition
"Requires attention as time permits"

High Thermal Condition
"Monitor until repair is completed"

Abnormal Condition
"Requires immediate action"

(c)

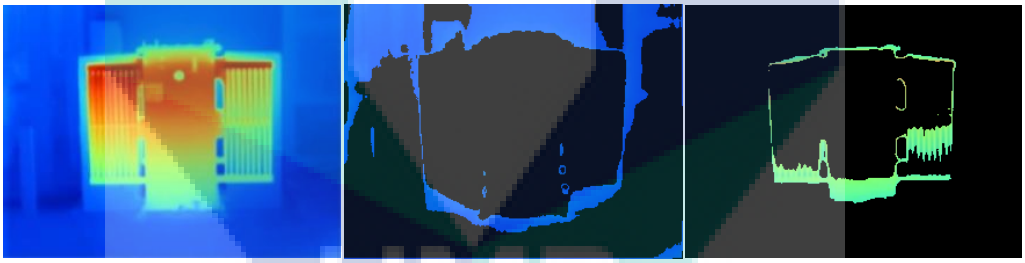

Original image

Ambient Temperature Region

Normal Condition
"No action required"

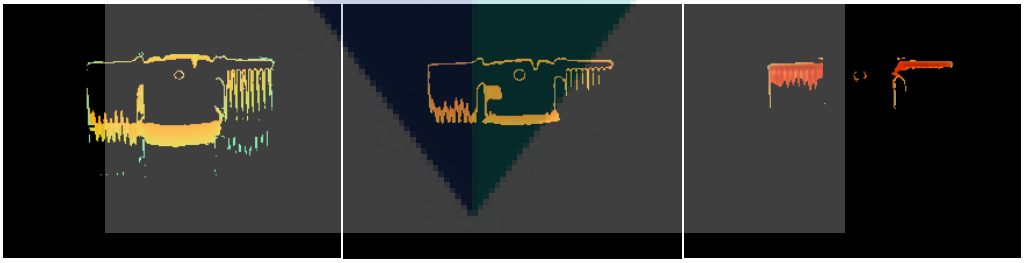

Warming Condition
"Requires attention as time permits"

High Thermal Condition
"Monitor until repair is completed"

Abnormal Condition
"Requires immediate action"

(d)

Original image | Ambient Temperature Region | Normal Condition "No action required"

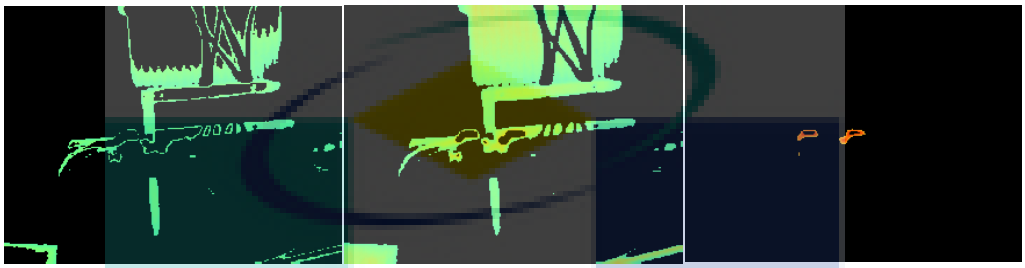

Warming Condition "Requires attention as time permits" | High Thermal Condition "Monitor until repair is completed" | Abnormal Condition "Requires immediate action"

(e)

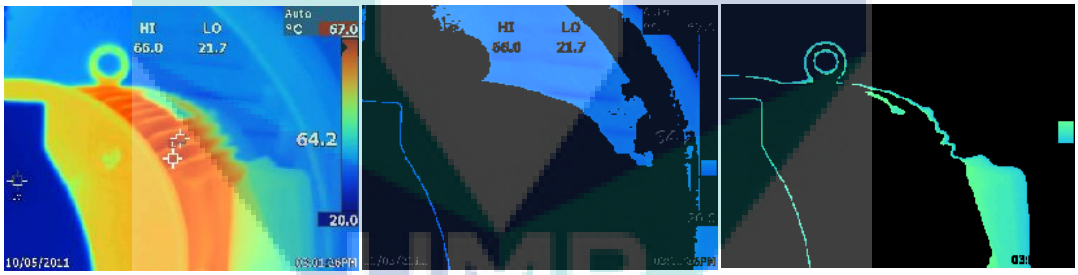

Original image | Ambient Temperature Region | Normal Condition "No action required"

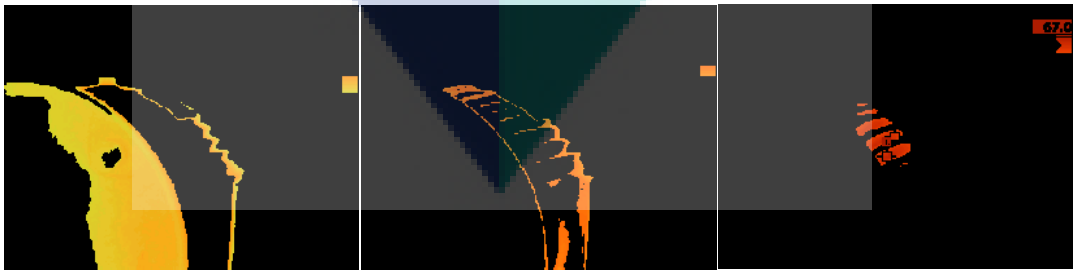

Warming Condition "Requires attention as time permits" | High Thermal Condition "Monitor until repair is completed" | Abnormal Condition "Requires immediate action"

(f)

Original image | Ambient Temperature Region | Normal Condition "No action required"

Warming Condition "Requires attention as time permits" | High Thermal Condition "Monitor until repair is completed" | Abnormal Condition "Requires immediate action"

(g)

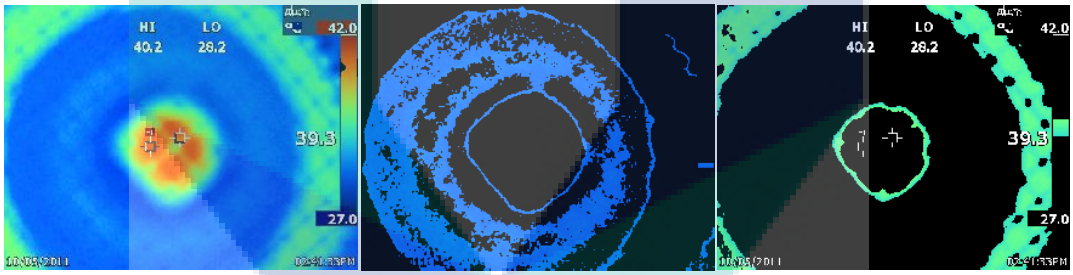

Original image | Ambient Temperature Region | Normal Condition "No action required"

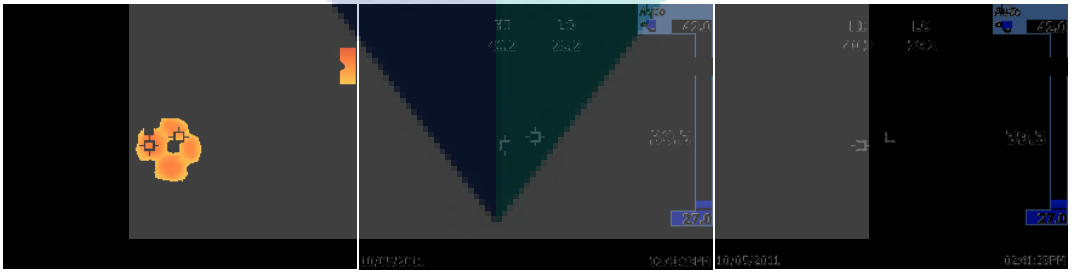

Warming Condition "Requires attention as time permits" | High Thermal Condition "Monitor until repair is completed" | Abnormal Condition "Requires immediate action"

(h)

Original image | Ambient Temperature Region | Normal Condition "No action required"

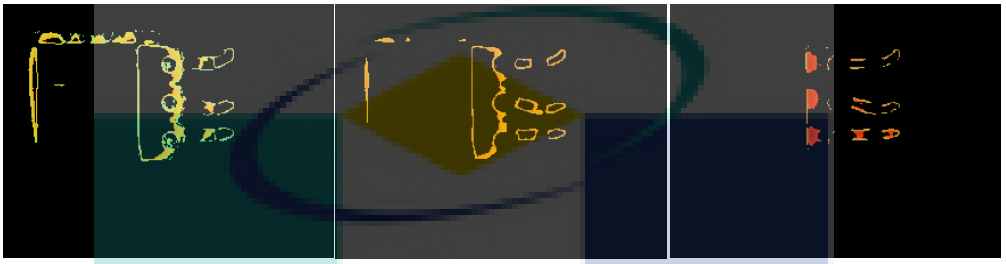

Warming Condition "Requires attention as time permits" | High Thermal Condition "Monitor until repair is completed" | Abnormal Condition "Requires immediate action"

(i)

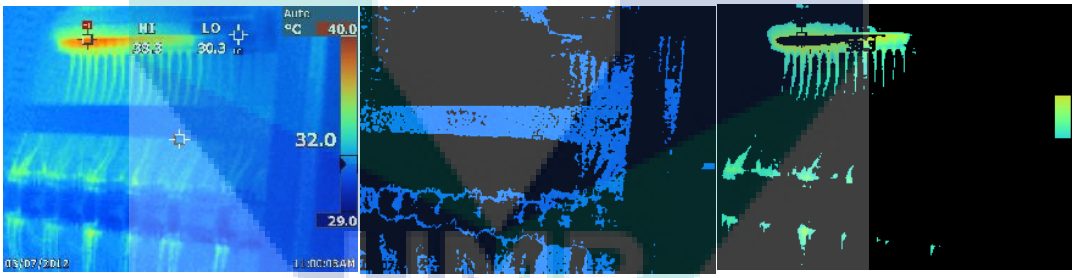

Original image | Ambient Temperature Region | Normal Condition "No action required"

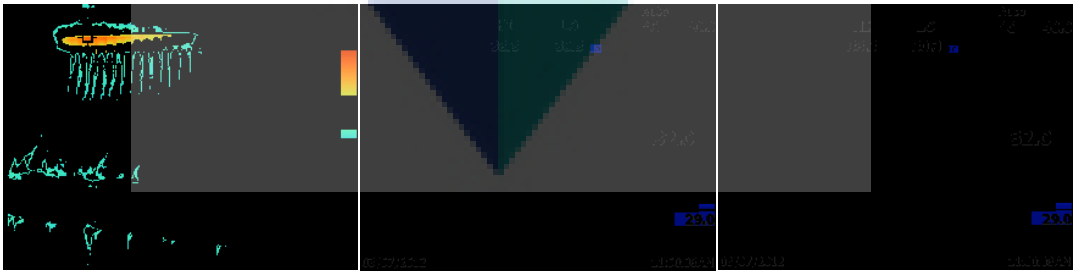

Warming Condition "Requires attention as time permits" | High Thermal Condition "Monitor until repair is completed" | Abnormal Condition "Requires immediate action"

(j)

Figure 4.12: Results of supervised K means classification

4.9 DEFECT DETECTION COMPARISON STUDY RESULTS

The comparative study on electrical power equipment and components defect detection technique was done between the supvervised RGB optimal threshold algorithm and the supvervised K means classification algorithm. For the RGB optimal threshold algorithm, the classification operation was based on the temperature range criteria refer to the defect detection training flow process in Figure 3.11 in subsection 3.7. While for the K means classification operation was programmically done based on the criteria of minimum distance to the centroid refer to the K means clustering algorithm flowchart in Figure 3.13 in subsection 3.7.

Within the limits of experimental errors, a total of one hundred eleven (111) samples of electrical power equipment and components was experimentally inspected and the same total number was also used for the comparision purpose in this research project. After equipment thermogram segmentation and classification using the two mentioned algorithms, it was confirmed that RGB optimal threshold algorithm proposed in this research is better than the K-means classification algorithm used for the same purpose of defect detection on electrical power equipment and components. It was observed that the supervised K-means classification algorithm sometimes do not give an accurate classification and judgement about equipment and components thermal operation status as can be seen in Figure 4.11, so understanding of the defective part of electrical power equipment and components based on the K means classification algorithm becomes difficult. In other words, there is inconsistency in defect detection with supervised K-means classification algorithm. Consequently, supervised K-means classification algorithm is not self explanatory like the supervised RGB optimal threshold algorithm. Also there are missing pixels as well as unnecessary repetitions among the processed image segments or clusters. It was also observed that K-means algorithm often produces empty blocks or clusters at higher iterations. Though supervised K-means classification algorithm can be used in situations where attention to specific regions of interest is needed such as defects in electrical equipment and components, but it takes longer processing time. However, K-means clustering algorithm has one unique advantage which is its undependability on the color palette

which means that, it has the ability to extract features from a color object or image irrespective of the color resolution involved.

The electrical power equipment and components thermogram in Figure 4.13 shows the results from the proposed RGB optimal threshold algorithm and the results of the supervised K-means classification algorithm. In Figure 4.13, eleven (*11*) processed samples of electrical power equipment and components were used to ascertain the accuracy level of the two algorithms (supvervised RGB optimal threshold and supvervised K means classification) implemented in this project for thermal defect detection on electrical power equipment and components. The results in Figure 4.13, showed that (*3/11*) processed samples of electrical power equipment were wrongly classified and judged by the supervised K means classification algorithm as compared with the proposed supervised RGB optimal threshold algorithm. The reason for the wrong classification and judgement was because of the inability of the supervised K means classification programme to accommodate wide range of threshold values which also led to the missing image pixels in the classification result. Secondly, the criteria for the minimum distance to the centiroid is automatically (unsupervised) determined in the image clustering algorithm prior to the supervised classification algorithm. This issue also affects the classification result. The first three (*3*) electrical power equipment in Figure 4.13 are samples of the wrongly judged and classified electrical power facilities and the other eight (*8*) electrical power equipment gave the same classification and judgement.

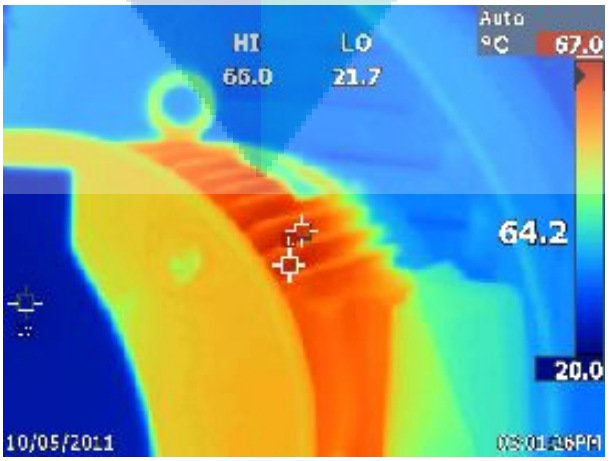

(a) Original image

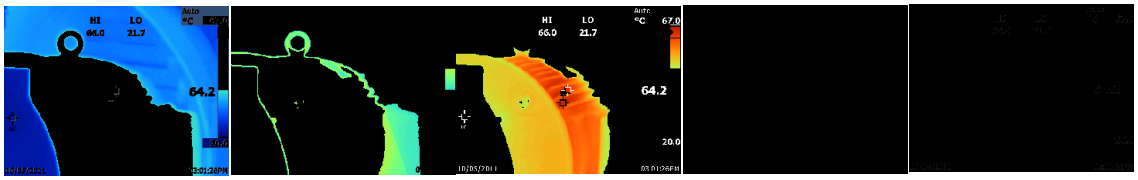

(Region b) (Region c) (Region d) (Region e) (Region f)

Supervised RGB optimal threshold classification result

(Region b) (Region c) (Region d) (Region e) (Region f)

Supervised K means classification result

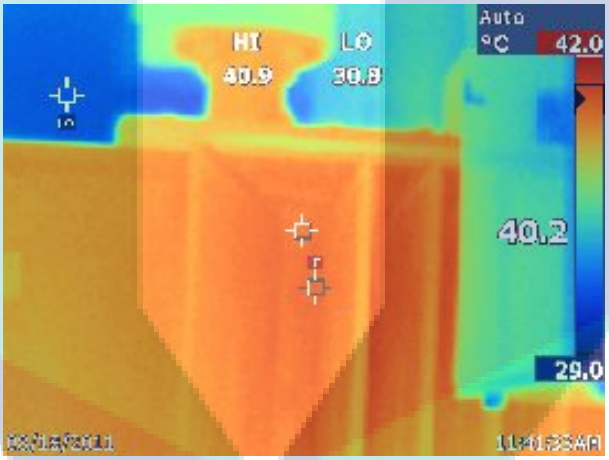

(a) Original image

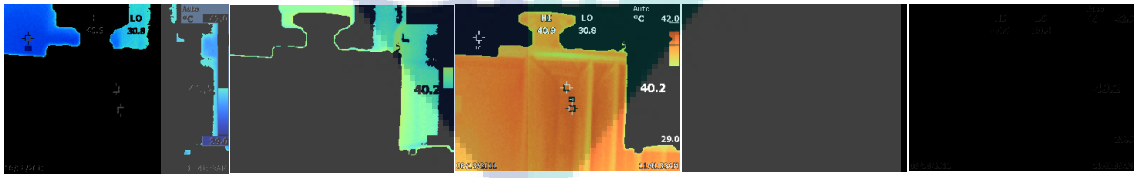

(Region b) (Region c) (Region d) (Region e) (Region f)

Supervised RGB optimal threshold classification result

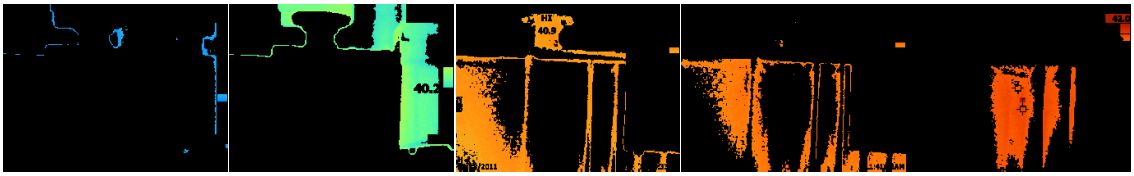

(Region b) (Region c) (Region d) (Region e) (Region f)

Supervised K means classification result

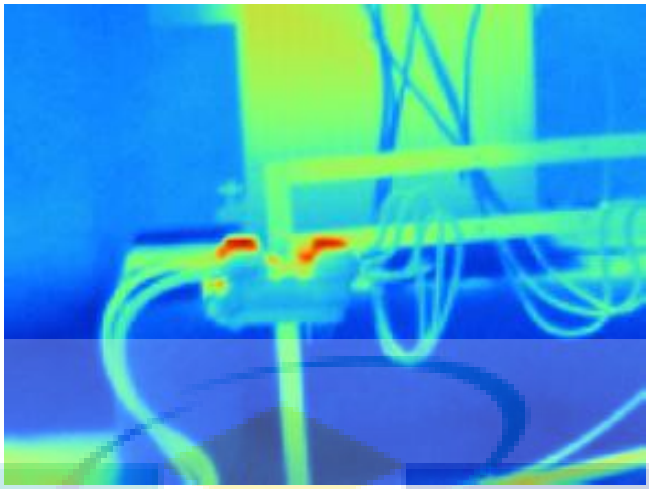

(a) Original image

(Region b) (Region c) (Region d) (Region e) (Region f)

Supervised RGB optimal threshold classification result

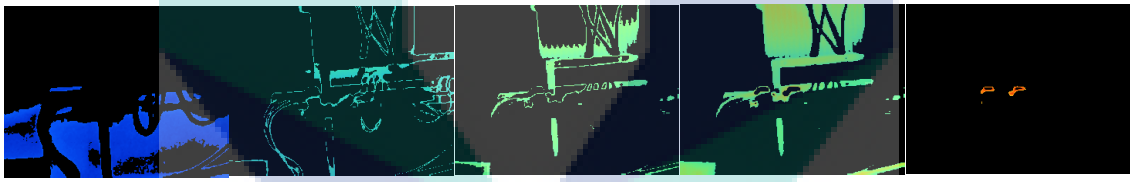

(Region b) (Region c) (Region d) (Region e) (Region f)

Supervised K means classification result

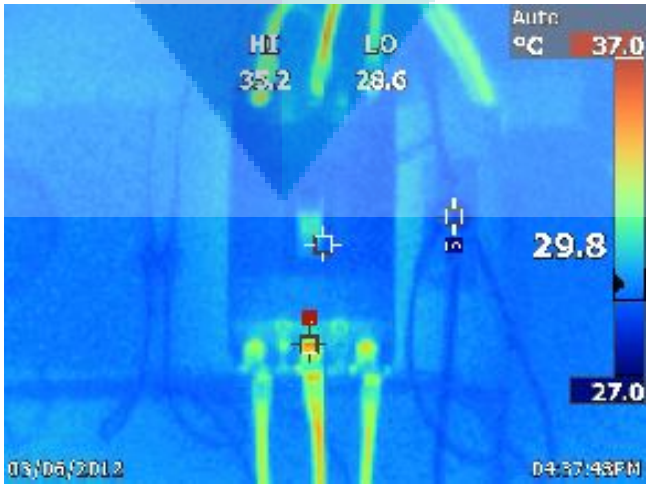

(a) Original image

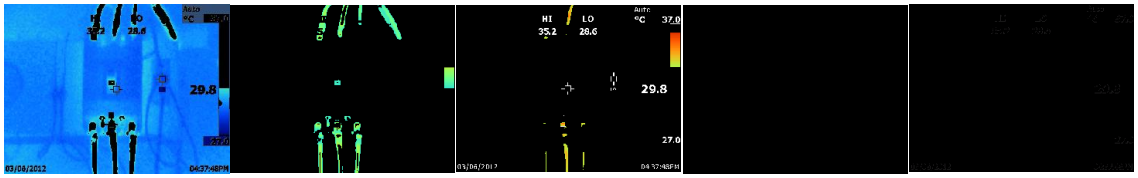

(Region b) (Region c) (Region d) (Region e) (Region f)

Supervised RGB optimal threshold classification result

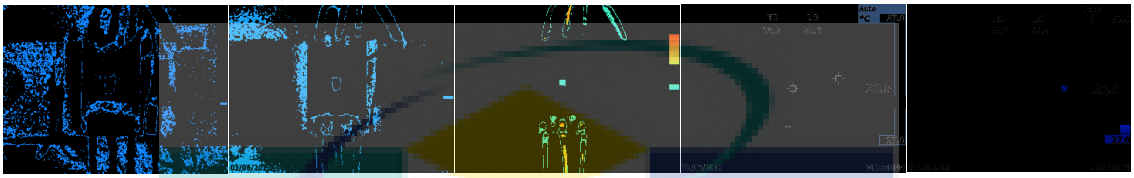

(Region b) (Region c) (Region d) (Region e) (Region f)

Supervised K means classification result

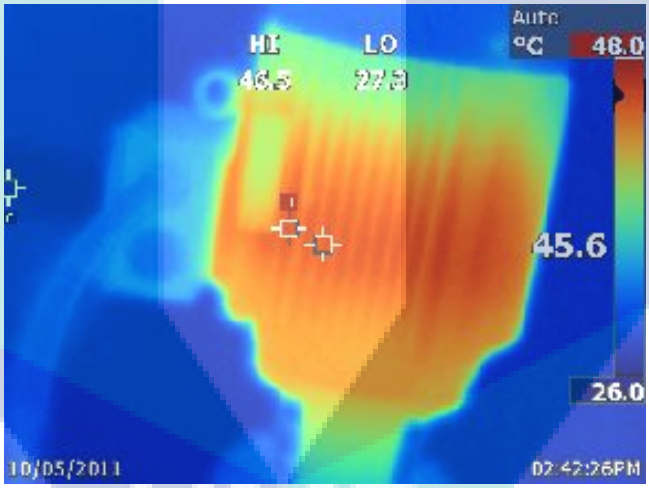

(a) Original image

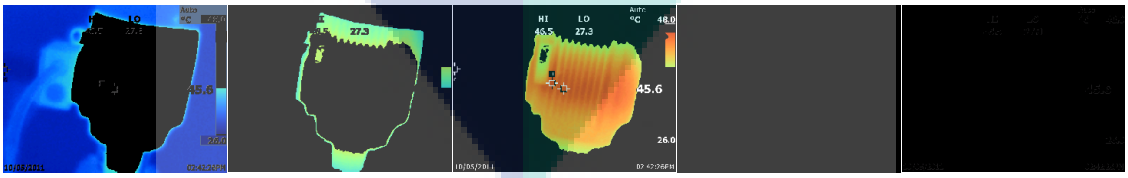

(Region b) (Region c) (Region d) (Region e) (Region f)

Supervised RGB optimal threshold classification result

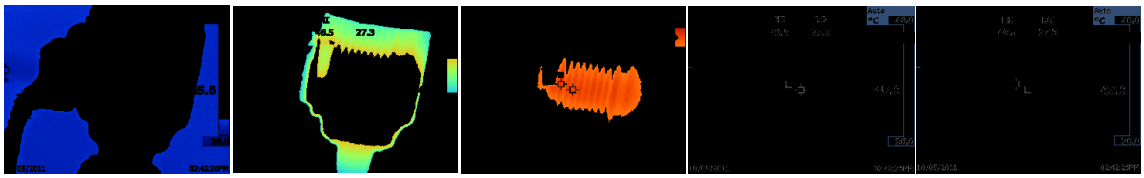

(Region b) (Region c) (Region d) (Region e) (Region f)

Supervised K means classification result

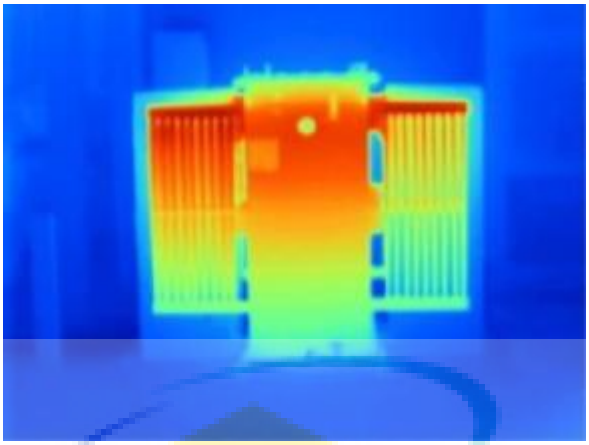

(a) Original image

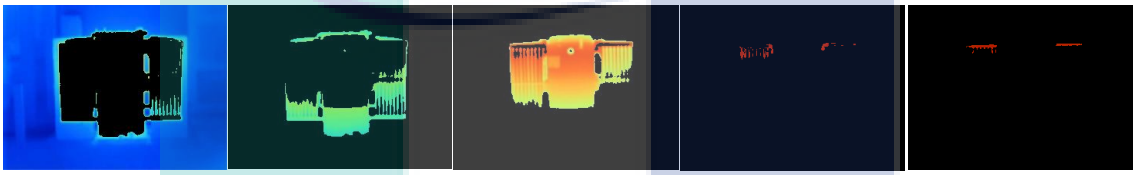

(Region b) (Region c) (Region d) (Region e) (Region f)

Supervised RGB optimal threshold classification result

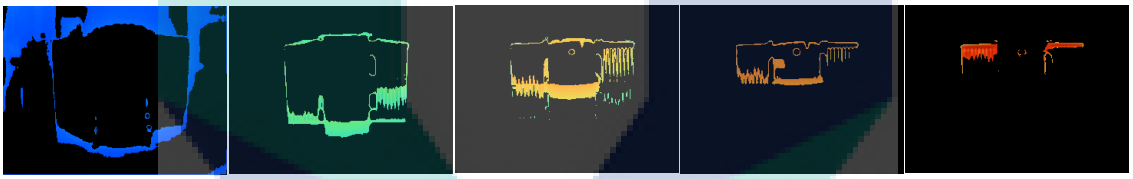

(Region b) (Region c) (Region d) (Region e) (Region f)

Supervised K means classification result

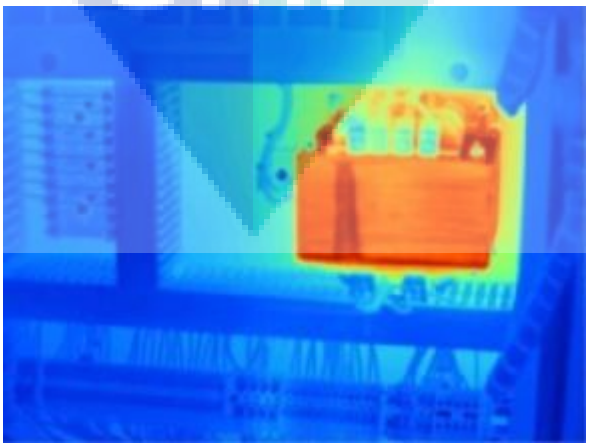

(a) Original image

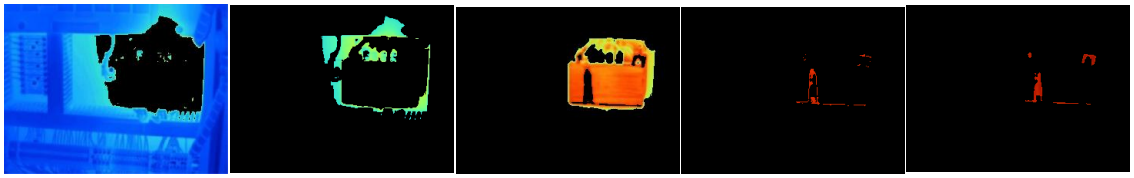

(Region b) (Region c) (Region d) (Region e) (Region f)

Supervised RGB optimal threshold classification result

(Region b) (Region c) (Region d) (Region e) (Region f)

Supervised K means classification result

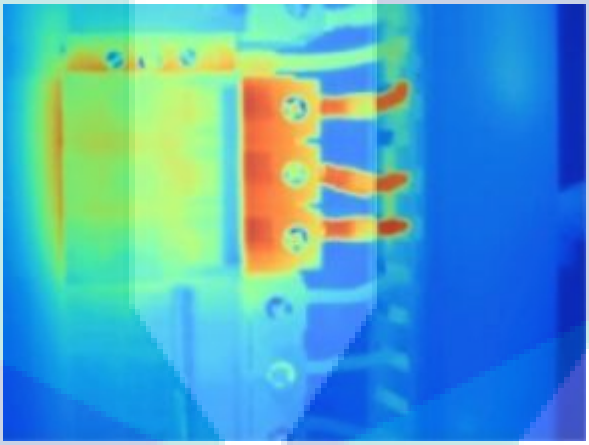

(a) Original image

(Region b) (Region c) (Region d) (Region e) (Region f)

Supervised RGB optimal threshold classification result

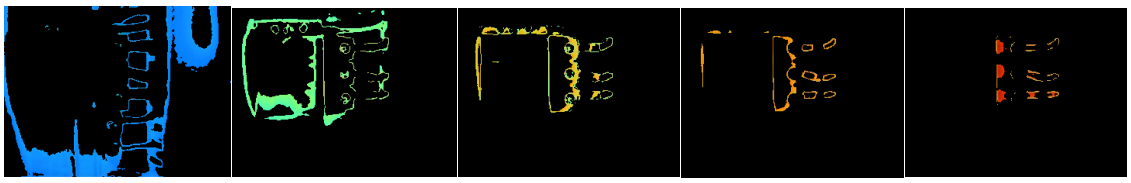

(Region b) (Region c) (Region d) (Region e) (Region f)

Supervised K means classification result

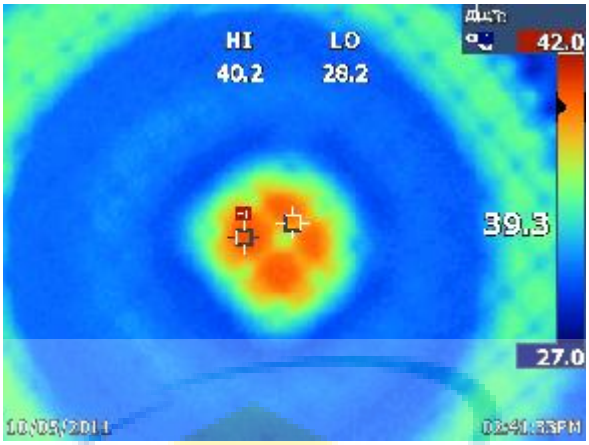

(a) Original image

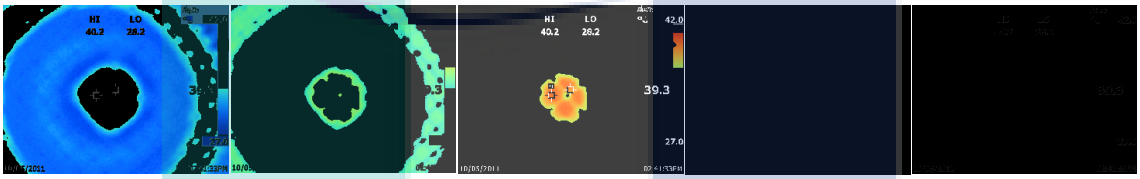

(Region b) (Region c) (Region d) (Region e) (Region f)

Supervised RGB optimal threshold classification result

(Region b) (Region c) (Region d) (Region e) (Region f)

Supervised K means classification result

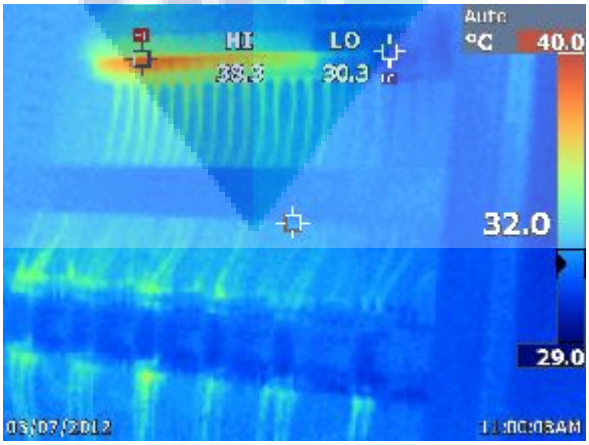

(a) Original image

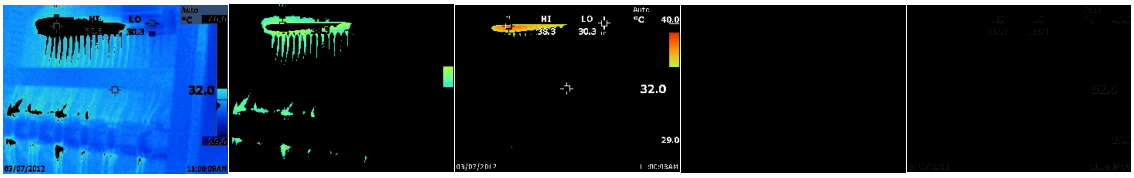

(Region b) (Region c) (Region d) (Region e) (Region f)

Supervised RGB optimal threshold classification result

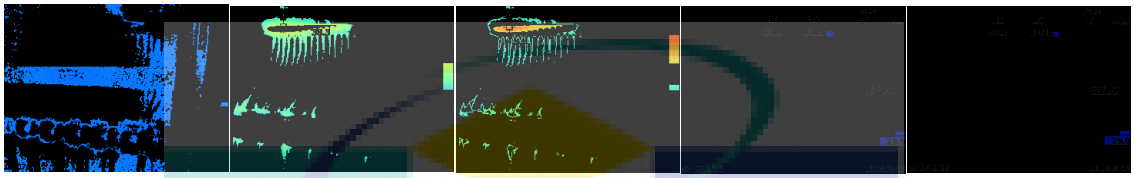

(Region b) (Region c) (Region d) (Region e) (Region f)

Supervised K means classification result

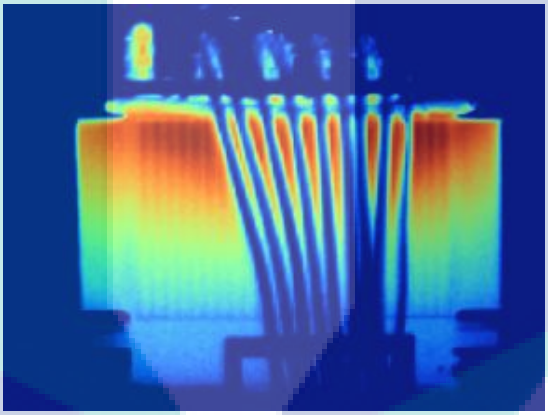

(a) Original image

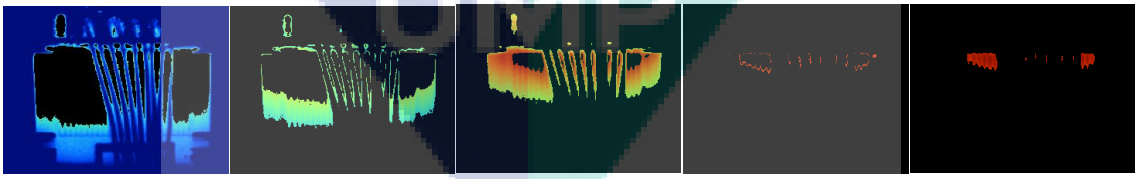

(Region b) (Region c) (Region d) (Region e) (Region f)

Supervised RGB optimal threshold classification result

(Region b) (Region c) (Region d) (Region e) (Region f)

Supervised K means classification result

Figure 4.13: Defect detection comparison results

The comparison result analysis in Table 4.5, open dots (○) and solid dots (●) were used to indicate image or object absence and presents after classification. In the Table 4.5, open dots represent the absence of an image or object and solid dots depicts presents of an image or object in the classified regions. The portions marked with yellow in the Table 4.5 showed where K means classification algorithm gave wrong equipment judgement after thorough defect detection scrutiny operations and classification. This conclusive result followed the defect detection comparison results between the proposed RGB optimal threshold and K means algorithms presented in Figure 4.13. The results analysis in Table 4.5, the yellow marks indicates the processed equipment samples that were wrongly judged by the supervised K-means classification algorithm as compared with the proposed RGB optimal threshold algorithm.

Table 4.5: Comparison analysis result table

	RGB Optimal Threshold Algorithm				**K Means Clustering Algorithm**			
No of Samples	**Abnormal**	**High Thermal**	**Warming**	**Normal**	**Abnormal**	**High Thermal**	**Warming**	**Normal**
1	○	○	●	●	●	●	●	●
2	○	○	●	●	○	○	●	●
3	○	○	●	●	○	○	●	●
4	●	●	●	●	●	●	●	●
5	●	●	●	●	●	●	●	●
6	○	○	●	●	●	●	●	●
7	○	○	●	●	●	●	●	●
8	○	○	●	●	○	○	●	●
9	○	○	●	●	○	○	●	●
10	●	●	●	●	●	●	●	●
11	○	○	●	●	●	●	●	●

Therefore thermal defect detection accuracy is evaluated based on the total number of inspected electrical power equipment and components minus the proportion of wrongly judged electrical power equipment and components divided by the total

number of inspected electrical power equipment and components and can be calculated using Formula (3.30),

$$Accuracy = [\frac{(Total\ inspected - wrongly\ judged) equipment}{Total\ number\ of\ inspected\ equipment} \times 100](\%) \quad (3.30)$$

Using the Formula 3.30, it is figured out that K means clustering algorithm was able to give 72.72% accuracy against 99.72% accuracy result from the proposed RGB optimal threshold algorithm. Therefore, the proposed RGB optimal threshold algorithm is confirmed better than the K means clustering algorithm.

CHAPTER 5

CONCLUSION AND RECOMMENDATIONS

5.1 INTRODUCTION

In summary, this research project proves the use of infrared thermal image or thermogram of electrical equipment as a non-invasive adjunctive diagnostic methodology for detecting electrical equipment faults. A thermal imager is used to collect thermal pictures of the tested electrical facilities under various operating conditions. These thermal pictures are used for thermal fault analysis base on the developed computer aided scrutiny system to detect the steady state or normal condition, the warming condition, the high temperature condition and abnormal thermal condition of electrical power equipment. From the experimental inspection results, it was proved that application of thermal imaging technology to analyze electrical faults is one of the safest means of testing, inspecting and in the preventive maintenance checks. Defect detection at early stage on electrical power components is very imperative in order to save cost, equipment and human life. Generally, thermal imaging technology and RGB optimal threshold technique is considered as robust non-destructive defect detection methodology in electrical power facilities with fast computational result and reasonable degree of accuracy. This chapter also presents summary and conclusion of the entire work according to chapters. Invaluable achievements and recommendations for future research are all summarized.

In chapter 1, the introduction of infrared thermal Imaging technology and its applications in electrical power engineering systems were explained. Imperativeness of thermography technology to quality safety testing and inspection for predictive or

preventive maintenance work are elaborately discussed. The scope and objective of this project are well spelled out.

In chapter 2, some thermography terminologies were explained. Review on relevant existing defect detection techniques and algorithms for thermal images and non-thermal images were surveyed. In addition, some advantages and disadvantages of these algorithms are discussed in the text. A brief introduction of the proposed technique is given at the end of the chapter.

In chapter 3, the proposed algorithm for defect detection on electrical equipment and components using thermal imaging technology and RGB optimal threshold technique was introduced and fully developed. Real life electrical power distribution equipment used during the training process of the defect detection scrutiny systemstemstem was pictorially shown in the text. Accuracy of IRT image segmentation proved using ideal ROC curve and the area under convex hull were well elaborated in the text. Results of performance measure showing the effect of flawed threshold values were presented in chapter 3.5.

In chapter 4, IRT images of different electrical equipment thermogram that were used for training the defect detection scrutiny system and for performance optimization presented. At the end of the training and performance optimization, the defect detection diagnostic system becomes very sensitive and performs defect detection operation. During comparison process, the RGB optimal threshold algorithm was found to be better than unsupervised k-means clustering algorithm. The efficacy and results of the proposed defect detection technique using thermal imaging technology and RGB optimal threshold algorithm were all discussed and presented in chapter 4. The overall result gotten from the defect detection scrutiny system showing various classified thermal regions (normal condition, warming condition, high temperature condition and abnormal condition) of inspected electrical equipment according to their surface thermal radiations were presented in chapter 4.5. Interpretations and classifications of the results were presented in chapter 4.6. Descriptions of decision making, sensitivity and accuracy of experimental thermal inspection on electrical power equipment and components were

presented in chapter 4.7. Results of K-means clustering algorithm were presented in chapter 4.8. Lastly, the results of comparative studies were presented in chapter 4.9.

The proposed defect detection scrutiny algorithm can detect subtle changes in equipment temperature that indicates varieties of abnormalities. This defect detection technique is very intuitive, interpretation-made-easy, cost and time effective yet the result is very satisfactory as shown in Figures 4.4 (A – D) and 4.5 (A – E) and Figures 4.6, 4.7, 4.8, 4.9 and 4.10. Therefore, the objective of this project for detecting defects in electrical power equipment and components using thermal imaging technology was successfully achieved.

5.2 ACHIEVEMENTS

Within the limits of experimental errors, the following objectives were also achieved:

Impact of electrical faults was studied and thoroughly analyzed following equipment thermal pattern. This is the doorway to defect detection on electrical equipment process, which accounts for the first objective.

A computer aided scrutiny system for defect detection on electrical power equipment that speedizes defect detection process, make a fault decision and recommend actions to be taken for proper preventive maintenance and repair actions was developed. This accounts for the second objective.

Thermal inspection results were compared with the international thermal evaluation standard and it was observed that the standard offered a useful guide. This accounts for the third objective.

Generally, the analysis results showed that 99.9% sensitivity was achieved from defect detection scrutiny system. Also 99.72% overall accuracy was achieved from a total of 111 samples of inspected electrical power equipment and components. The error rate value of 0.28% encountered was attributed to mistakes due to over and less caution.

The results suggested that, the defect detection scrutiny system technique that provides an accurate identification of defective parts of electrical component could be extended for further applications.

It also suggested that the system could improve the value and efficiency of consumable electrical power equipment, reducing the number of faults in the power distribution line, ensuring safety of the workers and users of electricity, protecting electrical power equipment from damage due to over-heating or fire.

Enhanced method of equipment situation report from tested and inspected equipment thermogram that helps preventive maintenance personnel and electrical power equipment inspectors was achieved.

Above all, testing, inspection and preventive maintenance work become robust, easier, and faster with a considerably high degree of accuracy.

5.3 RECOMMENDATION FOR FUTURE WORK

Based on the related problems discovered in the course of this research project, some suggested future work could continue from here:

In future, Infrared thermal imager and computer aided scrutiny software can be miniaturized into a portable small mobile device for easy electrical equipment inspection.

There could be a smarter scrutiny system with more sensitivity (artificial neural network system) if effectively implemented might offer infrared thermography inspection a greater chance to play its invaluable role in predictive or preventive maintenance operation.

There could be an advancement towards producing a system that will require little or no human interface in early fault detection process using infrared thermography technology.

LIST OF REFERENCES

Abbott J.A. 1999. *Quality measurements of fruits and vegetables.* 15. **207**. Postharvest. Biol.Technol.

Abbott J.A., Lu R., Upchurch B.L., Stroshine R.L. 1997. Technologies for nondestructive quality evaluation of fruits and vegetables. *Horticultural reviews.* J. Janick Wiley. **20**. Chichester, U.K.

Ahmed M. A. Haidar, Geoffrey O. Asiegbu, Kamarul Hawari, Faisal A. F. Ibrahim, 2012. Electrical defect detection in thermal image. *Advanced Materials Research,* **433-440**. 3366-3370.

Alan G. Glaros, Rex B. Kline. 1988. Understanding the accuracy of tests with cutting scores. *Journal of Clinical Psychology,* **44**(6).

Anil Z. Chitade, Dr S.K. Katiyar. 2010. Color based image segmentation using K–means clustering. *International Journal of Engineering Science and Technology,* **2** (10):5319-5325.

Blagojce Stojcevski, Akhtar Kalam. 2010. Fault location in overhead power lines using the iec61850. *International Protocol International Review on Computers and Software (IRECOS),* **3**(5): 888-899.

Braunovic, M., Myshkin N.K., and Konchits V.V. 2007. *electrical contacts fundamentals, applications and technology*. Paul G. Slade. Poland: CRC Press.

Brian J. McPartland, Frederic P. Hartwell and Joseph F. McPartland. 2011. *National electrical code handbook*. (Ed.). 27th. USA: McGraw-Hill.

Brunner, C.C., Maristany, A.G., Butler, D.A., VanLeeuwen, D., Funck, J.W. 1992. An evaluation of color spaces for detecting defects in Douglas-fir veneer. Industrial Metrology 2 (3/4), 169_ 184.

Butler, D.A., Brunner, C.C., Funck, J.W. 1989. A dual-threshold image sweep-and-mark algorithm for defect detection in veneer. *Forest Products Journal* 39(5): 25-28.

Butz P., Hofmann C., Tauscher B. 2005. Recent developments in non-invasive techniques for fresh fruit and vegetable internal quality analysis. *J Food Science* **70**, 131.

Carosena Meola. 2007. Infrared thermography of masonry structures. *Elsevier Journal Publication on Infrared Physics & Technology* **49**:228–233.

Chan Y. C., Fan Yeung, Guangchang Jin, Naikong Bao, and Chung P. **S**. 1995. Non-destructive detection of defects in miniaturized multilayer ceramic capacitors using digital speckle correlation techniques. *IEEE Transactions on Computers, Packaging and Manufacturing Technology-Part A.*

Chen X., Jing H., Tao Y., Carr L., Wheaton F. 2003. Real-time detection of physical hazards in de-bonded poultry using high resolution X-ray imaging. *Proceedings of the ASAE/CSAE Annual International Meeting,* Las Vegas, Paper #033084.

Chen, W. L., So, A. T. P., Lai, L. L. 2000. Three-dimensional thermal imaging for power equipment monitoring. *Proceedings IEEE Conference on Generation, Transmission, & Distribution,* **147**(6):355-360.

Chuck, H. 2001. *Handbook of Nondestructive Evaluation*. McGraw-Hill Professional.

Chunli F., Fengrui S., and Li Y. 2005. Investigation on nondestructive evaluation of pipelines using infrared thermography. *IEEE International Conference Terahertz Electronics,* **2**:339-340.

Churtin C., Ignatushin A. 1999. On-line & offline diagnostics for power station HV equipment. *IEEE International Conference on Electrical Insulation, Electrical Manufacturing, and Coil Winding,* 637-643.

Conners, R.W., McMillin, C.W., Ng, C.N. 1985. The utility of color information in the location and identification of defects in surfaced hardwood lumber. *Proceedings of the First International Conference on Scanning Technology in Sawmilling. Miller- Freeman Publications,* San Francisco, CA, pp. XVIII-1_ XVIII-33.

D.F. Bodies. in Food. 2007. M. Edwards. Woodhead Publishing Company, Cambridge.

Don A. Genutis. 2007. Infrared Inspections and Applications. *NETA World,* (online) http//www.netaworld.ld.org

Electric Power Engineering Center. 2007. Guide to Power Transformer Specification Issues. University of Canterbury. (online) http://www.scribd.com/doc/65031914/EPECentre-Guide-to-Transformer-Specification-Issues

Etehad M., Tavakol & S. Sadri & E. Y. K. Ng. 2008. Application of k- and fuzzy c-means for color segmentation of thermal infrared breast images. *Springer Science, Business Media, LLC.*

Faisal Shafaita, Daniel Keysersa, Thomas M. Breuelb. Efficient Implementation of Local Adaptive Thresholding Techniques Using Integral Image. (onlione). http://code.google.com/p/ocropus/ 2008.

Fluke. (online) http://thermalimagingblog.com/index.php/tag/ifovmeasurement/

Fournier D. and Amyot N. 2001. Diagnostic of overheating underground distribution cable joints. *IEE Conference Electricity Distribution,* **1**(482):18-21.

Franz Pernkopfa, Paul O'Leary. 2003. Image acquisition techniques for automatic visual inspection of metallic surfaces. *NDT&E International.* **36**: 609 - 617.

Funck, J.W., Zhong, Y., Butler, D.A., Brunner, C.C., Forrer, J.B.. 2003. Image segmentation algorithms applied to wood defect detection. *Journal Publication on Computers and Electronics in Agriculture*, **41**: 157- 179.

Gautam Biswas, Ravi Kapadia, Xudong W. Yu. 1997. Combined qualitative–quantitative steady-state diagnosis of continuous-valued systems. *IEEE Transactions on Systems, Man, and Cybernetics—Part A: Systems and Humans.*

Graves M., Batchelor B.G., Palmer S.C. 1994. *Three-dimensional X-ray inspection of food products.* A. G. Tescher. **248**. Applications of digital image, in Applications of Digital Image Processing XVII", SPIE Proceedings 2298.

Graves v, Smith A., Batchelor B.G. 1998. Approaches to foreign body detection in foods. *Trends. Food Sci. Technol.*

Hafizan Mat Som, Jasni Mohamad Zain and Amzari Jihadi Ghazali. 2011. Application of threshold techniques for readability improvement of jawi historical manuscript images. *Advanced Computing International Journal (ACIJ).*

Hamed Shah-Hosseini, Reza Safabakhsh. 2002. Automatic multilevel thresholding for image segmentation by the growing time adaptive self-organizing map. *IEEE Transactions on Pattern Analysis and Machine Intelligence.*

Hani, A., Almohair, K., Abd Rahman Ramli, Elsadig, A.M., Shaiful, B., Hashim, J. 2007. Skin detection in luminance images using threshold technique. *International Journal of Imaging Science and Engineering (IJISE),* GA,USA,ISSN:1934-9955,Vol.**1**; No.1.

Hari Kumar Singh, Shiv Kumar Tomar, Prashant Kumar Maurya. 2012. Thresholding techniques applied for segmentation of RGB and multispectral images. *Proceedings published by International Journal of Computer Applications® (IJCA)*- 7-8.

Hideaki Sato, Yasue Mitsukura, Minoru Fukumi, Norio Akamatsu. 2003. Thresholds decision method for fast object detection systems. *Proceedings of IEEE International Symposium on Computational Intelligence in Robotics and Automation,* Kohe, Japan.

Infrared Training and Infrared Certification Standard for infrared inspection of electrical systems & rotating equipment, Infraspection Institute, 2008 Article.

Infraspection Institute. 2008. Standard for infrared inspection of electrical systems & rotating equipment. In: Infraspection Institute, *Infrared Training and Infrared Certification.* 425 Ellis Street Burlington, NJ 08016, USA.

Jaspreet Kaur, Sinha, H.P. 2012. Automated localization of optic disc and macula from fundus images. *International Journal of Advanced Research in Computer Science and Software Engineering.*

Jayas D.S., Karunakaran C., Paliwal J. 2004. Grain quality monitoring using machine vision and soft X-ray for cereal grains. *Proceedings of the International Quality Grains Conference, Indianapolis.*

Jessy G. Smith, B Venkoba Rao, Vivek Diwanji, Shivaram Kamat. 2009. Fault diagnosis – isolation of malfunctions in power transformers. *Tata Consultancy Services Limited*, 10 June 2009.

Jha S.N., Matsuoka T. (Res.) 2000. Non-destructive techniques for quality evaluation of intact fruits and vegetables. Food Sci. Technol.

Jia Li , James Z. Wang , Gio Wiederhold. 2000. Integrated region matching for image retrieval (IRM). *Proceedings of The Eighth ACM International Conference on Multimedia*, 147-156.

Jifeng Ning, LeiZhang, DavidZhang, ChengkeW. 2010. Interactive Image Segmentation by Maximal Similarity Based Region Merging. *Pattern Recognition* **43**:445 – 456

Jim White, 2008, Electrical inspections using thermal imaging. Fluke Corporation. U.S.A. 6/2008 3358415 A-EN-N Rev A.

Jin Li, Pyanwei Wang, P Hong Liang, P Jie Weip, Dada Wang, P Hong Yu. 2012. X-Ray Image Defects Detection Algorithm Based on Digital Silhouette, *International Journal of Digital Content Technology and its Applications (JDCTA).*

Jonas Boberg. 2008. Early fault detection with model-based testing. *Proceedings of the Sigplan Workshop on Erlang*

José Martínez, Rodolfo Lagioia Edenor S.A. – Argentina Edenor S.A. 2007. Experience Performing Infrared Thermography in the Maintenance of a Distribution Utility. *19th International Conference on Electricity Distribution.* Vienna.

Jung-Shiong Chang, Hong-Yuan Mark Liaob, Maw-Kae Herb, Jun-Wei Hsieh, Ming-Yang Cherna. 1997. New automatic multi-level thresholding technique for segmentation of thermal images. *Image and Vision Computing* **15**:23-34.

L. M. Lavie. 2004. Electrical safety for an offshore power system. *IEEE Potentials,* **23**:(3):39-42.

Leemans, V., Magein, H., Destain, M.F. 1998. Defects segmentation on 'Golden Delicious' apples by using color machine vision. *Journal Publication on Computers and Electronics in Agriculture,* **20**:117–130.

Li, H., and Burgess, A. E., 2010. Evaluation of signal detection performance with pseudo-color display and lumpy backgrounds. J Med Syst 34:35–42 41 In: KundelH. L. (Ed.), SPIE, medical imaging: Image perception, 3036:143–149.

Liju Dong, Ge Yub, Philip Ogunbona, Wanqing Li. 2008. An efficient iterative algorithm for image thresholding. *Pattern Recognition Letters* **29**:1311–1316.

Lim K.S., Barigou M. 2004. X-ray micro-computed tomography of cellular food products. Food Res. Int. **37**:1001.

Lindquist T.M., Bertling L., Eriksson R. 2005. Estimation of disconnectors contact condition for modeling the effect of maintenance and ageing. *Power Tech IEEE Conference,* Russia.

Mair v. 1988. Industrial robotics. *Prentice Hall*, New York.

Majed Jabri, Houssem Jerbi, Naceur Benhadj Braiek. 2010. Fault detection of synchronous generator based on moving horizon parameter estimation and evolutionary computation. *International Review on Computers and Software (IRECOS),* **3** (1): 38-47.

Martin Technical Electrical Safety & Efficiency. 2012. Infrared Thermography Inspection.http://www.martechnical.com/infrared_inspections/electrical_infrared_inspection_service.php

Matian M., Marquis A.J., Brandon N.P. 2010. Application of Thermal Imaging to Validate a Heat Transfer Model for Polymer Electrolyte Fuel Cells. *International Journal of Hydrogen Energy,* **35**:12308-12316.

McGarry S.L. 1984. Acceptable quality levels are not acceptable any more. *Proceedings of Autofact*, 15:1 – 13.

Mehmet Sezgin, Biilent Sankd. 2001. Selection of thresholding methods for non-desctructive testing applications. *Image Processing, Proceedings ieeexplore*.

Mehmet Sezgin, Bu¨ lent Sankur. 2004. Survey over image thresholding techniques and quantitative performance evaluation. *Journal of Electronic Imaging* **13**(1):146–165.

Mohd Shawal Jadin, Soib Taib, Shahid Kabir, Mohd Ansor Bin Yusof. 2011. Image processing methods for evaluating infrared thermographic image of electrical equipment. *Progress In Electromagnetics Research Symposium Proceedings,* Marrakesh, Morocco.

Mythili Thiruganam, S.Margret Anouncia, Sachin Kantipudi. 2010. Automatic defect detection and counting in radiographic weldment images. *International Journal of Computer Applications.* **10(**2):0975 – 8887.

Nicholas Radaa, Gregory Tripletta, Samuel Graham. 2007. High-speed thermal analysis of high Power diode arrays. *Solid-State Electronics ISDRS,* College Park, MD, USA.

Prasoon Srivastava. 3rd February 2010. Zero defect policy is a culture. (online) http://www.ciol.com/News/Interviews/Zero-Defect-Policy-is-a culture/3210130972/0/

Rada N., Triplett G., Graham S., Kovaleski S. 2008. High-speed thermal analysis of high power diode arrays. *Solid-State Electronics ISDRS*, **52**. Issue 10:1602–1605.

Rajib Kumar Jha, Biswas P. K., Chatterji B. N. 2010. Image segmentation using suprathreshold stochastic resonance. *World Academy of Science, Engineering and Technology* **72**.

Robert M. Button. 2005. Soft-Fault Detection Technologies Developed for Electrical Power Systems. (online) http://powerweb.grc.nasa.gov/elecsys/

Ronald P. Haff. Natsuko Toyofuku. 2008. X-ray detection of defects and contaminants in the Food industry.

Rudi Heriansyah, S.A.R.Abu-Bakar. 2009. Defect detection in thermal image for non-destructive evaluation of petrochemical equipment. *NDT&E International* **42**: 729–740

Sangwook Lee, Color Image-based Defect Detection Method and Steel Bridge Coating, *ASC Annual International Conference Proceedings*, 2011

Shawal M., Taib S., Kabir S., Ansor M. 2011. Image processing methods for evaluating infrared thermographic image of electrical equipment. *Progress in Electromagnetics Research Symposium Proceedings*, Morocco, 1299-1302.

Slawomir Grys. 2012. New thermal contrast definition for defect characterization by active thermography. *Elsevier Journal Publication on Measurement.*

Smith B. 1993. Making war on defects: six sigma design. *IEEE Spectrum*, **30**(9): 43 – 47.

Snell J., and Renowden J. 2000. Improving results of thermographic inspections of electrical transmission and distribution lines. *Proceedings IEEE International Conference Transmission and Distribution Construction*, 135-144.

Soriano M., Huovinen S., Martinkauppi, Laaksonen. 2000. Skin detection in video under changing illumination conditions. *In Proceedings 15th International Conference on Pattern Recognition*. **1**:839– 842.

Tayyaba Azim, Arfan Jaffar, Anwar.M.Mirza. 2011. Automatic skin detection in luminance images using threshold technique. *International Conference on Computer Engineering and Applications* 2009 IPCSIT **2**.

Techniques and Select Industrial Applications of Thermal Imaging. 2011. (online) http://www.ndted.org/EducationResources/CommunityCollege/Other%20Methods/IRT/IR_Applications.htm

Timothy S. Newman, Anil K. Jain. 1995. A survey on automated visual inspection. *computer vision and image understanding.* **61**(2):231 – 262.

Vadivel A, Majumdar A K, Shamik Sural. 2003. Performance comparison of distance metrics in content-based Image retrieval applications. P*roceedings of International Conference on Computer Vision Application.*

Wagner G.G.. 1987. Combining X-ray imaging and machine vision, in optics, illumination, and Image sensing for machine vision II. D.J. Svetkoff. **850**. SPIE Proceedings.

Wahab, Md Saidin. 2003. Defect detection in high pressure die casting product using image processing technology. Master Thesis. University of South Australia, Australia.

Wei Zhan, Junkai Yang. 2012. Real time and automatic vehicle type recognition system design and its application. *International Conference on Mechanical Engineering and Automation Advances in Biomedical Engineering.*

Wenbing Tao, Hai Jin, Liman Liu. 2007. Object segmentation using ant colony optimization algorithm and fuzzy entropy. *Journal Publication on Pattern Recognition Letters* **28**:788–796.

Wen-Nung Lie. 1995. Automatic Target Segmentation by Locally Adaptive Image Thresholding. *IEEE Transactions on Image Processing*.

Wong, K. C. P.; Ryan, H. M. and Tindle, J. 1996. Power system fault prediction using artificial neural networks. *International Conference on Neural Information Processing*, Hong Kong.

Wretman, D., 2006. Finding regions of interest in a decision support system for analysis of infrared images. Master Thesis, Royal Institute of Technology. Stockholm, Sweden.

Yang Cao, Xiaoming Gu, Qi Jin. 2008. Infrared technology in the fault diagnosis of substation equipment. *Technical Session 1 Distribution network equipment*, Shanghai Electric Power Company Shanghai Branch Southern Power, 200030, SI-17 CP1377, CICED.

Ying-Chieh, Chou Leehter Yao. 2009. Automatic diagnosis system of electrical equipment using infrared thermography. *International Conference of Soft Computing and Pattern Recognition.*

Yingzi Du, Chein Chang, Paul David Thouin. 2004. Unsupervised approach to color video thresholding. *Optical Engineering*.

Yinxiao Liu. 2009. A new method of threshold and gradient optimization using class uncertainty theory and its quantitative analysis. Master Thesis, University of Iowa, Canada.

Yong Wu, Yuanjun He, Hongming Cai. 2005. Optimal threshold selection algorithm in edge detection based on wavelet transform. *Elsevier Journal Publication on Image and Vision Computing* **23**:1159–1169.

Youngbae Hwang, Jun-Sik Kim, Inso Kweon. 2006. Determination of color space for accurate change detection. *Proceedings of the International Conference on Image Processing, ICIP*. Atlanta, Georgia, USA.

Yu. P. Aksyonov, A. Golubev, A. Mochortov, V. Rodionov, V. Minein, B. Romanov, C. Churtin, A. Ignatushin. 1999. On-line & offline diagnostics for power station HV equipment. IEEE Int. Conf. Electrical Insulation, Electrical Manufacturing, and Coil Winding, 26-28:637-643.

Željko Hocenski, Suzana Vasilić, Verica Hocenski. 2006. Improved canny edge detector in ceramic tiles defect detection. *IEEE Industrial Electronics, IECON 2006 - 32nd Annual Conference*, 3328 – 3331.

APPENDIX A

TABLE -A Ti25 FLUKE THERMAL IMAGER SPECIFICATION

Temperature Measurement Range	-20 °C to +350 °C (-4 °F to + 662 °F)
Accuracy	± 2 °C or 2 % (whichever is greater)
On-screen Emissivity Correction	Yes
Field of View	23° x 17°
Spatial Resolution (IFOV)	2.5 mRad
Minimum Focus Distance	Thermal lens: 15 cm (6 in); Visible light lens: 46 cm (18 in)
Focus	Manual
Image Frequency	9 Hz refresh rate
Detector Type	160 X 120 focal plane array, uncooled microbolometer
Infrared Lens Type	20 mm F = 0.8 lens
Thermal Sensitivity (NETD)	≤0.1 °C at 30 °C (100 mK)
Infrared Spectral Band	7.5 µm to 14 µm
Visual Camera	640 x 480 resolution
Palettes	Ironbow, blue-red, high contrast, amber, hot metal, grey
Minimum Span (in manual mode)	2.5 °C (4.5 °F)
Minimum Span (in auto mode)	5 °C (9 °F)
IR-Fusion Information	Full infrared with MAX, MID, MIN; PIP with MAX, MID, MIN automatic blending (Visual and IR blending)
Picture-In-Picture (PIP)	Three levels of on-screen IR blending displayed in center 320 x 24 pixels
Full Screen (PIP off)	Three levels of on-screen IR blending displayed in center 640 x 480 LCD
Voice Annotation	60 seconds maximum recording time per image
Storage Medium	2 GB SD memory card
File Formats	Radiometric (.is2); Non-radiometric JPEG, BMP, GIF, PNG, TIFF, WMF, EXIF, and EMF

APPENDIX B

TABLE B-1 EMISSIVITY VALUES FOR METALS

Material		Emissivity		
		1.0 μm	1.6 μm	8 - 14 μm
Aluminum				
	Unoxidized	0.1-.0.2	0.02-.02	N.R.
	Oxidized	0.4	0.4	0.2-0.4
	Alloy A3003, Oxidized	N.R.	0.4	0.3
	Roughened	0.2-0.8	0.2-0.6	0.1-0.3
	Polished	0.1-0.2	0.02-0.1	N.R.
Brass				
	Polished	0.8-0.95	0.01-0.05	N.R.
	Burnished	N.R.	N.R.	0.3
	Oxidized	0.6	0.6	0.5
	Chromium	0.4	0.4	N.R.
Copper				
	Polished	N.R.	0.03	N.R.
	Roughened	N.R.	0.05-0.2	N.R.
	Oxidized	0.2-0.8	0.2-0.9	0.4-0.8
	Electrical Terminal Block	N.R.	N.R.	0.6
Gold		0.3	0,01-0.1	N.R.
Haynes Alloy		0.5-0.9	0.6-0.9	0.3-0.8
Inconel				
	Oxidized	0.4-0.9	0.6-0.9	0.7-0.95
	Sandblasted	0.3-0.4	0.3-0.6	0.3-0.6
	Electro-polished	0.2-0.5	0.25	0.15
Iron				
	Oxidized	0.4-0.8	0.5-0.9	0.5-0.9
	Unoxidized	0.35	0.1-0.3	N.R.
	Rusted	N.R.	0.6-0.9	0.5-0.7
	Molten	0.35	0.4-0.6	N.R.
Iron, Cast				
	Oxidized	0.7-0.9	0.7-0.9	06-0.95
	Unoxidized	0.35	0.3	0.2
	Molten	0.35	0.3-0.4	0.2-0.3
Iron, Wrought				
Dull		0.9	0.9	0.9
Lead				
	Polished	0.35	0.05-0.2	N.R.
	Rough	0.65	0.6	0.4
	Oxidized	N.R.	0.3-0.7	0.2-0.6
Magnesium		0.3-0.8	0.05-0.3	N.R.
Mercury		N.R.	0.05-0.15	N.R.

Molybdenum	Oxidized	0.5-0.9	0.4-0.9	0.2-0.6
	Unoxidized	0.25-0.35	0.1-.0.35	0.1
Monel (Ni-Cu)		0.3	0.2-0.6	0.1-0.14
Nickel				
	Oxidized	0.8-0.9	0.4-0.7	0.2-0.5
	Electrolytic	0.2-0.4	0.1-0.3	N.R.
Platinum				
	Black	0.95	0.9	N.R.
	Silver	N.R.	0.2	N.R.
Steel				
	Gold Rolled	0.8-0.9	0.8-0.9	0.7-0.9
	Ground Sheet	N.R.	N.R.	0.4-0.6
	Polished Sheet	0.35	0.25	0.1
	Molten	0.35	0.25-0.4	N.R.
	Oxidized	0.8-0.9	0.8-0.9	0.7-0.9
Stainless		0.35	0.2-0.9	0.1-0.8
Tin (Unoxidized)		0.25	0.1-0.3	N.R.
Titanium				
	Polished	0.5-0.75	0.3-0.5	N.R.
	Oxidized	N.R.	0.6-0.8	0.5-0.6
	Tungsten	N.R.	0.1-0.6	N.R.
	Polished	0.35-0.4	0.1-0.3	N.R.
Zinc				
	Oxidized	0.6	0.15	0.1
	Polished	0.5	0.05	N.R.

TABLE B-2 EMISSIVITY VALUES FOR NON-METALS

Material		1.0 μm	1.6 μm	8 -14 μm
Asbestos		0.9	0.9	0.95
Asphalt		N.R.	0.95	0.95
Basalt		N.R.	0.7	0.7
Carbon				
	Unoxidized	0.8-0.95	0.8-09	08-0.9
	Graphite	0.8-0.9	0.7-0.9	0.7-0.8
Carbrundum		N.R.	0.9	0.9
Ceramic		0.4	0.85-0.95	0.95
Clay		N.R.	0.85-0.95	0.95
Concrete		0.65	0.9	0.95
Cloth		N.R.	0.95	0.95
Glass				
	Plate	N.R.	0.98	0.85
	"Gob"	N.R.	0.9	N.R.

Gravel	N.R.	0.95	0.95
Gypsum	N.R.	0.4-0.97	0.8-0.95
Ice	N.R.		0.98
Limestone	N.R.	0.4-0.98	
Paint (Non Al)		0.9-0.95	0.9-0.95
Paper Any Color	N.R.	0.95	0.95
Plastic (Opaque, over 20 mils)	N.R.	0.95	0.95
Robber	N.R.	0.9	0.95
Sand	N.R.	0.9	0.9
Snow	N.R.		0.9
Soil	N.R.		0.9-0.98
Water	N.R.		0.93
Wood, Natural	N.R.	0.9-0.95	

APPENDIX C

C-1 Tools and Materials

Typical tools and materials used in this project include personal computer, 2GB SD memory card, and Ti25 model Fluke thermal Imager. Figure C-1 shows a pictorial representation of thermal date acquisition process.

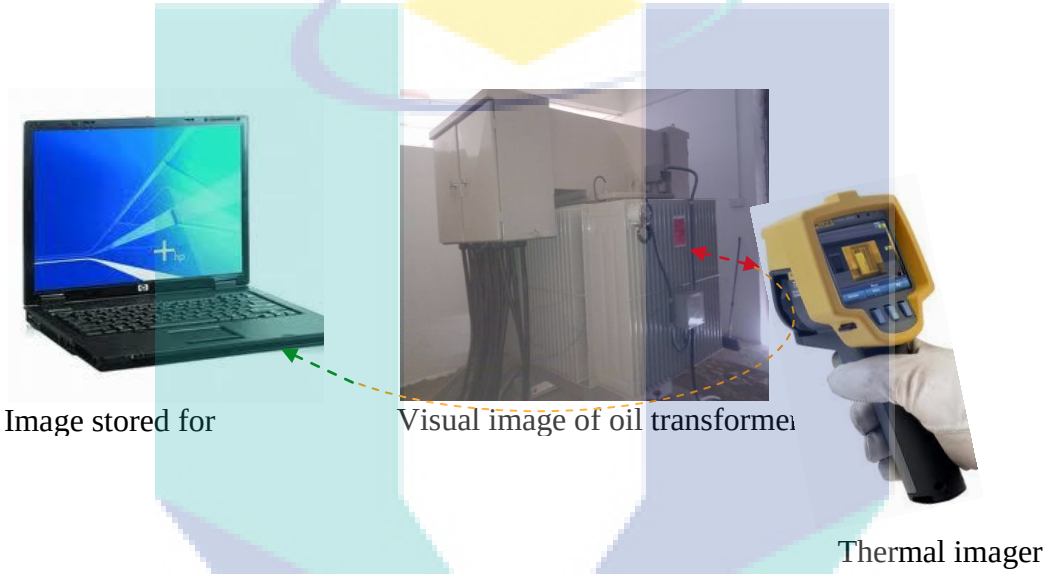

Figure C-1: Thermal Data acquisition Process (*image side 640×480*)

C-2 Thermal Picture Acquisition

Equipment inspection is the first stage of defect detection processes which thermal picture acquisition is an important aspect of the process. It is required that more precaution must be taken at this stage in order to have a minimal false positive images. A well-focused IRT image will facilitate defect detection analysis as well as reliable evaluation in decision making and situation report. Figure C-2 summarizes the concept in a brief flow chart.

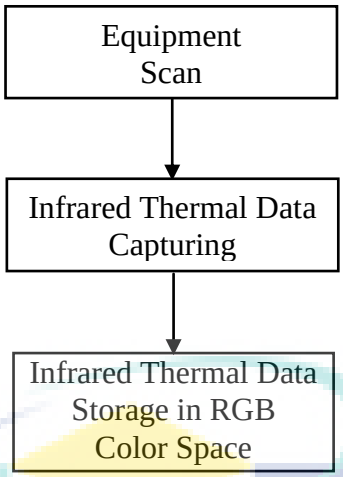

Figure C-2: Flow of Data Acquisition Process

In image acquisition stage, among other equipment thermogram that were captured are oil immerse distribution transformers, fuse boxes, dry type distribution transformers, circuit breakers, electric motors, connectors, contactors, capacitors, resistors, and inductors. Thermogram of all these equipment and components were taken under various loading conditions within University Malaysia Pahang (UMP) environment, Kuala Lumpur and Pahang electrical power distribution substations. In every equipment thermogram, there exist horizontal and vertical pixels or elements that contain a temperature value; a complex set of algorithm assigns a specific color level that corresponds with the temperature values that were found in the each specific *X-Y* coordinate. This color level is also known as *Palette*. This palette varies according to model and manufacturer specification such as IRBIS and IRBIS Plus V2.2 model from InfraTec GmbH Dresden has seven palettes: *varioscan*, *varioscan-printer*, *black-white*, *white-black*, *iron*, *blue-red*, and *stufen*. ThermaCAM Explorer 99 model from FLIR Systems produces as much as thirteen palettes: *glowbow*, *grey*, *grey10*, *grayred*, *iron*, *iron10*, *medical*, *midgreen*, *midgray*, *rain*, *rain100*, *rain900*, and *yellow*. While Ti25 model from Fluke gives six palettes: *Ironbow, blue-red, high contrast, amber, hot metal and gray*.

Figure C-3 is the different color palettes available in Ti25 model Fluke thermal imager used in this project. In whichever analyzer or algorithm adopted, the palette has to be predetermined before the captured data is stored. Secondly, all the captured data

are scaled along side with in depth analysis after transferring the data into a computer for processing and analysis.

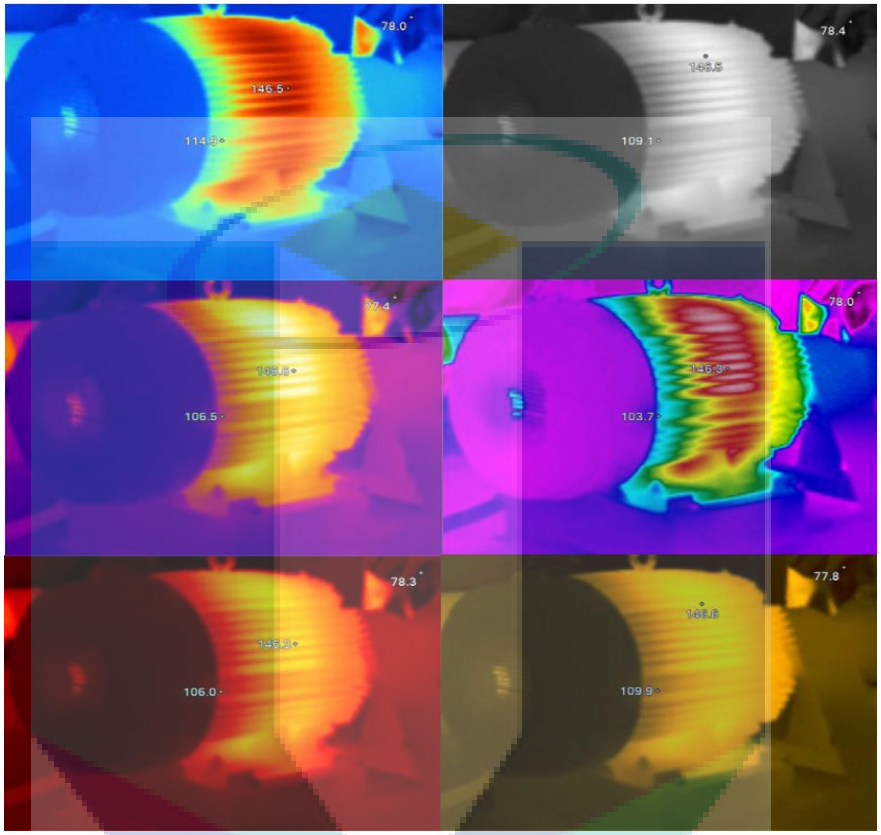

Figure C-3: Ti25 Fluke Thermal Imager Palettes

C-3 Factors for Measurement Accuracy

Beside the above-mentioned points, here are four listed and explained factors that facilitate measurement accuracy.

- Calibration of the Camera
- Emissivity Correction
- Reflected Temperature Compensation
- Distance-to-spot size ratio

C-4 Internal Calibration of Camera

When a thermal imager is switched on, it freezes briefly, which is normal as it is a process all thermal imagers go through especially at start up. During this time, the internal shutter briefly blocks the live image as it corrects and eliminates any offset variations and performs a recalibration sequence. Once the image has operated for a while, it will not need to self-calibrate as often. If you move to an environment with a very different temperature, it may again go through the process more frequently until it stabilizes once again. This is normal part of ensuring the accuracy of the measurement operation. This internal calibration process is also known as *Non-Uniformity Correction (NUC).*

C-5 Factory Calibration of Camera

The thermal imager is also factory calibrated in the Fluke Laboratory using exacting standards. It should be returned to maintain optimum performance. The interval between calibrations depends on how often the thermal imager is used as well as the specific model.

C-6 Emissivity Correction

This is an important factor for measurement accuracy; that is *emissivity correction.* In essence, emissivity is a material property that describes the efficiency with which an object radiates or emits heat. It is expressed as a value from 0.0 – 1.0, shiny metals, mirrors and reflectors have a low emissivity while blackbody, non-shiny metals, painted or heavily oxidized metals have a high emissivity. In qualitative measurements, it is preferable to set the thermal imager emissivity value to 1.0. If actual temperature value is required, then set the emissivity according to the material surface to be measured. Appendix C provides a reference list of some materials (metal and non-metal) with their corresponding emissivity values that can be used when it is not easy to determine the emissivity value experimentally. These emissivity values are only approximate and can be affected by any or all of the following parameters: temperature, angle of measurement, target Geometry (plane, concave, convex and so

on), thickness, surface quality (painted, polished, oxidized, shiny, rough and so on), Transmissivity (such as thin film plastics) and wavelength.

C-7 Reflected Temperature Compensation

Target surface that has low emissivity will reflect energy from neighboring objects. The additional reflected energy is added to the target's own emitted energy which could cause wrong evaluation especially in quantitative analysis where actual temperature readings is so required. There could be some circumstances where objects such as furnaces, electric motors, machines and other heat sources near target have a temperature much higher than that of the targeted surface. In such cases, it is necessary or even imperative to compensate for the reflected energy of those objects in order to have a reliable analysis and situation report. The concept of reflected temperature compensation is illustrated in Figure C-4. There is no need for reflected temperature compensation if the emissivity is (1.0) unity.

Figure C-4: Emitted, Reflected and Transmitted Energy

C-8 Distance-To-Spot Size Ratio

The Ti25 thermal imager views a portion of the scene that is $23^{\circ} wide \times 17^{\circ} hight$ that is the imager field of view (FOV) as shown in Figure C-5

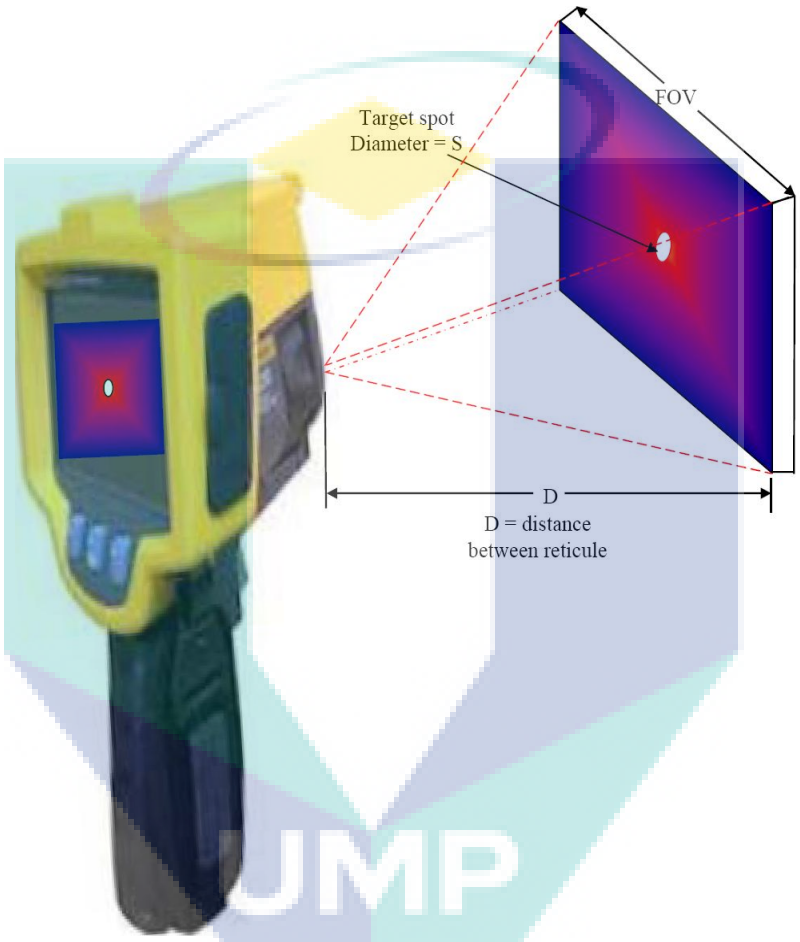

Figure C-5: Relationship between Target spot, FOV, and Reticule

This scene is displayed on the liquid crystal display (LCD) of the thermal imager. The single temperature displayed numerically at the lower edge of the LCD corresponds to a measurement of much smaller part of the scene. In essence, this corresponds to the average temperature of the area seen through the hole in the center of the reticule on the LCD display. The actual diameter of the measurement spot on the object is calculated by dividing the distance of the object by 75 (the D:S of the thermal imager). If the thermal imager is properly focused on the target of distance 120 inches, the diameter of the measurement spot will be $(120 \div 75 = 1.6 inches)$. To achieve the smallest

measurement spot (D:S = 75:1), the thermal imager must be properly focused on the object being measured as shown in Figure C-6.

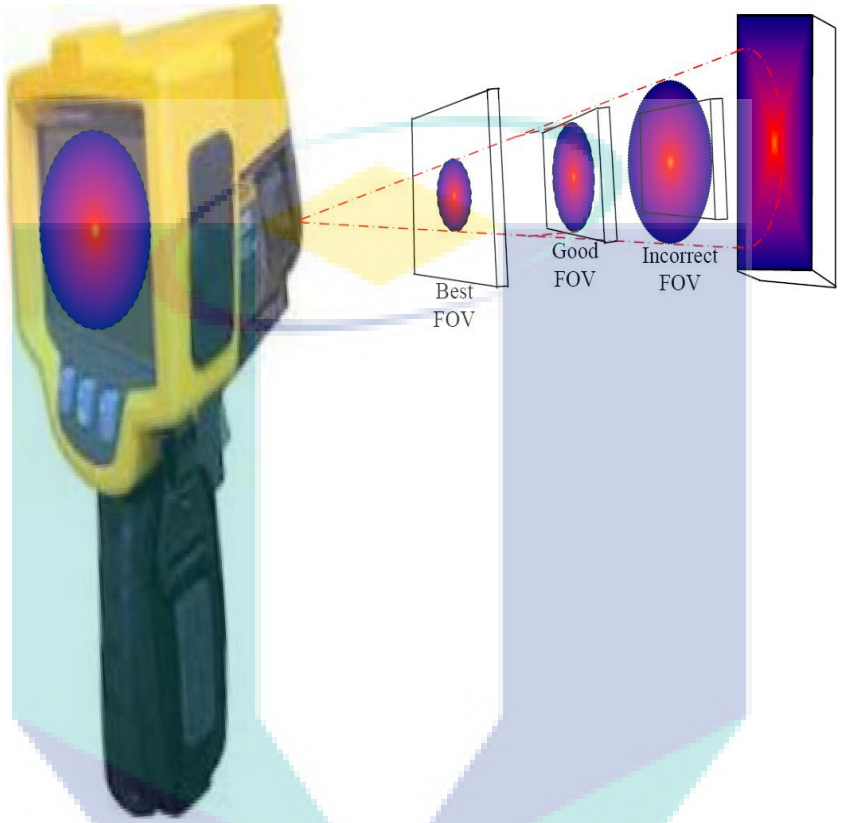

Figure C-6: Field Of View Measurements

C-9 Instantaneous Field of View (IFOV)

IFOV is a specification that describes measurement resolutions; thermal imagers can see an object at a greater distance than it can accurately measure the temperature of that object. This measurement resolution is of two types: IFOV (*theoretical*) and IFOV (*measurement*) *IFOV (theoretical):* This is related to the *distance to spot ratio (D:S)* on the thermal imager, and can tell how far away an object of a certain size can be seen. *IFOV (measurement):* This tells the distance at which an object's temperature can accurately be measured. For this, the distance is shorter. Just that an imager can detect an object; it does not mean that it can always accurately determine the temperature at long distances (thermal imaging blog.com).

C-10 Minimum Distance for Focus

At a minimum distance of 15 centimeters or 6 inches for thermal lens; 46 centimeters or 18 inches for visible light lens, Ti25 Fluke thermal Imager can accurately measure a targeted object as small as 7 millimeters or ¼ inches. It is always a good idea, whenever possible to move as close as safely can to fill the image with the target object. Even so, working within the distance to spot size ratio is necessary.

C-11 Correction Measurement

Adjust both the emissivity and reflected temperature compensation values in order to obtain optimized temperature measurement accuracy. In addition observe the following tips:-

- Avoid measuring shiny metal surfaces; they will often be unreliable.
- Use thermal Imager with shorter wavelength for the high temperature objects whenever possible.
- Ensure that the imager is held at perpendicular to the surface whenever the emissivity is less than 0.9 and at all times work within an angle of 30 degrees from the incidence.
- Measure high emissivity surfaces example, non-shiny metal such as oxidized metal, electrical insulation tapes or rough surface when possible.
- For partially transparent materials such as thin film plastics and glasses confirm that the background temperature is uniform or lower than the temperature of the target object.
- Be safe avoid touching hot or energized surfaces.
- Use emissivity tables mainly as guidelines.
- Use the correct ambient temperature after evaluating the environment and the temperature of the object being reflected.

APPENDIX D

LIST OF PUBLICATIONS

Geoffrey O. Asiegbu, Ahmed M. A. Haidar, Kamarul Hawari, "Thermal Defect Analysis on Transformer Using a RLC Network and Thermography," Circuit and Systems, 2013, 4, 52-60 doi:10.4236/cs.2013.41058.

Geoffrey O. Asiegbu, Ahmed M. A. Haidar, Kamarul Hawari, "Non-Destructive Defect Detection on Electrical Equipment Using Thermographic Technology," International Reviews on Computers and Software (I.RE.CO.S). Vol. 7, N. 3 may 2012. ISSN 1828-6003. (6.13 I.F.)

Ahmed M. A. Haidar, Geoffrey O. Asiegbu, Kamarul Hawari, Faisal A. F. Ibrahim, "Electrical Defect Detection in Thermal Image," Advanced Materials Research Vols. 433-440 (2012) pp 3366-3370

Geoffrey O. Asiegbu, Ahmed M. A. Haidar, Kamarul Hawari, "A Review of Defect Detection on Electrical Equipment Using Image Processing Technology," 4th International Conference on Signal and Image Processing. Lecture Notes in Electrical Engineering, 221 DOI:10.1007/978-81-322-0997-3_23 ©Springer India 2013.

Geoffrey O. Asiegbu, Ahmed M. A. Haidar, Kamarul Hawari, Defect Detection on Electrical Equipment, Malaysian Conference on Electrical, Electronic and Control Technology (MCEECT 2012), University Malaysia Pahang, February 16, 2012.

Geoffrey O. Asiegbu, Ahmed M. A. Haidar, "Defect Tracking of Electrical Components," United Kingdom-Malaysia-Ireland Engineering Science International Conference, (UMIES 2011) University Malaya, Kuala Lumpur, 12-14 July 2011.